

GALAXY GROUPS AND BINARIES AND THE VALUE OF Ω_0

by

Charles Grady Morgan
B.S., Memphis State University, 1966
M.S., Johns Hopkins University, 1969
Ph.D., Johns Hopkins University, 1970
M.Sc., University of Alberta, 1972

A THESIS SUBMITTED IN PARTIAL FULFILLMENT
OF THE REQUIREMENTS FOR THE DEGREE OF

MASTER OF SCIENCE

ACCEPTED
FACULTY OF GRADUATE STUDIES

in the Department

of

Physics

DATE

1986-10-20

DEAN

We accept this thesis as conforming
to the required standard

F. David A. Hartwick

John L. Climenhaga

Jeremy B. Tatum

Thomas W. Dingle

Charles J. Peterson

© Charles Grady Morgan, 1986
University of Victoria
July 1986

All rights reserved. This thesis may not be reproduced
in whole or in part, by mimeograph or any other means,
without the permission of the author.

OFFICE OF THE ATTORNEY GENERAL
STATE OF TEXAS

Q8858.7
M67

Supervisor: Professor F. David A. Hartwick

ABSTRACT

A new technique, which uses Ω_0 as an input variable, for identifying gravitationally bound, dynamically isolated, virialized groups of galaxies from a magnitude limited catalog is developed. The technique has been applied to the CfA redshift survey. In this thesis only the binary systems have been analyzed. Using a self-consistency argument, a value of $\Omega_0 = 0.03 \pm 0.01$ was obtained.

Examiners:

[Redacted]

F. David A. Hartwick

[Redacted]

John L. Climenhaga

[Redacted]

Jeremy B. Tatum

[Redacted]

Thomas W. Dingle

[Redacted]

Charles J. Peterson

TABLE OF CONTENTS

Title page	1
Abstract	ii
Table of contents	iii
List of tables	v
List of figures	vi
Acknowledgements	ix
Chapter I: Introduction	1
Chapter II: The theory of finding groups	14
II.A: The catalog requirements	14
II.B: The general framework algorithm	15
II.C: The companionship criteria	20
II.C.1: The brightest galaxy criterion	21
II.C.2: The escape velocity criterion	25
II.C.3: The density criterion	33
Chapter III: Binary galaxies	38
III.A: Binary samples	38
III.B: Binary calculations	39
III.C: Variable interrelationships	42
III.D: The problem of faint companions	46
Chapter IV: Applications and results	54
IV.A: Initial conditions	54
IV.B: Resultant binary galaxies	56
IV.C: Variable interrelationships	58
IV.D: Results of the cull procedure	62

IV.E: Simulations	68
IV.F: Determination of Ω_0	70
Chapter V: Discussion and conclusions	74
V.A: Discussion	74
V.B: Conclusions	79
Tables	81
Figures	124
Bibliography	165

LIST OF TABLES

Tables	81
Table 1: Unculled binaries, $\Omega_0 = 0.20$	82
Table 2: Unculled binary galaxies, $\Omega_0 = 0.20$	90
Table 3: Unculled binaries, $\Omega_0 = 0.03$	102
Table 4: Unculled binary galaxies, $\Omega_0 = 0.03$	109
Table 5: Effect of culling procedure on sample size	121
Table 6: Omega determination	122
Table 7: Velocity dispersion comparisons	123

LIST OF FIGURES

Figures	124
Figure 1: Projection geometry	125
Figure 2: Observable luminosity density function, H ₀ = 100	126
Figure 3: L vs ΔV , unculted binaries, $\omega = 0.2$	127
Figure 4: L vs R _p , unculted binaries, $\omega = 0.2$...	128
Figure 5: ΔV vs R _p , unculted binaries, $\omega = 0.2$	129
Figure 6: M/L vs R _p , unculted binaries, $\omega = 0.2$	130
Figure 7: M/L vs R _p , unculted binaries, $\omega = 0.03$	131
Figure 8: ΔV vs redshift, unculted binaries, $\omega = 0.2$	132
Figure 9: R _p vs redshift, unculted binaries, $\omega = 0.2$	133
Figure 10: L vs redshift, unculted binaries, $\omega = 0.2$	134
Figure 11: M vs redshift, unculted binaries, $\omega = 0.2$	135
Figure 12: M/L vs redshift, unculted binaries, $\omega = 0.2$	136

Figure 13: M/L vs redshift, unculted binaries, $\omega = 0.03$	137
Figure 14: M vs L, unculted binaries, $\omega = 0.2$	138
Figure 15: M vs L, unculted binaries, $\omega = 0.03$	139
Figure 16: M/L vs L, unculted binaries, $\omega = 0.2$	140
Figure 17: M/L vs L, unculted binaries, $\omega = 0.03$	141
Figure 18: Effect of cull on R_p , $\omega = 0.2$	142
Figure 19: Effect of cull on ΔV , $\omega = 0.2$	143
Figure 20: Effect of cull on M, $\omega = 0.2$	144
Figure 21: Effect of cull on M, $\omega = 0.03$	145
Figure 22: Effect of cull on L, $\omega = 0.2$	146
Figure 23: Effect of cull on L, $\omega = 0.03$	147
Figure 24: Effect of cull on M/L, $\omega = 0.2$	148
Figure 25: Effect of cull on M/L, $\omega = 0.03$	149
Figure 26: M vs L, binaries culled at 13.8, $\omega = 0.2$	150
Figure 27: M vs L, binaries culled at 13.4, $\omega = 0.03$	151
Figure 28: M/L vs R_p , binaries culled at 13.8, $\omega = 0.2$	152

Figure 29: M/L vs R_p , binaries culled at 13.4, $\omega = 0.03$	153
Figure 30: M/L vs L, binaries culled at 13.8, $\omega = 0.2$	154
Figure 31: M/L vs L, binaries culled at 13.4, $\omega = 0.03$	155
Figure 32: Binned projection factor, bin width = 0.01	156
Figure 33: Binned triangle distribution, bin width = 5	157
Figure 34: Binned exponential distribution, bin width = 5	158
Figure 35: Binned log normal distribution, bin width = 5	159
Figure 36: Delta function simulation, $\omega = 0.2$...	160
Figure 37: Triangle simulation, $\omega = 0.2$	161
Figure 38: Exponential simulation, $\omega = 0.2$	162
Figure 39: Log normal simulation, $\omega = 0.2$	163
Figure 40: ω --out as a function of ω --in	164

ACKNOWLEDGEMENTS

I would like to express my sincere appreciation to my colleagues in the Department of Physics for their willingness to allow me to participate in their classes as a student. I have certainly learned a great deal from them over the years, and their classes have been a source of much pleasure to me.

My deepest thanks go to David Hartwick. I never cease to be impressed by his intellectual power, as well as by his enthusiasm for astrophysics. He has been a constant source of inspiration to me. In addition, his patience, his personal humility, his humor, and his very warm human qualities are unsurpassed. I could not ask for a better friend.

CHAPTER I

INTRODUCTION

Assuming relativistic cosmology, a certain "critical" mean mass density is required in order to close the universe. If the actual mean mass density is less than the critical value, then the universe will expand forever. If the actual mean mass density is greater than the critical value, the universe will eventually collapse. See Weinberg (1972) for details. The ratio of the actual mean mass density to the critical value is frequently designated by Ω_0 . Thus, astrophysically, the actual mean mass density of the universe is one of the most fundamental empirical determinations which could be made. A determination of the mean mass density would immediately yield a value of Ω_0 and tell us the gross future history of the universe.

The following line of reasoning suggests that the mean mass density of the universe can be determined from a study of the galaxies. First we note that almost all of the electromagnetic radiation, particularly in the optical range, that we are able to detect seems to be associated with galaxies. Assuming that the mass of the universe is generally associated with the radiation, we naturally conclude that virtually all of the mass of the universe is associated with the galaxies. (If the mass were not associated with the radiation, then a "mass to light ratio" would be practically useless, perhaps on a par with the

ratio of the number of trees to the number of blades of grass in Canada.) Carefully note that the assumption that the mass of the universe is associated with the radiation is not equivalent to the assumption that all of the mass is radiative. All that is required is the assumption that the radiative matter is a reasonable tracer of all matter. It then follows that the galaxies are reasonable tracers of all matter. Galaxies are easily identified by their output in the optical portion of the spectrum. So, the mean luminosity density of the universe is relatively easy to determine from the observation of the galaxies. Thus a determination of the mean mass to light ratio (henceforth designated by M/L) of the galaxies would provide a determination of the mean mass of the universe.

Various techniques have been employed to determine the masses of galaxies and to determine a value for galaxy M/L . A really major problem is that there are serious discrepancies in the values for galaxy mass and M/L obtained by the different techniques. For an excellent review of the various techniques and the results obtained, consult Faber and Gallagher (1979). For convenience, we can divide techniques for galaxy mass determination into two major classes. We will use the terms "non-interactive" and "interactive" to refer to these two classes. By "non-interactive" we mean all those techniques which do not

utilize gravitational interaction among galaxies; some non-interactive techniques do use gravitational effects, but not gravitational effects involving more than one galaxy.

We count the following as non-interactive methods:

extrapolation from the mass to light ratio observed locally in the vicinity of our sun, applications of Boltzmann/hydrodynamical equations and test particles (stars, globular clusters, etc.), galaxy rotation curves, and the application of the virial theorem to elliptical galaxies. By "interactive" we mean those techniques which use gravitational interaction among galaxies to measure their masses. The two most frequently encountered interactive techniques are the analysis of binary galaxy systems and the application of the virial theorem to larger groups of galaxies.

A general trend has become clear: the larger the size of the system to which the technique is applied, the greater the value of M/L determined by the technique. For example application of the virial theorem to groups of galaxies gives M/L values much higher than those determined by other techniques. Dynamical analyses of binary galaxies yield M/L values smaller than those determined from large groups, but generally greater than those determined from the analysis of spiral galaxy rotation curves. And the values determined from spiral galaxy rotation curves are

generally greater than M/L values determined from extrapolating from the local material in our own galaxy.

This general trend has led to the now widely accepted view that a great deal of the matter in the universe is "dark", i.e., non-luminous. This dark matter is usually postulated to be dissipationless. That is, although subject to gravitational attraction, the dark matter does not dissipate energy through collisions, radiation, etc. It is supposed that initially the ordinary and dark matter are uniformly mixed. As "globs" of the mixed matter are formed through gravitational clumping, the associated luminous matter begins to dissipate energy and thus collapses, forming galaxies and groups of galaxies at the present epoch.

As general background, we assume a general theory of galaxy formation commonly known as hierarchical clustering--see Faber (1982), Peebles (1980), and White and Rees (1978). In its simplest terms, the over-all picture is quite easy to understand. It is assumed that the universe originated in a "Big Bang" and continues to expand, corresponding to a Friedmann model. It is further assumed that the distribution of matter in space is primarily affected only by cosmological expansion and by gravitationally induced clumping.

For example, consider two isolated particles at rest

relative to each other at some proper time t_0 . At some later time t , the separation between the two particles will tend to be increased by the general cosmological expansion; at the same time, this increase in separation will be countered by the tendency of the two particles to move toward each other as a result of their mutual gravitational attraction. If the gravitational attraction between two particles is sufficiently great to overcome the cosmological expansion, the particles will form a "bound" system and eventually clump together, forming a "particle" whose mass is the sum of the masses of the original two. Since the gravitational attraction between particles is an increasing function of the masses of the particles, bound systems of particles will tend to grow, "sweeping up" nearby particles.

Because gravitational forces depend on mass and particle separation, at each (reference) point in time there is a certain minimum "local" density required in order for a collection of particles to become gravitationally bound against the universal expansion by some specified later time. The time between the reference point and the point at which the particle collection of interest ceases to expand is called the "turn around" time for that collection. Obviously, the greater the density of the collection and the smaller the rate of cosmological

expansion at the reference time, the shorter the time to turn around will be.

If all particles were identical in all physical respects, initially at rest, and uniformly distributed at equal distances from each other, we would get an expanding (or contracting) lattice. But such a picture is unreasonable on thermodynamic grounds. Of course, in general the motions of the particles will be the result of their "initial" velocities, the cosmological expansion factor, and the force of gravitational attraction, as well as collisions, radiation, and a host of other effects.

The over-all picture is that due to gravitational clumping, "primordial" density fluctuations grow by the present epoch to form objects the size of galaxies or groups of galaxies; these galaxies and groups of galaxies are composed of luminous matter (the visible portion of the galaxies) imbedded in halos of dark matter. Further gravitational clumping has formed objects the size of clusters, etc. A gravitationally bound collection of galaxies may be swimming in a "soup" of dark matter. This soup may be either the primordial blob out of which the constituent galaxies of the collection condensed or it may be a merger of the dark matter "halos" of the constituent members.

This simple picture can easily account for the fact

that mass to light determinations based on larger systems are generally larger than mass to light determinations based on smaller systems. The greater the size of the system over which a mass determination is made, the higher the ratio of dark to luminous matter, so the greater the value obtained for M/L. Rotation curves and analyses based on Boltzmann equations measure the mass of systems with radii on the order of several tens of kpc. Binary galaxy systems typically have radii on the order of several hundreds of kpc. The virial theorem applied to groups of galaxies will measure the mass of systems with typical radii of several Mpc. So, if we postulate the existence of very large amounts of dark matter, in halos perhaps as large as groups of galaxies (the large halo hypothesis) then the substantial increase in the values obtained for M/L with increasing system size is easily explained.

It is important to recognize that the amount of dark matter postulated is crucial. If the dark matter exists in halos surrounding galaxies but only on the order of at most several times the size of a galaxy (the small halo hypothesis), then one would expect to find values for M/L increasing as one moves from local extrapolation to rotation curve analysis or to a Boltzmann type analysis at large galactic radii. But under the small halo assumption, one may not find any further increase in the transition

from non-interactive to interactive techniques; at least one should not find any difference in the values of M/L as determined by binary studies and as determined by the virial analysis of groups. So, the dark matter hypothesis is quite robust, in the sense that an adjustment in the amount of dark matter postulated can accommodate substantially different empirical findings.

There are many problems associated with the simple dark matter - hierarchical clustering picture. From our point of view, one of the most important difficulties concerns the determination of Ω_0 . As noted above, one can use a value of M/L to determine a value for Ω_0 . An independent value of Ω_0 may be obtained by nucleosynthesis considerations. See Yang *et al.* (1984) for a survey of techniques and recent results. To date, values of Ω_0 computed from M/L values determined by interactive techniques are significantly greater than values of Ω_0 computed on the basis of nucleosynthesis studies. Unless the dark matter is postulated to be non-baryonic, either the nucleosynthesis work must be incorrect or the analyses based on interactive techniques must be incorrect.

There is at least one very serious difficulty with galaxy M/L determinations based on interactive techniques which could account for the discrepancy with the nucleosynthesis work. In order to obtain reasonable results

from the mathematics of binary dynamics or from the virial theorem applied to larger collections, we must first be able to identify systems of galaxies that are (i) gravitationally bound, (ii) virialized, and (iii) dynamically isolated. For example, consider an arbitrary pair of galaxies. If the galaxies are not gravitationally bound, then in general we cannot use the mathematics of binary orbits to determine the mass of the pair. If the pair is not virialized, then the two galaxies have not settled into an equilibrium configuration to which various statistical treatments would correctly apply. And finally, if the pair is not isolated from perturbing influences, then at the very least, the center of mass of the pair cannot be assumed to be moving uniformly under the influence of just the Hubble flow, and thus our determinations of projected radial separation and absolute luminosity may be greatly in error; and at worst, the pair may not be behaving as a binary system at all, but rather as part of a larger, more complicated ensemble.

One of the major problems addressed by this thesis is the development of simple, intuitively plausible criteria which may be collectively used as the basis of a technique for the identification of gravitationally bound, virialized, dynamically isolated systems of galaxies on the basis of available observational parameters. We have

applied the technique to the CfA redshift survey, Huchra et al. (1983), and have obtained a new list of galaxy groups. We have concentrated attention on the analysis of the binary systems, leaving the analysis of the larger groups for a later time.

One apparent drawback with our technique for galaxy group identification is that it requires the input of three crucial parameters. (i) One parameter is the absolute magnitude limit of the brightest possible galaxy. This parameter can be reasonably estimated from fairly secure observational data. It should be noted that the value of this parameter may change with a change in the value of the Hubble constant H_0 . However, as we will report below, our results depend very little on this parameter. (ii) Another required input parameter is the value of H_0 . The value of H_0 is input only as a convenience in the program. We will show, both experimentally and theoretically, that except for the small dependence in the magnitude parameter mentioned above, our results are independent of H_0 ; thus some arbitrary indicative value could be used. (iii) The last parameter is the value of Ω_0 . As will become obvious, the results obtained using our technique depend crucially on the value of this parameter.

There are a number of advantages which may be claimed for our technique. First, it is totally objective. Once the

initial parameters are selected, there is no point at which individual judgement can intervene. All groups are treated exactly alike; group membership does not depend on whether or not the collection appears to be a group to some observer. In addition, there is a dependence on only two parameters, only one of which (namely Ω_0) is really crucial. Further, the dependence on that crucial parameter is totally transparent, which has not always been the case with other group-finding routines. For example, any galaxy group finding technique which makes use of criteria based on relative isolation or density enhancement obviously has a covert dependence on Ω_0 , as well as perhaps on H_0 .

It may appear at this point that our technique cannot be used as a basis to obtain an independent value for Ω_0 , since an input value of Ω_0 is required. However, there is a way around this seeming difficulty. We have used the binary systems for a given input value of Ω_0 to determine a value for M/L and thus a computed value for Ω_0 . That is, we have treated our technique as a "black box function", which computes a value of Ω_0 as a function of an input value of Ω_0 .

$$\Omega_{0\text{out}} = \text{BBF}(\Omega_{0\text{in}})$$

We then adjusted the input value of Ω_0 until it agreed with

the computed value. That is, we simply applied a self-consistency criterion. It is interesting to note that our value of Ω_0 so derived is in good agreement with the value obtained from nucleosynthesis studies.

Of course underlying our application of the self-consistency analysis to the binary data is the assumption that the true distribution in M/L is reasonably sampled by the dynamics of the binary systems. This assumption may be questioned, particularly in light of the large halo hypothesis discussed above. Perhaps a more adequate approach would be to apply the self-consistency analysis for Ω_0 to the groups determined by our technique. However, that approach would also involve a major assumption, namely that the true distribution in M/L is reasonably sampled by the dynamics of larger groups. Many will view this latter assumption as less problematic than the corresponding assumption concerning the binaries. Nevertheless, just as with the binary assumption, it is always possible that dark matter halos extend for a considerable distance well beyond the boundaries of the groups.

At the very least, we hope to have demonstrated the feasibility of our group-finding technique and of the related self-consistency analysis. Further, even if the large halo hypothesis is correct, our analysis of the binary systems provides a lower bound on the value of M/L

and hence a lower bound on the value of Ω_0 . And, what is perhaps most important of all, we have demonstrated the crucial role that the assumed value of Ω_0 plays in any attempt to identify gravitationally bound, dynamically isolated, virialized systems of galaxies. We suggest that there is no way to identify such systems that is independent of Ω_0 . If our suggestion is correct, then a self-consistency sort of analysis is the only way to use binaries and larger groups to determine Ω_0 .

We now turn our attention to a few words about the notation used in this thesis. We have used subscripts and a few special symbols to make the reading of equations easier. In all cases, special notation will be defined in the text. We use the notation " $\sqrt{\quad}$ " to indicate the extraction of roots. Frequently a numerical superscript will be used to indicate the root. Thus " $^3\sqrt{(M_1 + M_2)}$ " should be taken to represent the cube root of the quantity $M_1 + M_2$. In other cases, normal mathematical notation will be employed, where possible, including superscripts to indicate exponentiation.

Chapter II

The Theory of Finding Groups

II.A: The catalog requirements

Henceforth, we will apply the term "group" to collections of galaxies which are gravitationally bound, virialized, and reasonably dynamically isolated. Before presenting the details of the group finding algorithm, it is first necessary to discuss the data set requirements for which the algorithm was designed. As a matter of fact, the algorithm was designed specifically for the CfA redshift survey, as given in Huchra et al. (1983). However, our algorithm is not limited to this one catalog but is applicable to any catalog sharing certain characteristics with the CfA survey. In particular, we assume that the catalog is a magnitude limited sample, with known apparent magnitude limit m_{lim} . The solid angle θ_c covered by the catalog must also be known. For each galaxy in the catalog, we require the following information: an angular position given as right ascension and declination, a redshift velocity with associated error estimate, and an apparent magnitude. Morphological information was not used in the group finding algorithm.

II.B: The general framework algorithm

In some elementary respects, the general framework of our technique for finding groups of galaxies is similar to that used by Huchra and Geller (1982) and to that used by Press and Davis (1982). The catalog of galaxies being examined is first partitioned (in the mathematical sense of "partition") according to a general "companionship" scheme. We begin by considering all possible pairs of galaxies from the galaxy catalog. Each pair is analyzed according to a set of "primary" companionship criteria; each partition class is completed by iteratively adding companions of companions. For later convenience, we refer to this portion of our group finding algorithm as "pass one." Our companionship criteria differ from those of both Huchra and Geller (1982) and Press and Davis (1982) and will be discussed in detail in the next sections.

The framework of our group finding procedure differs from that of Huchra and Geller (1982) in one very important respect. They took groups to be the partition classes determined by the companionship scheme applied to just the original catalog (what we have called pass one). However, such an approach ignores possible higher-order clumping which might occur among groups themselves or between groups

and individuals. Without taking into account such higher-order clumping, one cannot ensure that the groups obtained are dynamically isolated. Thus our algorithm involves two additional steps, which we refer to as "pass two" and "pass three." Press and Davis (1982) do include an additional step to try to pick up individual galaxies captured by a group, but the criterion employed is simple closeness (add galaxies that fall within one rms radius of the group), and does not involve their original companionship criterion; and they completely ignore group-group clumping.

For both pass two and pass three, a list of pseudo-galaxies is formed corresponding to the characteristics of the groups. The parameters for a pseudo-galaxy include the number of galaxies in the group, a (luminosity weighted) center of mass position given as right ascension and declination, an harmonic radius, a (luminosity weighted) redshift, and an apparent magnitude. In pass two, we apply the iterated companionship technique to pairs of pseudo-galaxies. If any new companions are found, we merge the groups involved, form new pseudo-galaxies and repeat the procedure. We continue the process until no further changes are found. In pass three, we take the updated pseudo-galaxies from pass two and compare every pseudo-galaxy with every galaxy from the original catalog which is not already in the group corresponding to the given pseudo-

galaxy. Any isolated galaxy found to be a companion of a group is added to the group; if a member of one group is found to be a companion of another group, then the two groups are merged. If any new companions are found during pass three, then a new pseudo-galaxy list is formed and we return to pass two. We continue cycling through pass two and pass three until no further changes occur.

In practice, our algorithm works by maintaining a "galaxy companion list." The galaxy companion list is just a list of ordered pairs of integers $\langle i, j \rangle$, where i and j are the ordinal numbers of galaxies in the galaxy catalog (j may be 0, as explained below). For each galaxy i , there will be one and only one pair $\langle i, j \rangle$ on the galaxy companion list. Thus it is perhaps easier to think of the galaxy companion list as a function, which we can write as $C(i) = j$. We will henceforth use the phrases "galaxy companion list" and "galaxy companion function" interchangeably. Each partition class (galaxy group) will be indexed by the first galaxy in the class, i.e., by the smallest ordinal number corresponding to a galaxy in the class. For example, an entry $C(92) = 8$ on the galaxy companion list says that galaxy number 92 belongs to a group whose first member found was galaxy number 8.

The galaxy companion function is initialized for each galaxy i by setting $C(i) = 0$, indicating that galaxy number

i has not yet been found to be a member of any group. Updating the galaxy companion function is very simple and could be done by considering a multitude of cases. However, the following easily stated procedure will clearly do the job. Suppose galaxies m and n are found to be companions. Take m^* to be m if $C(m) = 0$ and let it be $C(m)$ if $C(m) \neq 0$; define n^* similarly. Then to update the galaxy companion function, we step through all the galaxies and for each i , if $C(i) = \max(m^*, n^*)$ we set $C(i) = \min(m^*, n^*)$; and if either $C(m)$ or $C(n)$ is 0, we set both to $\min(m^*, n^*)$.

When a list of pseudo-galaxies is formed, we keep a corresponding "first member function" $F(i) = j$, which stores the information that galaxy number j is the first member of pseudo-galaxy (group) number i . Using the first member function, it is an easy matter to update the galaxy companion function when two pseudo-galaxies, say those with ordinal numbers m and n , are found to be companions. For each galaxy i , if $C(i) = \max(F(m), F(n))$ then we set $C(i) = \min(F(m), F(n))$; and we set $F(m)$ and $F(n)$ to be $\min(F(m), F(n))$ so that if additional pseudo-galaxy companions are found, the subsequent update of the galaxy companion function will be done correctly.

Similarly, we may easily update the galaxy companion function when a galaxy, say number k , is found to be a

companion of pseudo-galaxy number m . The two main cases to consider are $C(k) = 0$ and $C(k) \neq 0$. First, suppose $C(k) = 0$; that means that galaxy k was not a member of any group. If $F(n) \angle k$, we just set $C(k) = F(n)$; otherwise for each galaxy i , if $C(i) = F(n)$ we set $C(i) = k$, and we set both $C(k)$ and $F(n)$ to be k . On the other hand, suppose $C(k) \neq 0$; that means that galaxy k was a member of another group. Let r be $\min(C(k), F(m))$ and let s be $\max(C(k), F(m))$. For each galaxy i , if $C(i) = s$, we set $C(i) = r$; and if $C(k) \angle F(m)$, we set $F(m) = C(k)$.

Abstracting from these details, the general framework algorithm is quite easy to follow. We state it in the following six simple steps:

1. (pass one) For each pair of galaxies, i and j , see if i and j are companions. If so, then update the galaxy companion list. When finished, go to step 2.
2. Use the galaxy companion list to form a list of pseudo-galaxies. Go to step 3.
3. (pass two) For each pair of pseudo-galaxies, m and n , see if m and n are companions. If so, then update the galaxy companion list. When finished, go to step 4.

4. If step 3 resulted in any changes in the galaxy companion list, then go to step 2; otherwise go to step 5.
5. (pass three) For each pair consisting of a pseudo-galaxy m and a galaxy i not a member of m , check to see if m and i are companions. If so, then update the galaxy companion list. When finished, go to step 6.
6. If step 5 resulted in any changes in the galaxy companion list, then go to step 2; otherwise halt.

We wish to emphasize again that pass two and pass three are necessary to help ensure that the groups found are in fact reasonably dynamically isolated from other objects in the catalog.

II.C: The companionship criteria

Our companionship criteria amount to a particular application of what is sometimes called the "hypothetico-deductive method." The general scheme is to initially hypothesize that the two objects in question (two galaxies, two groups, or a galaxy and a group) do constitute a gravitationally bound, virialized system. On the basis of this hypothesis, a number of consequences are derived. If

any of the consequences are at odds with physical theory then we reject the hypothesis. If all of the consequences are consistent with physical theory, then we cannot reject the hypothesis.

In short, for each pair of objects, we are trying to determine whether or not there is a consistent interpretation of the observational data under which the pair may be regarded as gravitationally bound and virialized. As we will show below, the tests we employ are all quite conservative, in the sense that if a pair really is a bound, virialized system, then in general our criteria will all be satisfied.

At the beginning of our routine, the user is asked to supply three input parameters for use in the companionship criteria: (i) the absolute magnitude of the theoretically brightest possible galaxy, (ii) the value of H_0 , and (iii) the value of Ω_0 . We employ three distinct criteria, which we call (c.1) the brightest galaxy criterion, (c.2) the escape velocity criterion, and (c.3) the density criterion.

II.C.1: The brightest galaxy criterion

The intuitive idea behind the brightest galaxy criterion is that the calculated brightness of a galaxy

must not be beyond the range of that of the theoretically brightest possible galaxy. Hence, our first criterion requires the specification of a theoretical limit on the brightest possible galaxy. The user could have been asked to supply such a limit as either an absolute luminosity or an absolute magnitude; we have arbitrarily chosen to request an absolute magnitude value, M_{\max} . The value of M_{\max} supplied is assumed to be from the same band width as the apparent magnitudes given in the catalog. The basic idea is that if we assume that two objects are bound, we can then compute their true distance, from which we can compute their true absolute magnitudes. If both objects are single galaxies, then we just need to check to see if either absolute magnitude would have to be outside the theoretically permissible range. If either of the objects is a group, then we could convert the absolute magnitude to a luminosity, divide by the number of objects in the group to get a mean luminosity, and then convert back to an absolute magnitude to make the comparison.

Since our other criteria require computation of the absolute luminosity of the two objects, we actually convert M_{\max} to a maximum absolute luminosity L_{\max} and compare luminosities rather than magnitudes. We use the following equation to convert absolute magnitudes to absolute luminosities in solar units:

$$(1) \quad L/L_{\odot} = 10^{(.4 \times (M_{\odot} - M))}$$

Since we will always be using solar units when speaking of luminosity, we will henceforth write "L" instead of "L/L_⊙".

Let the two objects being considered be designated by 1 and 2, with redshift velocities V_1 in km/s, and apparent magnitudes m_1 . If the two objects really are gravitationally bound, then they are at approximately the same redshift distance. Assuming that mass goes roughly as luminosity, we calculate a luminosity weighted redshift for the pair. First we calculate an indicative luminosity l_1 for each object:

$$(2) \quad l = 1 / 10^{(.4 \times m)}$$

The luminosity weighted pair redshift velocity is then given by:

$$(3) \quad V_{12} = ((l_1 \times V_1) + (l_2 \times V_2)) / (l_1 + l_2)$$

If equation (3) yields a value less than 300, then we set $V_{12} = 300$. The distance to an object with redshift velocity V can be easily calculated from the relation:

$$(4) \quad d = V / H_0$$

Generally H_0 is given in units of km/s/Mpc, and V is given in units of km/s; under these circumstances, d will be in units of Mpc. For d in Mpc, the absolute magnitude M_1 of each object can be calculated using:

$$(5) \quad M = m - 25 - 5 \log d$$

As discussed above, we convert the absolute magnitudes M_1 to absolute luminosities L_1 in solar units using equation (1). For each composite object (group) i , we have the number n_1 of galaxies making up the object; for single galaxies, we set $n_1 = 1$. What we have called our brightest galaxy criterion thus amounts to the following requirement for each object:

$$(6) \quad L_1 \leq n_1 \times L_{\max}$$

It can easily be seen from (1-5) that for fixed values of the m_1 , the values of L_1 are proportional to H_0^{-2} . For example, if we halve the value of H_0 , then the calculated values of the L_1 will be larger by a factor of 4, and hence (6) will be more easily violated. Thus, unless the theoretical value M_{\max} is adjusted to be an appropriate

function of H_0 , the brightest galaxy criterion will be a function of H_0 .

II.C.2: The escape velocity criterion

Our second criterion is based on the fact that if two objects are moving in a gravitationally bound orbit about their center of mass, then their relative velocity at a given separation cannot exceed the escape velocity at that separation. And the escape velocity at a given separation is just the square root of two, times the velocity needed to maintain a circular orbit with the given radius. Thus, we have the familiar inequality:

$$(7) \quad V_{rel} \leq \sqrt{2 \times G \times (M_1 + M_2) / R_{12}}$$

Of course G is the gravitational constant, V_{rel} is the true relative velocity between the two objects, R_{12} is the true separation between the two objects, and the M_i represent the masses. One major problem in the application of (7) to galaxies is that we have no way of unambiguously determining the values of V_{rel} , R_{12} , and the M_i . We will address these factors one at a time.

First we consider the relative velocity term. If we hypothesize that the two objects under consideration really

are gravitationally bound, we can in general obtain a good approximation of their relative velocity in the radial direction by using the difference ΔV in their given radial velocities.

$$(8) \quad \Delta V_{12} = |V_1 - V_2|$$

We propose to use ΔV_{12} in place of V_{rel} in (7). Of course (8) is only an approximation due to the finite angular separation between the two objects. We could define two distinct radial relative velocities using:

$$(9) \quad \Delta V\langle ij \rangle = |V_i - V_j \times \cos \theta|$$

where θ is the separation angle between i and j . In general, $\Delta V\langle 12 \rangle$ will not be the same as $\Delta V\langle 21 \rangle$, and neither will equal ΔV_{12} . For large values of θ , the differences may be quite substantial; however, for values of θ less than a few degrees, the differences will be negligible. We will return to this point below.

At this point, it is important to note that ΔV_{12} always underestimates at least one of the values $\Delta V\langle ij \rangle$, and in some cases, it is smaller than both. (For example, for values of θ greater than $\pi/2$, ΔV_{12} will be smaller than both values for $\Delta V\langle ij \rangle$.) Further, the relative velocity in

one dimension is clearly a lower bound for the true relative velocity. Thus, using ΔV_{12} in place of V_{rel} in (7) is conservative, in the sense that no pair that is really bound would violate the resulting condition.

We now turn our attention to the separation between the two objects, R_{12} . Since we cannot know the true value of R_{12} , we propose to use instead a projected separation $R_{p,12}$, to be defined shortly. Of course, the projected separation will be a lower bound for the true separation. Thus, once again it is clear from (7) that using the projected separation instead of the true separation is conservative, in the sense that no pair that is truly bound would be ruled out.

We now need to define the projected separation between two arbitrary objects. We begin by a determination of the angular separation Θ_{12} between the two. Let the right ascension and declination of each object be represented by α_1 and δ_1 , respectively. Then the angular separation between the two objects is given by the usual relationship from spherical trigonometry:

$$(10) \quad \Theta_{12} = \cos^{-1} \left((\sin \delta_1 \times \sin \delta_2) + (\cos (\alpha_2 - \alpha_1) \times \cos \delta_1 \times \cos \delta_2) \right)$$

For very small separations, the following plane triangle

approximation is often useful in overcoming round-off errors:

$$(11) \quad \Theta_{12} = \sqrt{(\bar{d}_2 - \bar{d}_1)^2 + ((\alpha_2 - \alpha_1) \times \cos \bar{d}_2)^2}$$

As we stated above, if we hypothesize that the two objects under consideration do form a bound system, then we can use V_{12} , defined in equation (3), as an estimator of the true redshift distance. We propose to use the angular separation of the pair and the redshift distance of their center of mass to calculate an estimated projected separation. There are a number of alternatives, the differences being quite negligible for the range of variables which will be of interest to us. Our adopted technique is to assume that the midpoint of the projection of a line joining the two objects is at the distance of the center of mass. Then the geometry of the situation dictates that the projected separation is given by:

$$(12) \quad R_{p.12} = 2 \times V_{12} \times \sin(\Theta_{12} / 2) / H_0$$

We are still left with the troublesome mass terms in the initial statement of the escape velocity criterion (7). Our technique is to use the luminosity as an indicator of mass. We begin by using the mass to light ratio to replace

the sum of the masses by the sum of the luminosities:

$$(13) \quad M_1 + M_2 = (L_1 + L_2) \times M/L$$

Under the assumption that the two objects are gravitationally bound, we have already calculated the values of the L_1 using (1-5). The value of M/L could be obtained from the appropriate densities, which we represent by ρ with corresponding subscripts:

$$(14) \quad M/L = \rho_{M.\text{mean}} / \rho_L$$

Since Ω_0 is just the ratio of the mass density to the well-defined "critical" density, we can determine the mass density from Ω_0 :

$$(15) \quad \rho_{M.\text{mean}} = (3 \times \Omega_0 \times H_0^2) / (8 \times \pi \times G)$$

The only remaining term to be determined is the luminosity density ρ_L . Since we know the solid angular coverage of the catalog, we could use the catalog to compute a mean luminosity density. But such an approach would be grossly in error. The legitimacy of the shift from the sum of the masses to the sum of the luminosities in (13) depends on treating M/L as mass to observed

luminosity. The point is subtle, but quite important. If we just naively used a constant value for M/L , we would be able to show a sharp fall-off of mass with increasing redshift. That is, we would be committed to the absurd result that there is substantially more mass close to us than far away, a result that directly violates the cosmological principle! Obviously the problem is that with a magnitude limited sample, the luminosity density falls off with increasing redshift. Thus we need to make luminosity density a function of redshift.

Using equations (4-5), for any given redshift we can compute from the apparent magnitude limit of the catalog the absolute magnitude of the faintest galaxy observable at that redshift. So, instead of making luminosity density a function of redshift, we can equivalently make luminosity density a function of the limiting observable absolute magnitude at the given redshift. We can derive the desired function directly from the catalog.

For the purposes of deriving the catalog luminosity density function, we treat the redshift velocity of each galaxy as though it were pure Hubble flow, and we compute the corresponding absolute magnitude M_i and luminosity L_i of the galaxy using equations (1,4, and 5). Using the apparent magnitude limit of the catalog and the absolute magnitude of the galaxy, we can also use (5) to compute a

value of $d_{\max.i}$, the maximum distance at which the galaxy would still be observable. We consider the luminosity of each galaxy to be distributed uniformly in a sphere of radius $d_{\max.i}$, of which only that portion determined by the solid angular coverage θ_c of the catalog contributes to the total. If the solid angular coverage of the catalog is given in steradians, then the required luminosity density function is given by:

$$(16) \quad \rho_L(M) = \sum_{M_1 \leq M} (3 \times L_i) / (\theta_c \times d_{\max.i}^3)$$

That is, the luminosity density, at a redshift corresponding to a limiting observable absolute magnitude M , is just the sum of the contributions to the luminosity density made by galaxies in the catalog which would be observable at that redshift. Our technique here for dealing with the faint galaxy problem is effectively the same mathematically as that used by Huchra and Geller (1982), although their presentation is a bit different from ours.

Thus far in the discussion, we have treated all objects as point masses. While that is appropriate for galaxies, it will not be appropriate for groups. One particle orbiting the center of a spherical cloud of particles is dynamically affected only by the mass of particles within its orbital radius. Consequently, there may be cases in which the mass

terms in (7) must be scaled by an appropriate fraction. Given (13), we accomplish the same effect by scaling the luminosity terms. In order to compute an appropriate scale factor, we define a characteristic radius for each group. There are various ways a characteristic radius could be defined (e.g., mean pair-wise separation). Since we are using the radius in a dynamic context, we calculate an harmonic radius that would be appropriate for the virial theorem. For each group i , with n_i members, we compute the harmonic angular radius $\theta_{h,i}$ from the angular separations θ_{jk} of all pairs of group members, j and k , using the following equation:

$$(17) \quad \theta_{h,i} = n_i^2 / \sum_{j,k} (1 / \theta_{jk})$$

Note that in (17), each physical pair gets counted twice, once by θ_{jk} and once by θ_{kj} . For single galaxies, we define the harmonic angular radius to be 0. Now, suppose we are considering an arbitrary pair of objects, 1 and 2, which may both be galaxies, both groups, or a galaxy and a group. Then we may assign to each a scale factor S_i based on the angular separation of the two objects, as follows:

$$(18) \quad S_1 = 1 \quad \text{if } \theta_{h,1} \leq \theta_{12}$$

$$= (\theta_{12} / \theta_{h,1})^3 \quad \text{if } \theta_{h,1} > \theta_{12}$$

We simply multiply the luminosities in (13) by the appropriate scale factors.

We are now in a position to state our escape velocity criterion. For convenience in writing out the criterion, we first square both sides of (7) and then make the substitutions discussed above.

$$(19) \quad \Delta V_{12}^2 \leq \frac{3 \times \Omega_0 \times H_0^2 \times ((S_1 \times L_1) + (S_2 \times L_2))}{4 \times \pi \times R_{p.12} \times \rho_L(M_{lim})}$$

From equations (1,4, and 5), it is clear that L is proportional to H_0^{-2} , and hence the numerator of (19) has no H_0 dependency. Having noted the relation between L and H_0 , equations (4 and 16) guarantee that $\rho_L(M_{lim})$ is proportional to H_0 . But (12) assures us that $R_{p.12}$ is proportional to H_0^{-1} . Hence there is no H_0 dependency in the denominator of (19) either. So our escape velocity criterion is independent of H_0 and depends only on Ω_0 .

II.C.3: The density criterion

The last criterion we will employ concerns the minimum mass density for gravitationally bound, virialized groups. The intuitive idea is that the internal density of a

gravitationally bound, virialized region must be sufficiently greater than that of the background for the region to have stopped expanding with the Hubble flow and to have become virialized by the present epoch.

Consider a small region of space, and let χ represent the density enhancement, i.e., the ratio of the internal mass density of the region to the mean background mass density. Recall from the hierarchical clustering model that if a region is sufficiently overdense, then gravitation will eventually overcome the Hubble expansion, at which point the region will stop expanding and begin to collapse. For values of $\Omega_0 < 1$, Gott and Rees (1975) derive the following criterion for the minimum density enhancement required in order for a region to be gravitationally bound in virial equilibrium at present cosmic time t_0 :

$$(20) \quad \chi = (18 \times \pi^2) / (\Omega_0 \times H_0^2 \times t_0^2)$$

We use the following equation from Weinberg (1972) to compute the present cosmic time:

$$(21) \quad t_0 = H_0^{-1} \times [(1-\Omega_0)^{-1} - (\Omega_0/2) \times (1-\Omega_0)^{-3/2} \times \cosh^{-1}((2/\Omega_0)-1)]$$

So, for a pair of objects, say 1 and 2, we can express a restriction on the mass density $\rho_{M.12}$ determined by the pair and the mean background mass density.

$$(22) \quad \rho_{M.12} \geq \rho_{M.mean} \times X$$

Once again, we must deal with a mass term, and we use the same technique discussed above in the circular velocity criterion. We relate the mass density $\rho_{M.12}$ of a pair to the luminosity density $\rho_{L.12}$ of the pair.

$$(23) \quad \begin{aligned} \rho_{M.12} &= \rho_{L.12} \times M/L \\ &= \rho_{L.12} \times \rho_{M.mean} / \rho_L(M_{lim}) \end{aligned}$$

Putting (22) together with (23) gives:

$$(24) \quad \rho_{L.12} \geq \rho_L(M_{lim}) \times X$$

Thus we can actually replace the mass density restriction with a restriction on the luminosity density.

To compute the luminosity density, we assume that the luminosity is distributed within a sphere whose radius is the separation between the two objects. Since we do not know the true separation between two objects, we use the projected separation $R_{p.12}$ defined in (12). To obtain the

total luminosity, we must again worry about the case when one or both of the objects are groups. As before, we use the scale factors defined by (18). Hence, we can compute the luminosity density determined by a pair as follows:

$$(25) \quad \rho_{L.12} = \frac{3 \times ((S_1 \times L_1) + (S_2 \times L_2))}{(4 \times \pi \times R_{p.12}^3)}$$

Obviously density is inversely proportional to the cube of the radius. Hence, using the projected separation means that our density criterion is conservative in the sense that any pair that is really gravitationally bound would satisfy our restriction.

We now turn our attention to the H_0 dependency. Since the L_i are proportional to H_0^{-2} and $R_{p.12}$ is proportional to H_0^{-1} , we know from (25) that $\rho_{L.12}$ is proportional to H_0 . From our previous discussion, we know that $\rho_L(M_{lim})$ is proportional to H_0 . Equations (20 and 21) guarantee that X is independent of H_0 . Thus, our restriction (24) is independent of H_0 .

Finally we return to our approximation (8) for the relative velocity in the radial direction for the pair of objects under consideration. We noted that for small values of angular separation θ_{12} , ΔV_{12} is a good approximation to the radial component of the relative velocity; however, for

larger values of angular separation, the true value may differ substantially from our approximation. For example, suppose $V_1 = V_2$; if $\theta_{12} = \pi$, then $\Delta V_{12} = 0$, whereas the true value would be $2 \times V_1$. So there is no upper limit on the size of the potential error. Our escape velocity criterion (19) provides no restriction for the case $V_1 = V_2$. However, as θ_{12} increases, the projected separation $R_{p,12}$ defined in equation (12) also increases. But from (25), we know that the luminosity density of the pair is inversely proportional to the cube of the projected separation. Consequently, our density criterion (24) will legitimately rule out pairs with very large angular separation.

Chapter III

Binary Galaxies

III.A: Binary samples

Once the general group finding techniques described in the previous chapter have been applied, the galaxy connection function can trivially be used to obtain a list of those groups which have only two members. As discussed previously, all the groups will be gravitationally bound, they will be dynamically isolated from each other and from the remaining single galaxies in the catalog, and they will be virialized. Consequently, the sub-sample of binaries will also share these properties. As already noted, each binary sample will be independent of H_0 , being a function of only the input value of Ω_0 and the value for the theoretically brightest galaxy. We will use the binary samples so obtained to compute mean values for M/L corresponding to a range of values for Ω_0 . We will then use the self-consistency technique to obtain a best value for Ω_0 .

III.B: Binary calculations

From the dynamics of binary systems, we know that the sum of the masses of a bound pair is given by:

$$(26) \quad M_1 + M_2 = V_{rel}^2 \times R_{12} / G$$

The true values of V_{rel} and R_{12} cannot be determined for a binary galaxy system. Consequently, in our study of binary galaxies, we are limited to statistical techniques. In particular, we hope to use mean values from a large binary sample to estimate the true value of M/L .

As before, we replace V_{rel} by ΔV_{12} , defined by (8), and we replace R_{12} by $R_{p.12}$, defined by (12). From the observations, we can then obtain an "observed" value of M/L for the pair from the absolute luminosities calculated on the basis of the redshift determined by the pair.

$$(27) \quad (M/L)_{o.12} = \frac{\Delta V_{12}^2 \times R_{p.12}}{G \times (L_1 + L_2)}$$

We wish to find the mean value of M/L as given in (27) for our binary sample. However, if there are known errors ϵ_1 in the observed radial velocities V_1 , then statistically speaking, (27) will be a biased estimator. The corrected

estimator is given by the following:

$$(28) \quad (M/L)_{c.12} = \frac{(\Delta V_{12}^2 - \epsilon_1^2 - \epsilon_2^2) \times R_{p.12}}{G \times (L_1 + L_2)}$$

In actual applications, these "corrected" values will in some cases be negative and hence have no physical significance. Further, the statistical characteristics of the corrected values will not in general be the same as the statistical characteristics of the uncorrected values. The corrected values will have a lower mean but a higher standard deviation. However, the mean of the corrected values will in general be a better estimate of the true mean of the population than will the mean of the uncorrected values. Of course if the errors are all 0, then (27) and (28) coincide.

Because of projection effects, ΔV_{12} and $R_{p.12}$ will underestimate V_{rel} and R_{12} , respectively. Figure 1 gives the geometry of the situation. It is easy to see that the following relationships hold, where in all cases we are interested only in the absolute values:

$$(29) \quad R_{p.12} = R_{12} \times \sin \theta$$

$$(30) \quad \Delta V_{12} = V_{rel} \times \sin \phi \times \sin \theta$$

$$(31) \quad 0 \leq \theta \leq \pi/2$$

$$(32) \quad 0 \leq \phi \leq 2\pi$$

Hence, we immediately have:

$$(33) \quad (M/L)_{o.12} = f \times (M/L)_{t.12}$$

where we use "f" to represent the projection function, we use the subscript "o" to represent the value of M/L computed from "observed" quantities, and we use the subscript "t" to represent the true value of M/L. The projection function f is given by:

$$(34) \quad f = \sin^2 \phi \times \sin^3 \theta$$

As before, we must worry about the statistical bias introduced by the square of the error terms in the values of the V_i . If we intend to use mean values, then instead of simply taking the mean of both sides of (33), it is more appropriate to use the following, where angular brackets denote mean values:

$$(35) \quad \langle (M/L)_{c.12} \rangle = \langle f \times (M/L)_{t.12} \rangle$$

III.C: Variable interrelationships

In our discussion of our three criteria, we have already noted that the escape velocity criterion and the density criterion are both independent of H_0 . Further, it is obvious that neither depends on the input value of the absolute magnitude of the brightest possible galaxy. Thus both of these criteria depend only on the value of Ω_0 . The only possible dependency on H_0 is in the brightest galaxy criterion, and that dependency can trivially be removed by appropriately scaling the input parameter with change of H_0 value. In actual experiments with the CfA survey, using values of Ω_0 from 1 down to .01 and a constant value of -23 for the input magnitude parameter, we found that changing the value of H_0 from 100 to 50 made a difference of only two or three out of 150 to 175 pairs. Thus even with no change in the magnitude parameter, there is virtually no dependence on H_0 .

As we discussed in the introduction, it is becoming commonly accepted that there is a relationship between the size of the region over which mass is determined and the calculated value of M/L ; the larger the region, the higher the value of M/L . Indeed, one of the most influential arguments for the dark matter hypothesis was based on a

claimed increase in M/L with increasing projected separation for a sample of binary galaxies; see Einasto et al. (1974). In order to use our binary sample to check this currently popular view, it is important to determine whether or not our companionship criteria themselves induce such a relationship.

From equation (19) of the escape velocity criterion, we see that the minimum allowed total luminosity of a binary is proportional to the product of the square of the radial velocity difference and the projected separation:

$$(36) \quad L_{\min} \propto \Delta V^2 \times R_p$$

From the escape velocity criterion alone, we would expect that a plot of total luminosity L against the quantity $\Delta V^2 \times R_p$ should be a scattergram with all points falling at or above a line of non-zero slope. Comparing (36) with the equations for calculating M/L, namely (27-28), we see that there is no induced relationship between the maximum allowed value of M/L and projected separation. Assuming no relation inherent in the data itself, a plot of M/L against R_p should be a scattergram, all points falling below a line of constant M/L. So the escape velocity criterion does not induce a spurious relation between M/L and R_p .

From equations (24-25) of the density criterion, we see

that the minimum total luminosity of a binary is proportional to the cube of the projected separation:

$$(37) \quad L_{\min} \propto R_p^3$$

So the density criterion together with the escape velocity criterion, i.e., (36) together with (37), make ΔV proportional to R_p , as one would expect. Consequently, there is no relationship between M/L and R_p induced by the combination of the escape velocity criterion and the density criterion. And trivially, no such relationship is induced by the brightest galaxy criterion.

Since the ratio of mass to observed light increases with distance, we should expect there to be a relation between the maximum allowed ΔV for a pair and the distance from the observer. Assuming the distribution of matter is uniform throughout space, the further away a pair is, the more unseen matter there must be in the vicinity of the pair. Thus a pair with given apparent magnitudes will support a higher velocity difference at larger redshifts than at smaller redshifts. We should then expect a relationship between ΔV and distance. Indeed, the equation for the escape velocity criterion (19) together with the standard equations (1 and 5) yield the following relationship:

$$(38) \quad \Delta V \leq d^{3/2} \times \rho_L(M_{lim})$$

The true relationship between ΔV and distance depends on the way in which $\rho_L(M_{lim})$ varies with distance, and this latter variation may differ from one catalog to another.

From equations (36-38), we are led to expect some relationship between the minimum absolute luminosity of binaries observed at a given distance and the distance. However, any effect induced by our selection criteria is likely to be completely overshadowed by the effect due to the fact that our original catalog is an apparent magnitude limited sample. From equations (1, 4, and 5), we obtain the standard result for any apparent magnitude limited sample that the minimum absolute luminosity observed at a given distance is proportional to the square of the distance. But the members of a binary galaxy are presumed to be at the same distance. Since the absolute luminosity of a binary is just the sum of the absolute luminosities of the constituent galaxies, the minimum luminosity of binary galaxies observed at a given distance will also be proportional to the square of the distance.

A final note of some importance concerns the relationship between our companionship criteria and the projection angles θ and ϕ . Unlike previous work in the

field (e.g. Page (1952), Karachentsev (1972), Turner (1976), and Peterson (1979)), our criteria make no explicit separate appeal to any cut-off in velocity difference or projected separation, nor do we use directly any positional isolation requirement. As a result, the projection angles remain random variables. Indeed, we have already noted that no true binary system would be ruled out by our three criteria. Since true binary systems may be presented to the observer through any random projection angles, our criteria cannot introduce any bias in these angles. Thus it will be appropriate to divide the mean value of M/L from our sample by the mean of the projection function in order to obtain the true value of M/L .

III.D: The problem of faint companions

As we have pointed out above, our criteria are all conservative, in the sense that generally speaking, a true binary pair will not be rejected. However, there is a problem of significant contamination of our sample by "imposters", i.e., by pairs that do not really form binary systems. Obviously, from our point of view, some imposters are much worse than others. To put the matter succinctly, bad imposters are those that foul up the statistics. Given our goals and techniques, there is nothing to be gained in

trying to identify imposters that do not affect the statistics of the sample; only the bad imposters need to be eliminated.

The most obvious sort of bad imposter is a larger group masquerading as a binary because of the observational limit of the original catalog. Any pair in our sample may have close companions that are fainter than the observational limit of the catalog. If the faint companions are similar in mass to the visible objects, then the mathematics of binary dynamics cannot be appropriately used. To put the matter slightly differently, for cases of significant mass contamination, calculations based on binary dynamics will provide very misleading values of M/L . It is easy to describe scenarios in which the spurious values will be low as well as high. But statistically speaking, the mean of a distribution weights larger values more than smaller values, so the mean M/L of a contaminated sample will be larger than it should be. Further, because the M/L values of the bad imposters tend to be extreme, the standard deviation in M/L for the contaminated sample will be greater than the corresponding standard deviation for the sample with the bad imposters removed.

It is important to recognize that eliminating randomly chosen true binaries from the sample will not affect the statistics, assuming of course that we do not eliminate so

many that small numbers become a serious problem. This fact has two very important consequences. First, we need not worry if our procedures for eliminating bad imposters are quite draconian and eliminate many true binaries as well; as long as the cull procedure introduces no bias in the orientation angles which determine the projection function, the elimination of such randomly selected true binaries will not affect the statistical results. And second, if our cull procedure is designed to progressively eliminate more and more pairs, we will be able to tell when the bad imposters have been eliminated by simply noting the point at which the statistical characteristics of the remaining sample become stable. Thus, that very quality of bad imposters to which we object (they significantly affect the statistics of the sample) will in fact enable us to cull them from the sample, as we will now discuss.

Since we are assuming that mass is roughly proportional to light for galaxies, an unseen companion will have a greater dynamical effect on galaxies close to the catalog observational limit than on brighter galaxies. Hence, if either member of a pair in our sample is close to the observational limit of the catalog, then we must be suspicious that the pair might be a bad imposter. In fact, the closer to the limit either member of the pair is, the greater should be our suspicion. In light of this

observation, a simple culling procedure suggests itself: we should cull any pair in which at least one member is "close to" the observational limit of the catalog.

We have used the difference between the apparent magnitude of the faintest member of the pair and the observational limit of the catalog as the "closeness" parameter for our procedure. We have implemented a progressive culling technique by starting with a closeness parameter of 0 (culling first at the catalog limit) and then increasing the closeness parameter in steps of one tenth of a magnitude. From equations (1 and 5) we can obtain the following relationship:

$$(39) \quad dL/L = (-.4 / \log e) \times dm \approx -.921 \times dm$$

So, assuming a constant value of M/L , each step in one tenth apparent magnitude means a change in mass by a factor of almost one tenth.

As suggested above, we continue our progressive culling procedure until the statistical characteristics of the remaining sample have stabilized; the particular characteristics of interest are the mean and standard deviation in the calculated value of M/L . It is possible to predict fairly precisely how the mean and standard deviation should behave under our culling procedure if our

characterization of the bad imposters has been correct. It will be important to use these predictions as a check on the correctness of our proposals.

Let A and B represent any two variables such that one is the product of some independent projection function f times the other.

$$(40) \quad A_i = f_i \times B_i$$

In our case, the "A" represents values of M/L calculated from our sample, while B represents the true value of M/L. Hereafter we will use angular brackets around variables to denote mean values, and we will use "σ" with appropriate subscripts to denote standard deviations. Given (40), the following two relationships are easy to establish (see Reif (1965) and Squires (1976)):

$$(41) \quad \langle A \rangle = \langle f \rangle \times \langle B \rangle$$

$$(42) \quad (\sigma_A / \langle A \rangle)^2 = (\sigma_f / \langle f \rangle)^2 + (\sigma_B / \langle B \rangle)^2$$

For the case of interest to us, the projection function is given by (34) above. To obtain the mean of the projection function, we must consider the probability distribution of the angles. We assume that there is no

preferred direction for the axes, i.e., for the relative velocity vector and the line joining the two galaxies. In other words, if we think of a "point of view" as a location on the hemispherical shell determined by the ranges of θ and ϕ , then each point of view is equally probable. Hence the probability that θ is in the range θ to $\theta + d\theta$ and ϕ is in the range ϕ to $\phi + d\phi$ is just the element of solid angle, $\sin \theta \times d\theta \times d\phi$, divided by the total solid angle in the hemisphere, 2π . Using this probability and equation (34), we find:

$$(43) \quad \langle f \rangle = 3\pi/32 \approx 0.295$$

$$(44) \quad \sigma_f = \sqrt{((6/35) - (9\pi^2/1024))} \approx 0.291$$

So, the ratio of the mean of the projection function to its standard deviation is about 1. Thus, from (42), we obtain the following important relationship:

$$(45) \quad \sigma_A \approx \langle A \rangle \times \sqrt{(1 + C)}$$

Of course C in (45) is just the square of the ratio of the standard deviation in B to the mean of B .

We are now in a position to predict how the mean and standard deviation in M/L should behave under our culling

technique. As discussed above, both the mean and the standard deviation should show a steady decline as the extreme values of the bad imposters are eliminated. More importantly, from equation (45), we can predict that the standard deviation should be a bit greater than the mean. The ratio of the standard deviation in the true M/L value to its mean is of course unknown, but on a priori grounds, we would not expect it to be large. After all, if the standard deviation is much larger than the mean, then the mass to light ratio ceases to be of much value on any scale less than that of the entire universe. In any case, once the bad imposters are removed from the sample, the mean and the standard deviation in calculated M/L should both level off and remain a constant distance apart.

We could have used this predicted behaviour as an indication of where to stop the cull. However, it seemed to us better to use the predicted relationship between the mean and the standard deviation as a check on our underlying assumptions and to use a more objective criterion for ending the cull. Thus, in actual practice, we computed statistics on samples culled at one tenth magnitude intervals over a range of one and a half magnitudes; we then used that sample which had the lowest standard deviation in computed M/L. In all cases which we examined, using values of Ω_0 from 1 to .01, the means and

standard deviations behaved exactly as predicted (see the following chapter).

It is extremely important to note that our culling procedure does not in any way bias the sample in terms of the projection angles. Note that a faint galaxy may occur in a pair with any arbitrary projection angles, as may a bright galaxy. Culling on the basis of apparent magnitude amounts to simply using only a shallower sub-catalog of the original. If the original catalog was complete to some limiting apparent magnitude, then it should be complete at all smaller apparent magnitudes.

Since corrected values of M/L computed according to equation (28) introduce spuriously high standard deviations, we used statistics based on the uncorrected values of M/L , computed according to equation (27), when performing the culling procedure. However, when calculating the true value of M/L , we used the mean of the corrected values, as in equations (28 and 35) in order to be statistically unbiased.

Chapter IV

Applications and Results

IV.A: Initial conditions

As stated previously, our techniques were designed primarily for the CfA survey, Huchra et al. (1983). We obtained the CfA survey on computer tape and found it to differ in only three records from the published version; our version contained data on 2398 galaxies. Morphological information was not used by the group finding algorithm. Further, no attempt was made to use the CfA supplied major and minor axis data to correct magnitudes for galaxy inclination. Velocities were converted from heliocentric to galactocentric values and corrected for Virgo-centric flow as in Geller and Huchra (1983). By direct integration of the boundary conditions of the survey, it was determined that the catalog coverage totals 2.674 steradians, as opposed to the value of 2.66 reported in Huchra et al. (1983).

In order for the results of applying the group finding algorithm to be at all accurate, the catalog must be reasonably complete to some limiting magnitude. The CfA survey is stated to be complete to apparent magnitude 14.5.

Just to be sure, we performed a V/V_{\max} test, see Schmidt (1968), in two versions on the CfA survey. In one version, we adjusted all redshifts quoted at less than 300 km/s to 300 km/s; we obtained a test value of 0.474. In the other version, we eliminated the 22 galaxies with quoted redshifts less than 300 km/s; we then obtained a test value of 0.477. On the basis of these tests, we concluded that the CfA survey is reasonably complete to the stated limiting magnitude.

During the course of the group finding algorithm, if the computation of the redshift velocity of the center of mass of a pair resulted in a value less than 300 km/s, the value was revised to be 300 km/s. In all cases, we used a value of -23 for the limiting absolute magnitude of the brightest possible galaxy. This value was selected following Schmidt and Green (1983) as the upper edge of the galaxy distribution and the lower edge of the quasar distribution. As indicated previously, we found virtually no change in our binary lists when changing our value of H_0 from 100 to 50, even when all other parameters remained constant. Thus, we will henceforth assume an H_0 value of 100 km/s/Mpc. Recall that only the brightest galaxy criterion depends on H_0 . Thus from equations (4 and 5), a change in H_0 by a factor of two is equivalent to a change in the limiting absolute magnitude of about 1.5.

Consequently it is clear that our results depend very little on the value chosen for the limiting absolute magnitude. For Ω_0 , we used the following values: 1.0, 0.2, 0.1, 0.05, 0.04, 0.03, 0.02, and 0.01. For speed in computation, the observable luminosity density function, defined by equation (16), was calculated at half-magnitude points. A plot of the result as a function of redshift distance is given in figure 2.

A very strong body of opinion presently seems to support the value of 0.2 for Ω_0 ; see Davis and Peebles (1983) and Peebles (1984). Remarkably, our self-consistency technique comes up with a value of about 0.03, as we will discuss below. Consequently, instead of reproducing complete data for all values of Ω_0 actually tried, we will concentrate our analysis on the results obtained for the two cases 0.2 and 0.03.

IV.B: Resultant binary galaxies

A complete list of the binary galaxies for Ω_0 equal to 0.2 and 0.03 will be found in tables 1-4. Tables 1 and 3 give the characteristics of the binaries themselves. The column labeled "No." is just the ordinal number assigned to the binary. The numbers in table 1 do not correspond to the numbers in table 3. The column labeled "BCPT" is a

transparent code for purposes of comparison: "B" means the binary is on the unculled lists for both Ω_0 values 0.2 and 0.03.; "C" means the binary passes the culling procedure for the given value of Ω_0 ; "P" means the binary was also identified as such by Peterson (1979); and "T" means the binary was also identified by Turner (1976). The column labelled "R.A." gives the computed right ascension for the center of mass in hours and minutes. The column labelled "Dec." gives the computed declination for the center of mass in degrees and minutes. Coordinates are all given in epoch 1950. The column labeled "mag." gives the computed apparent photographic magnitude of the binary. The column labeled "V" gives the computed galactocentric redshift velocity of the center of mass in km/s; note that these velocities have also been corrected for Virgo-centric flow as in Geller and Huchra (1983). The column labeled " ΔV " gives the radial velocity difference between the two galaxies in km/s. The column labeled " θ " gives the computed angular separation in degrees between the two galaxies.

Tables 2 and 4 list the characteristics of the galaxies. This information is all taken from the CfA survey, Huchra et al. (1983). As before, the column labeled "No." gives the ordinal number assigned to the binary. The numbers in table 2 correspond to those in table 1, while the numbers in table 4 correspond to those in table 3. The

numbers in table 2 do not correspond to those in table 4. The column labeled "Name" gives the designation from the CfA survey, and is either the NGC number, the IC number, or a positional designation. The columns labeled "R.A.", "Dec.", and "mag." give the information described above, only for the individual galaxies rather than for the binary itself. The column labeled "V" gives the galactocentric red shift velocity in km/s, and it has been corrected for Virgo-centric flow as in Geller and Huchra (1983). The column labeled "E" gives the estimated error in the red shift. The column labeled "Mor." gives the morphological characteristics from the CfA survey.

For $\Omega_0 = 0.2$, an initial total of 174 galaxy pairs were identified. Of these, 78 were identified by Peterson (1979) and 25 were identified by Turner (1976). For $\Omega_0 = 0.03$, an initial total of 166 galaxy pairs were identified. Of these, 77 were identified by Peterson and 32 were identified by Turner. The lists for the two values of Ω_0 have 107 pairs in common.

IV.C: Variable interrelationships

As a check on our procedures, we made various scatter plots of the unculled data to illustrate the expected interdependencies among the variables. The plots for all

values of Ω_0 were quite similar in shape, so for illustrative purposes, we have chosen to include only some plots for 0.2 and some for 0.03. It should be carefully noted that plots of actual data will exhibit a convolution of variable dependencies induced by our techniques with variable dependencies inherent in the data.

We will first deal with the variable dependencies on projected separation. Equations (36-37) lead us to expect that the minimum L will be proportional both to the cube of ΔV and to cube of R_p . However, the effect of the magnitude limited sample and equation (38) combine to alter the dependency somewhat. The relationships between L and ΔV and between L and R_p are quite evident in figures 3 and 4, respectively. In both cases, note the diagonal edge of the envelope of points and the absence of points on the lower right of the plot. In each case, a line of slope 3 has been included for reference. In both cases the edge of the plot appears closer to slope 2 than to 3.

The relationship between ΔV and R_p is illustrated in figure 5. Note the absence of points on the upper left of the plot. Since we expect the one variable to be directly proportional to the other, we have included a reference line of slope 1 along the edge of the points.

In figures 6 and 7, we have plotted M/L against projected separation for the two values of Ω_0 . For the 0.2

plot, there does seem to be an increase in maximum M/L over the entire range 5 to 1000 kpc. But for the 0.03 plot, maximum M/L seems to be constant up to about 50 kpc, at which point it increases out to 100 kpc where it again levels off. However, we must caution that these apparent relationships may be due to the presence of bad imposters in the unculled sample, and we will comment more fully when we discuss the culled samples.

Next we consider variable dependencies on redshift. The relationship expected from equation (38) between ΔV and redshift is illustrated in figure 8. We used the observable luminosity density function and equation (38) to derive the shape of the expected upper bound on ΔV , which we have plotted on the diagram for reference.

From equations (36-38), we expect a relationship between R_p and redshift, and this relationship shows up clearly in figure 9. As with figure 8, we have included a plot of the expected boundary curve as derived from equations (36-38) and the observable luminosity density function.

In figure 10 we have plotted the relationship between absolute luminosity and redshift. As we discussed previously, we expect this relationship to be determined primarily from the fact that we are working with a catalog with an apparent magnitude limit. As we have illustrated on the

plot, the lower boundary of the points is a good fit to a line determined by the square of the distance.

From the binary mass calculation given in equation (26) we can see from equation (36) that luminosity and mass should have inverse dependencies on redshift; that expected trend can be seen by comparing figures 10 and 11. Consequently, we would expect M/L to show no dependency on redshift. Figure 12 for the 0.2 case is weakly suggestive that such a trend may be present, but the data points are too sparse on the upper edge to really decide the issue. Figure 13 for the 0.03 case shows no such trend. Thus any such trend present in the 0.2 case is most likely inherent in the data and not due to our techniques.

Figures 14 and 15 are of considerable interest, as we have plotted mass against luminosity for the two indicated values of Ω_0 . For reference, we have included the two lines for $M = 1000 L$ and $M = 100 L$. In both plots, the upper edge is the crucial part, the lower portions obviously being due to the effects of the projection function. It does appear that a power law exponent different from 1 would be a better fit for the 0.2 case; however, a power of 1 seems to fit the 0.03 case quite well. But, in both cases, the upper edge is too sparsely populated to be precisely defined. We wish to emphasize that no firm conclusions can be drawn from the unculled samples due to the likely presence of bad

imposters.

To check the possibility of an induced relationship between M/L and L, we have plotted L vs M/L for the unculled binaries in figures 16 and 17. A very weak trend may be present in figure 16, but no such trend appears in figure 17. Since the trend does not show up in both cases, it cannot be a systematic effect due to our technique.

IV.D: Results of the cull procedure

We now turn our attention to the effects of our culling procedure. In table 5 we have recorded the effect of the culling procedure on the number of binaries in the samples for all values of Ω_0 . It is interesting to note that at each level of culling, the numbers of binaries in the samples for different values of Ω_0 are remarkably consistent.

The effects of the culling procedure are clearly apparent in figures 18-25. Note that progression to the right along the abscissa includes more and more of the original set of binaries, until at the extreme right (culling all pairs with at least one member fainter than apparent magnitude 14.5) no pairs at all are culled. In other words, the culling is more severe as we move from the right to the left along the abscissa. For illustrative

purposes, figures 18-25 deal only with Ω_0 values of 0.2 and 0.03. The corresponding diagrams for other values of Ω_0 are quite similar in shape.

Figure 18 deals with projected separation. Recall from equation (29) that the projection function for separation is just $\sin \theta$, so we do not expect the same variation in projected separation that we do in M/L. At about 14.1, both mean and standard deviation become quite stable, with very little change until we begin to cull at 13.5. Even so, the mean changes by only about 50 kpc throughout the entire range. In general, the culling procedure seems to affect the distribution of projected separations very little, as is especially apparent from the behaviour of the median.

Figure 19 deals with ΔV . Recall from equation (30) that the projection function for ΔV is $\sin \phi \sin \theta$, so again we do not expect the same variation in ΔV that we do in M/L. Nevertheless, the graph exhibits the characteristic trend of marked decrease in standard deviation as we begin to cull (moving from right to left along the abscissa) until a point of stabilization is reached, after which the standard deviation remains relatively constant. The mean shows a similar, but less drastic change, reaching stability at the same point as the standard deviation. Of particular importance to note is the behaviour of the median, which

remains practically constant throughout. The constancy of the median in the face of large changes in standard deviation is an indication that the relative percentages of higher vs lower values of the variable remain unaffected by the culling procedure. Thus the culling procedure does not introduce any particular bias toward higher or lower values.

Projected separation and ΔV are combined as in equation (26) to compute an indicative total mass. Mass is subject to the total projection function given in (34). However, we do expect considerable inherent variation in the mass of galaxies, because there is so much variation in their absolute luminosities. The effect of the culling procedure on mass is illustrated in figures 20 and 21. For the $\Omega_0 = 0.2$ case, figure 20, the mean and standard deviation remain relatively parallel, except at the sharp downward steps. At these steps, the difference between the mean and the standard deviation decreases slightly, remaining rather constant until the next sharp downward trend. However, the case for $\Omega_0 = 0.03$, figure 21, follows the more characteristic pattern we expect from our previous discussion of the theory of our culling procedure. Note the characteristic steep change and leveling off of both the mean and standard deviation as the culling proceeds. In both cases, note the relative constancy of the median in

spite of the changes in mean and standard deviation.

Figures 22 and 23 deal with absolute luminosity. Absolute luminosity is not subject to projections based on the angles θ and ϕ , so we do not expect the distribution to be affected by our culling procedure in the same way as distributions of variables that are subject to such projections. The mean and standard deviation continue to change in non-parallel ways throughout the range of the cull procedure, while the changes in the median roughly parallel the changes in the mean. The general trend in mean luminosity is downward as more pairs are culled, indicating that we are eliminating the binaries with greatest combined luminosity.

Figures 24 and 25 give the changes in M/L throughout the culling procedure. As we predicted earlier, the standard deviation and the mean both drop as the cull begins, until both level out, the standard deviation remaining greater than the mean. The same strong trend was very evident for all values of Ω_0 . As above, it is important to note that the median is extremely stable throughout the cull procedure, indicating that no systematic bias toward higher or lower values has been introduced.

We suggest that the point at which it is appropriate to stop the cull is quite evident from the graphs--simply

select the point at which the mean and standard deviation settle down and "march along together." However, we feel that a more objective criterion might be deemed desirable, so we have used the point at which the standard deviation reaches its lowest value. Of course the choice of this criterion has an element of subjectivity to it as well. In any case, once the statistical characteristics of the sample have settled down, it will not matter much where we choose to stop the cull. Thus for $\Omega_0 = 0.2$, we used the sample culled at apparent magnitude 13.8, while for $\Omega_0 = 0.03$, we used the sample culled at apparent magnitude 13.4.

Returning to tables 1 and 3, we can see the differences made by the value of Ω_0 in the culled samples. For $\Omega_0 = 0.2$, 19 out of 53 binaries in the "culled list" (the list remaining after the cull procedure) are not on the original list for $\Omega_0 = 0.03$. For $\Omega_0 = 0.03$, 23 out of 42 binaries are not on the culled list for the other value of Ω_0 . (Recall that the cull criterion for $\Omega_0 = 0.2$ is 13.8, while for $\Omega_0 = 0.03$ it is 13.4.)

In figures 26 and 27 we have plotted mass against absolute luminosity. In figure 26, $\Omega_0 = 0.2$, we have included the two reference lines $M = 1000 L$ and $M = 100 L$. In figure 27, $\Omega_0 = 0.03$, we have included the two reference lines $M = 100 L$ and $M = 10 L$. In both cases it seems clear

that the upper edge of the distribution falls between the two reference lines. If only the distributions contained many more points, it would be possible to obtain an accurate determination of the true value of M/L in each case directly from the graph. Since the distributions are so sparse, we must instead utilize the mean of the projection function and the means of the samples.

In figures 28 and 29, we have plotted M/L against separation to check for any trend. In figure 28, $\Omega_0 = 0.2$, the trend tentatively noted in the uncultured sample can still be seen. There seems to be a trend to increasing M/L with increasing separation out to 100 kpc, where values appear to level off. But the data points are even more sparse than before, so any conclusions based on figure 28 must remain tentative at best. Figure 29, $\Omega = 0.03$, shows no trend in M/L with increasing separation. However, as before, there are too few data points to warrant any firm conclusions.

In figures 30 and 31 we have plotted L vs M/L for the culled samples. For the 0.2 case, figure 30, M/L still seems to vary with L . However, for the 0.03 case, figure 31, there is no such trend. Recall from equation (37) that minimum absolute luminosity observed at a given separation is proportional to the cube of the separation. Thus if the data contains an intrinsic relationship between M/L and

separation, this relationship will also be exhibited as a relation between M/L and L . For the 0.2 case, we seem to have found a relation between M/L and separation, and hence we also see a relation between M/L and L . But for the 0.03 case, there is no inherent relation between M/L and separation, and hence we find no relation between M/L and L . Thus there appears to be no induced systematic relation between M/L and L .

IV.E: Simulations

As an additional check on our approach, we attempted to reproduce sample distributions of M/L from a simulation of the projection function and various presumed "true" distributions in M/L . All of our simulations were 10,000 points. Figure 32 is a plot of 10,000 points for the projection function distribution. The mean and standard deviation of the simulation (0.295 and 0.291) are the analytically determined values. The median (0.186) was empirically determined from the distribution of points.

We will report only on the simulations for $\Omega = 0.2$, as the other cases were all quite similar. We used four different simulations for the "true" M/L distribution: a delta function, a triangle distribution, an exponential distribution, and a log normal distribution. We simply

divided the mean of the sample M/L as determined by equation (27) by the mean of the projection function to obtain the mean of the "true" distribution. Of course for the delta function, 100% of the values were at the mean. For the triangle distribution, an isosceles triangle was used, the base of the triangle being twice the mean. The standard deviation for the log normal distribution was determined from that of the sample by using equation (42). A plot of all distributions except the delta function are given as figures 33-35.

The points in the simulated distributions were obtained by taking the product of a randomly selected projection and a randomly selected "true" value. The simulations are plotted with the actual sample distribution in figures 36-39.

To analytically check the goodness of fit, we binned the actual distribution and the simulations into bins of width 5 and performed a chi-square test for each simulation. In each case we used the simulation as the expected distribution. For all cases except the delta function, we used the simulated values out to four times the mean of the simulation when calculating the test statistic; since the delta function yielded zero expected frequency at four times the mean, we used simulated values only to three times the mean. The highest value of the test

statistic was 0.58 for the delta function simulation; the test for the delta function simulation was made over 30 bins, while the test for the others was made on the basis of 41 bins. Thus in all cases, the differences between the simulation and the actual distribution were statistically quite negligible.

The good success of our simulations points to two important points. First, it should be obvious that except for the mean value, virtually no details about an underlying "true" distribution in M/L can be obtained from the observed sample. The effects of the projection function are so strong that they mask all other details. Second, our successful simulations provide yet one more piece of evidence that our original companionship criteria and our cull procedure do not bias the resulting sample with respect to the projection angles. Consequently, it will be legitimate to use the means of the sample distributions and the projection function to obtain a "true" mean value for M/L.

IV.F: Determination of Ω_0

As indicated previously, we have obtained binary samples for values of Ω_0 from 0.01 to 1. The results are summarized in table 6. The column labeled " Ω_0^{in} " is the

input value of Ω_0 . The column labeled "Cull" gives the apparent magnitude at which the standard deviation in M/L was least; we eliminated all pairs with at least one member fainter than the indicated apparent magnitude. The column labeled "#" gives the number of binaries left in the culled sample. The column labeled " $\langle M/L \rangle_c$ " contains the mean statistically corrected values of M/L in solar units, as in equation (28). The column labeled " $\langle M/L \rangle_t$ " lists the proposed "true" values of M/L in solar units; the values are obtained from the " $\langle M/L \rangle_c$ " column by dividing by the mean of the projection function. Finally, the column labeled " $\Omega_{0\text{out}}$ " contains the values of Ω_0 calculated from the "true" M/L values. Using equations (14 and 15), we have:

$$(46) \quad \Omega_0 = \frac{8 \times \pi \times G \times \rho_L}{3 \times H_0^2} \times M/L$$

The value of ρ_L is just the total luminosity density obtained from the catalog. We found $\rho_L \approx 1.781 \times 10^8$ in units of suns per cubic Mpc. For our units, we used the following equation:

$$(47) \quad \Omega_0 = \langle M/L \rangle_t / 1558$$

The data in table 6 are plotted in figure 40. For convenience in plotting the data, the point for $\Omega_0^{\text{in}} = 1$ has been omitted. For reference, we have included the line indicating equality of Ω_0^{in} and Ω_0^{out} . It is abundantly clear, both from the table and from the graph, that the self-consistency requirement dictates Ω_0 between 0.02 and 0.03.

It should be emphasized that the standard deviation in our observed M/L is not a good guide to the errors in our technique. The standard deviation in observed M/L is a convolution of the standard deviation in the projection function, the standard deviation inherent in the true M/L distribution, the errors in the input data, and the internal errors resulting from our approach.

One simple way to estimate the error in $\langle M/L \rangle_c$ is to recall that once the mean and standard deviation stabilize during the cull procedure, they change very little. From an examination of the results of the culling procedure for all the values of Ω_0 used, we can state that the maximum change in the value of $\langle M/L \rangle_c$ over the range of statistical stability is 10%. Thus the internal error in the values of $\langle M/L \rangle_c$ for each value of Ω_0^{in} may be taken to be 10%. Obviously 10% errors in the values of $\langle M/L \rangle_c$ yield corresponding 10% errors in the values of Ω_0^{out} computed for the values of Ω_0^{in} . Another source of uncertainty in

our adopted value of Ω_0 arises from the step size in Ω_0^{in} in the vicinity of the equilibrium point between Ω_0^{in} and Ω_0^{out} . And finally, some uncertainty is due to the "graininess" of the samples; that is, the small number of binaries in the samples means that our "black box function" is not very smooth, and hence the degree of resolution is rather limited. There is no analytic way to calculate an error based on all these considerations. However, from figure 40, we estimate that the potential internal error in identifying Ω_0 is about 0.01. Thus from our analysis, we suggest that the appropriate value is $\Omega_0 = 0.03 \pm 0.01$.

Chapter V

Discussion and Conclusions

V.A: Discussion

Almost every attempt to determine a value for Ω_0 seems to yield a different value. Hence it is not too surprising that our value of 0.03 agrees with some and disagrees with others. We have already noted that our value is in better agreement with the generally low values of Ω_0 which result from nucleosynthesis analyses than the currently popular values of 0.2 and higher; see Yang et al. (1984) for a good summary of recent work in this area. It is also worth noting that using a different technique from ours for finding groups, Press and Davis (1982) obtain a lower bound of 0.07 from the CfA survey.

In spite of these agreements, we must comment on the fact that Davis and Peebles (1983) analyze the CfA survey based on two-point correlations and argue for $\Omega_0 \approx 0.2$. Although their approach is different from ours, both assume that gravity is the primary force affecting the galaxies. Thus it is quite surprising that the two approaches give such different results when applied to the same data base. Without going into tremendous detail, it is easy to point

to many places in their analysis where Davis and Peebles make a choice, not dictated by the data, which substantially affects the outcome. We will mention only three such points.

The first point concerns certain model parameters used in the analysis. As part of the analysis, Press and Davis attempt to model the relative velocity distribution and fit it to the observations. Two free parameters are the pair-wise relative velocity dispersion and a factor designated by F . Note that Davis and Peebles use " σ " for the dispersion, while in keeping with statistical practice, we have used the same symbol for standard deviation. Henceforth, to avoid confusion we will use " σ_d " for the pair-wise velocity dispersion. Note that the pair-wise velocity dispersion is presumed to vary with the separation of the individuals. As the authors note, the data do not provide enough sensitivity to simultaneously fit for both F and σ_d . They opt to use a value of 1 for F , in part because the value of σ_d does not seem to vary much with F in the range 0.8 to 1.5.

However, the choice of a value of F is intimately connected with the crucial cosmological parameter Ω_0 . As the authors note (p. 474) "A small value of F implies that galaxies on all scales are expanding with the Hubble flow...", while larger values of F imply that gravitational

forces are more effective in overcoming the Hubble flow. In brief, a lower value of F yields lower values for the velocity dispersions at various separations, as Davis and Peebles clearly indicate. Using a value of $F = 1.0$, Davis and Peebles note (p. 474) that for small separations (less than 200 kpc) "...we get a value of σ that we suspect is unrealistically large...". Similarly, they note that for large separations (greater than 6.4 Mpc) the data do not fit the model. For these reasons they choose not to use the values from their model for both small and large separations. We would suggest that a lower value of F would yield more reasonable results. A lower value of F would yield a lower velocity dispersion from the data, and hence a lower value of Ω_0 ; consequently, F is obviously not independent of the cosmological parameter the authors are trying to derive.

The second point concerns the relationship between the pair-wise velocity dispersion and the single-galaxy one-dimensional (peculiar) velocity dispersion, which we will designate by $\langle v_p \rangle$. Because the observed redshift is a vector sum of the peculiar velocity of the galaxy as well as its true Hubble recession velocity, we cannot determine a single galaxy peculiar velocity directly from the observations. Hence the pair-wise velocity dispersion must be used as a basis for estimating the peculiar velocity

dispersion. Davis and Peebles note that N-body studies indicate that $\langle vp \rangle$ is about half the value of σ_D at a separation of 1 Mpc. However, for certain analytical reasons, the authors expect $\langle vp \rangle$ to be roughly equal to σ_D at 1 Mpc separation. They opt to use $\langle vp \rangle$ equal to σ_D at 1 Mpc. For dispersions in km/s, they use the following to compute Ω_0 :

$$(49) \quad \Omega_0 \approx (\langle vp \rangle / 660)^2$$

From their analysis, they find $\Omega_0 = 0.27$. Note that simply taking $\langle vp \rangle$ to be one half σ_D at 1 Mpc would reduce the value of Ω_0 by a factor of 4, giving $\Omega_0 = 0.07$, in much better agreement with our result.

The final point we will note concerns the pair-wise velocity dispersion at small separations. Because of perceived inadequacies with their model, Davis and Peebles opt to use the binary galaxies of Turner (1976) to determine the velocity dispersion at smaller separations. It should be carefully noted that Davis and Peebles use the velocities reported in White et al. (1983); these velocities were determined by methods similar to those used for the CfA survey and are more accurate than those originally given by Turner.

As we have already noted, selection criteria of the

sort that Turner employed involve covert assumptions about Ω_0 . Using a different set of binaries selected on the basis of other criteria might very well yield different results. For purposes of comparison, in table 7 we have tabulated the velocity dispersions in km/s, corrected for statistical bias due to observational errors, binned at various separations, for each of our unculled binary lists. We have also listed the corresponding values for the Turner sample taken from Davis and Peebles (1984). The columns headed "10", "30", "90", and "270" are for the bins 5-15, 15-45, 45-135, and 135-405, respectively, all in kpc. Obviously the distributions of velocity dispersions for our samples are all quite different from the Turner data, and with the exception of the 90 kpc bin for $\Omega_0 = 0.2$ and 0.1, all of our values are substantially lower than the corresponding Turner sample values. Our culled samples would have produced even smaller dispersions than those listed in table 7.

In summary, it would be very surprising if two analyses of the same data, both based on the same underlying force, would yield radically different results. We suggest that there are enough free choices in the Davis and Peebles analysis to bring their result into good agreement with ours.

V.B: Conclusions

In conclusion, there are a number of important points that warrant emphasis. First, we do not believe that it is possible to identify gravitationally bound, dynamically isolated, virialized groups of galaxies independently of assumptions about crucial cosmological parameters. In this thesis, we have clearly illustrated the very significant effect even apparently small changes in these parameters will have on even the binaries selected. If our contention is true, then a self-consistency analysis is the only logically appropriate way to determine the value of Ω_0 on the basis of galaxy binaries and groups.

Further, a value of $\Omega_0 = 0.03 \pm 0.01$ is clearly indicated by our analysis. We caution that this result applies only to the region of the universe sampled by the CfA survey. Other regions may be more or less dense, and the same analysis applied elsewhere may yield different results. We also caution that our result is based only on the binaries. Our data did not show a clear trend in M/L with increasing separation, but they did not rule out such a trend either. Consequently, it may very well be the case that the present result is appropriate only for small separations and will be revised upward when we analyze the groups.

We should note several ways in which our technique might be improved. As indicated before, we did not attempt to correct the apparent magnitude data for galaxy inclination. Thus, we have probably underestimated the luminosities and hence overestimated the value of M/L . Secondly, we have made no attempt to cull pairs that are close to the edge of the area covered by the CfA. However, it may easily happen that a pair we have identified as a binary is actually part of a larger system whose other members are outside the coverage of the CfA. One could progressively cull based on an edge distance parameter, again checking to see where the statistical parameters of the remaining distribution stabilize. We did not pursue such a course primarily because the numbers in our samples were already quite small.

It would be extremely useful to be able to apply our technique to other regions of the sky or to a deeper survey in the same region. With more data points, the edge of the distribution of mass versus light would become quite clear, and it would be possible to determine M/L independently of the projection function. We look forward to having such data available.

TABLES

Table 1: Unculled Binaries, $\Omega_0 = 0.20$

No.	BCPT	R.A.	Dec.	mag.	V	ΔV	θ
1	B P	0 7.50	25 36.83	12.69	4563	16	0.1643
2	P	0 26.58	2 34.38	12.53	4419	1127	0.1065
3		0 38.35	25 15.81	12.89	4484	132	0.4715
4		0 39.70	-2 8.64	13.11	5120	5	0.3732
5	B P	0 45.48	27 22.22	13.01	5035	216	0.1493
6		0 48.65	-3 44.42	12.78	3840	222	0.4874
7	B P	0 55.04	30 4.05	12.28	4934	126	0.1065
8	C	1 12.94	-2 37.72	11.95	1613	156	0.7515
9	BCP	1 17.37	3 9.00	11.87	2174	37	0.0766
10		1 26.40	-1 0.08	13.34	5280	17	0.4005
11	B	1 34.06	15 32.11	10.05	542	23	0.8509
12	BC	1 46.39	5 40.85	10.43	1347	77	0.4614
13		1 47.37	27 16.31	12.84	3439	89	0.4507
14	B T	1 56.59	18 45.80	11.34	2389	54	0.0559
15	B P	1 58.78	26 16.16	13.37	5007	93	0.0625
16	B PT	2 1.05	14 29.06	13.50	3513	7	0.0395
17	B	2 3.24	29 37.25	13.47	4898	166	0.1856
18	B P	2 15.14	14 19.02	12.52	3741	169	0.1938
19		2 24.14	-1 28.93	13.37	6152	30	0.3593
20	B T	2 36.67	10 36.69	13.19	3380	163	0.1119
21	B P	2 37.31	1 18.94	13.70	5778	165	0.1047
22		2 37.88	17 41.68	13.70	8708	405	0.4266
23		2 46.68	-2 57.56	13.41	6687	671	0.1887

Table 1: continued

No.	BCPT	R.A.	Dec.	mag.	V	ΔV	θ
24	B P	2 50.96	12 44.96	12.81	3438	19	0.1736
25	B	2 52.63	-1 36.93	13.11	8354	176	0.0122
26	B P	2 55.65	3 11.22	13.11	2912	28	0.1413
27		2 57.60	5 33.66	13.25	7410	2069	0.1047
28		3 9.68	-1 27.40	13.70	6612	21	0.2639
29	B PT	8 53.22	52 17.23	13.07	4147	252	0.0559
30	B PT	9 9.31	35 11.42	12.76	2156	66	0.1282
31	B P	9 14.16	20 19.83	13.20	8288	442	0.1506
32	B P	9 14.23	42 12.75	12.96	1962	149	0.0251
33		9 17.38	33 59.99	13.00	7060	138	0.4813
34	B P	9 20.70	49 25.96	13.10	2907	94	0.0484
35	B P	9 31.22	10 21.17	13.24	3282	83	0.0815
36		9 34.49	23 37.79	13.49	7681	9	0.4365
37	BCP	9 40.06	32 6.53	11.97	1496	27	0.0949
38		9 45.81	44 20.97	12.44	4970	171	0.3298
39	CP	9 46.42	33 41.73	12.07	1725	3	0.5166
40	BC	9 47.55	13 1.84	12.67	1560	60	0.1101
41	BC	9 52.64	59 32.28	12.71	3234	59	0.0280
42	C	9 53.18	16 51.93	13.00	3881	40	0.4571
43	BC	9 58.49	55 54.72	11.31	1368	58	0.1631
44	B	10 10.99	38 58.50	13.14	6842	623	0.1467
45	BC	10 19.07	57 12.69	12.34	1453	66	0.2887
46		10 29.72	28 49.63	12.36	1616	12	0.5128
47	BC	10 29.37	65 11.36	12.48	2094	157	0.2921

Table 1: continued

No.	BCPT	R.A.	Dec.	mag.	V	ΔV	θ
48	CP	10 33.49	22 3.57	11.98	1500	21	0.5319
49		10 33.91	14 17.97	12.84	3133	2	0.4715
50	C	10 43.80	72 59.54	12.14	3102	118	0.4419
51		10 44.97	26 49.43	13.70	6492	8	0.3159
52	B	10 48.80	8 40.19	13.47	6530	365	0.2654
53		10 58.10	45 57.17	13.49	10142	2531	0.2579
54	C	10 57.95	29 14.54	11.01	903	33	0.7271
55	C	11 0.70	45 26.45	12.43	6564	540	0.4837
56	B	10 59.95	17 0.00	13.75	1211	1	0.0342
57		11 0.67	50 16.43	13.70	7516	83	0.4252
58	BC	11 0.74	18 23.11	11.29	1177	158	0.2056
59	BC	11 0.68	28 15.69	11.52	1723	140	0.1824
60	B	11 3.35	0 13.93	9.81	904	166	0.8774
61		11 7.70	47 12.00	13.55	7819	85	0.3851
62	B P	11 15.60	23 42.06	13.43	6948	122	0.1426
63	BC	11 18.65	53 24.65	11.09	1467	55	0.4997
64	B	11 19.15	20 27.10	12.01	4424	248	0.1170
65	BC	11 21.84	38 59.18	11.72	2340	37	0.2423
66		11 22.47	63 48.15	12.74	3836	274	0.3007
67	BC T	11 25.71	58 50.18	11.91	3415	14	0.0079
68	B	11 26.21	9 22.52	13.70	6409	121	0.1028
69	B P	11 29.10	28 31.80	13.60	7229	4	0.2203
70	BCPT	11 29.77	1 5.31	12.58	6080	72	0.0280
71	BC	11 30.29	53 22.13	11.20	1332	110	0.1998

Table 1: continued

No.	BCPT	R.A.	Dec.	mag.	V	ΔV	θ
72	C	11 33.51	54 45.15	11.99	1558	95	0.6224
73	C	11 36.77	60 1.11	12.80	3636	231	0.5004
74	C	11 38.00	11 50.45	11.23	1172	19	0.9325
75	BCPT	11 37.10	32 12.14	12.59	2900	30	0.0342
76	B PT	11 37.60	15 36.78	12.81	3511	15	0.0198
77	P	11 43.55	14 1.93	12.96	3378	106	0.3220
78	B PT	11 46.25	59 42.27	12.56	3560	47	0.0280
79	C	11 46.97	27 4.71	12.05	2045	9	0.5692
80		11 47.11	26 20.32	13.43	3924	135	0.2698
81	BCP	11 52.25	58 43.43	12.02	3554	137	0.1282
82	CPT	11 56.17	43 0.49	12.43	1045	101	0.0559
83	B PT	11 59.64	30 7.48	13.60	3396	88	0.0625
84		12 1.38	18 46.55	12.38	1226	194	0.4247
85	B P	12 1.81	11 2.49	12.74	2643	125	0.3032
86		12 1.94	2 9.60	12.74	6331	1064	0.1251
87	B	12 4.38	67 27.60	12.76	2826	90	0.0625
88	BCP	12 5.42	3 5.15	11.57	1488	6	0.2220
89	B	12 6.43	29 30.44	13.19	4057	97	0.1595
90	BC	12 7.80	39 52.34	10.66	1286	44	0.4934
91	BC	12 11.30	28 44.72	12.84	4178	139	0.2549
92	B PT	12 14.04	33 48.77	13.27	6878	363	0.0395
93		12 16.89	49 55.12	13.21	4258	469	0.4528
94	B P	12 20.97	58 42.53	13.21	4901	119	0.1454
95	BCP	12 24.19	65 7.90	12.89	1725	103	0.2669

Table 1: continued

No.	BCPT	R.A.	Dec.	mag.	V	ΔV	θ
96	B	12 23.94	9 17.82	13.55	7770	3	0.0198
97	C	12 32.18	26 11.54	10.15	1545	119	1.1429
98	CP	12 30.14	0 26.48	11.18	1379	399	0.2914
99	BCP	12 31.78	2 39.02	10.67	1959	82	0.4715
100		12 38.19	1 31.76	13.21	2003	139	0.2947
101	B PT	12 39.06	26 19.17	13.23	5007	94	0.0395
102	C	12 39.24	7 43.79	12.04	2052	94	0.3951
103	B P	12 40.91	55 8.05	13.34	5021	391	0.1385
104	B	12 44.69	54 45.78	13.28	5326	91	0.2112
105	P	12 45.67	35 36.53	13.60	4477	200	0.2853
106	BC	12 48.08	25 47.02	10.14	1489	16	0.4073
107		12 49.08	73 12.04	12.41	1851	34	0.4731
108	C	12 52.15	4 38.41	12.01	969	14	0.6691
109	B	12 52.50	8 19.98	12.84	3022	37	0.0000
110		12 53.03	58 43.06	12.86	2869	10	0.4257
111	BCP	12 57.71	37 34.98	12.24	4993	24	0.3165
112	P	13 3.16	29 22.27	12.99	6670	1165	0.2907
113		13 14.28	31 14.75	13.14	5905	41	0.3274
114	BCP	13 19.53	38 56.54	12.35	1299	39	0.2315
115	B P	13 21.79	14 16.71	12.94	7284	412	0.1235
116		13 27.52	46 54.39	12.88	2806	84	0.3183
117	BC T	13 27.77	47 27.96	8.86	832	84	0.0791
118	B	13 30.10	7 30.48	13.65	7031	72	0.1802
119	B P	13 30.47	62 59.80	12.71	3234	89	0.0685

Table 1: continued

No.	BCPT	R.A.	Dec.	mag.	V	ΔV	θ
120	B	13 32.20	34 59.38	13.70	7777	491	0.0906
121	BCPT	13 37.35	1 5.51	13.00	7003	213	0.0280
122	B	13 39.68	55 54.78	13.13	7931	24	0.0484
123	BCP	13 43.12	41 52.98	12.47	2901	67	0.2185
124	B	13 49.86	14 20.47	13.70	7150	69	0.0713
125	B P	13 51.10	38 8.66	12.49	3976	16	0.2027
126	C	13 54.38	41 57.01	11.78	2583	82	0.6723
127	B	13 55.28	15 36.07	13.64	5839	58	0.2247
128	B	13 58.30	39 11.91	12.80	5554	281	0.2518
129		13 59.74	8 9.31	13.31	4965	274	0.3511
130	BC	14 0.96	49 24.89	11.86	2367	27	0.0118
131	BCPT	14 4.61	50 57.65	12.41	2270	144	0.0523
132	B	14 7.63	17 50.33	13.01	5433	444	0.1866
133	P	14 12.90	14 26.70	13.39	5579	590	0.2382
134	PT	14 14.37	39 47.68	13.06	7554	1850	0.0862
135	B P	14 15.89	7 42.28	13.40	7769	406	0.2238
136	B PT	14 17.25	18 5.47	13.70	5974	111	0.0342
137	B P	14 20.84	40 34.71	13.39	5909	158	0.1251
138	B	14 26.80	70 2.68	13.70	9539	375	0.2349
139		14 27.51	3 23.83	12.39	1849	145	0.5055
140		14 27.40	29 7.44	12.71	4584	434	0.4648
141	B P	14 33.86	48 55.74	12.89	2550	113	0.2037
142	P	14 34.65	36 45.58	13.29	4532	180	0.3013
143	BCP	14 42.26	2 5.42	11.47	1914	150	0.3103

Table 1: continued

No.	BCPT	R.A.	Dec.	mag.	V	ΔV	θ
144	B PT	14 49.07	35 45.85	13.59	1592	66	0.0685
145	B P	14 52.81	42 43.77	13.13	5834	33	0.1897
146	P	14 55.05	30 16.15	12.93	2135	15	0.3449
147	CP	14 58.26	1 57.99	11.60	1973	609	0.3516
148	B PT	15 5.27	19 46.35	13.12	5072	10	0.0342
149		15 7.37	54 48.81	13.24	3471	38	0.3403
150	C	15 12.77	56 42.29	11.01	1063	109	1.0780
151	BCP	15 14.53	55 39.36	11.90	3724	82	0.2307
152	B T	15 24.36	41 51.00	13.03	2949	67	0.0186
153		15 27.35	43 4.98	13.53	5913	79	0.2921
154	BCP	15 32.80	12 4.02	12.55	2142	68	0.3159
155	B PT	15 42.66	41 16.13	13.29	9909	60	0.0395
156	B	15 47.82	19 6.69	13.04	4191	242	0.2572
157		15 54.67	48 6.03	13.49	6330	65	0.2961
158	P	16 18.27	58 0.78	12.69	5083	457	0.3522
159		16 27.54	41 5.79	13.39	8985	385	0.4829
160	B P	23 4.77	22 42.09	13.60	6236	50	0.1747
161	B PT	23 12.15	4 15.56	12.52	2534	41	0.0593
162	B P	23 12.80	18 43.27	13.24	4921	468	0.0862
163		23 13.84	13 4.85	13.64	4463	341	0.3577
164	B P	23 25.30	23 18.02	12.39	3446	140	0.1153
165	B PT	23 26.31	3 14.43	13.05	5017	12	0.0685
166	B	23 36.57	26 47.87	13.33	9306	357	0.3334
167		23 41.03	25 49.01	12.13	761	10	0.7574

Table 1: continued

No.	BCPT	R.A.	Dec.	mag.	V	ΔV	θ
168	B P	23 39.05	3 27.56	13.64	2799	89	0.0280
169	B P	23 44.57	29 11.73	12.86	5197	38	0.0280
170	B P	23 48.35	26 51.18	13.34	8084	110	0.0685
171	BCP	23 48.67	19 51.16	12.45	4239	167	0.0989
172	P	23 59.19	12 46.50	13.27	5315	230	0.2867
173	B P	23 58.90	31 9.49	13.60	4918	121	0.0170
174	B P	23 59.13	23 13.35	12.74	4418	147	0.0280

Table 2: Unculled Binary Galaxies, $\Omega_0 = 0.20$

No.	Name	R.A.	Dec.	mag.	V	E	Mor.
1	N 23	0 7.31	25 38.70	13.12	4558	15	1BOS
	N 26	0 7.90	25 33.00	13.90	4574	15	2AOT
2	N 125	0 26.30	2 33.00	13.83	5206	24	0AO
	N 128	0 26.70	2 34.98	12.92	4079	21	-2 OP
3	0036+2522	0 36.80	25 22.02	14.50	4586	29	-3 0
	N 214	0 38.80	25 13.98	13.17	4454	20	5X1R
4	0038-0159	0 38.80	-2 1.02	14.40	5123	21	1AO
	N 227	0 40.10	-2 12.00	13.51	5118	28	-5 0
5	N 252	0 45.30	27 21.00	13.40	4969	31	-2 0
	N 260	0 45.90	27 25.02	14.30	5185	25	5 OP
6	N 271	0 48.20	-3 51.00	13.20	3912	22	3BO
	N 279	0 49.60	-3 30.66	14.00	3690	23	-2 0
7	N 311	0 54.80	30 0.00	14.10	5037	16	-2 0
	N 315	0 55.10	30 4.98	12.50	4911	18	0-5A
8	N 448	1 12.80	-2 7.02	13.20	1719	22	-2 0
	N 450	1 13.00	-2 52.02	12.37	1563	10	6X8S
9	N 470	1 17.20	3 9.00	12.75	2195	10	3AOT
	N 474	1 17.50	3 9.00	12.51	2158	21	-2AOP
10	0126-0049	1 26.40	-1 10.98	14.00	5272	23	2 0
	N 570	1 26.40	-2 46.98	14.20	5289	30	1BOT
11	N 628	1 34.00	15 31.98	10.07	542	2	5A1S
	0137+1539	1 37.50	15 39.00	14.38	519	10	10 9
12	N 676	1 46.30	5 40.02	10.50	1342	20	0 0
	N 693	1 47.90	5 54.00	13.50	1419	24	0 0
13	I1731	1 47.30	26 57.00	14.20	3375	39	5AO
	N 684	1 47.40	27 24.00	13.20	3464	20	3 0
14	N 770	1 56.50	18 43.02	14.20	2439	22	-5 0
	N 772	1 56.60	18 46.02	11.42	2385	23	3A1S
15	0158+2615	1 58.70	26 15.00	13.90	5043	35	1 0
	0158+2618	1 58.90	26 18.00	14.40	4950	15	1XOS

Table 2: continued

No.	Name	R.A.	Dec.	mag.	V	E	Mor.
16	I 195	2 1.00	14 28.02	14.30	3517	28	-2 0
	I 196	2 1.10	14 30.00	14.20	3510	21	-3B0
17	0203+2933	2 3.20	29 33.00	14.00	4962	28	-3 0
	0203+2944	2 3.30	29 43.98	14.50	4796	25	3 0
18	N 871	2 14.50	14 19.02	14.30	3605	10	5B0S
	N 877	2 15.30	14 19.02	12.76	3774	10	4X1T
19	N 926	2 23.60	-1 27.00	13.90	6164	38	4BOT
	N 934	2 25.00	-1 31.98	14.40	6134	22	-2 0
20	N1024	2 36.50	10 37.98	13.80	3310	25	2AOR
	N1029	2 36.90	10 34.98	14.10	3473	18	0 0
21	I1827	2 37.10	1 19.98	14.50	5692	26	1A0
	N1038	2 37.50	1 18.00	14.40	5857	25	1 0
22	N1030	2 37.10	17 49.02	14.50	8496	41	1 OP
	I 248	2 38.60	17 34.98	14.40	8901	45	1 0
23	I1856	2 46.30	-1 1.98	14.50	6261	30	3B0
	0246-0105	2 46.90	-2 55.02	13.90	6932	32	3B0
24	N1134	2 50.90	12 48.00	13.20	3444	20	2 OP
	I 267	2 51.10	12 37.98	14.10	3425	21	3B0
25	N1143	2 52.60	-1 37.20	14.20	8242	31	-2 OP
	N1144	2 52.64	-1 36.78	13.60	8418	32	10 OP
26	N1153	2 55.50	3 10.02	13.50	2921	22	-5 0
	0256+0314	2 56.00	3 13.98	14.40	2893	28	-5 OP
27	0257+0536	2 57.50	5 36.42	14.00	6375	32	0 0
	0257+0530	2 57.70	5 30.90	14.00	8444	27	0 0
28	0309-0035	3 9.20	-1 25.02	14.40	6622	35	3B0
	0310-0030	3 10.20	-1 30.00	14.50	6601	21	0B0
29	0853+5218	8 53.10	52 18.00	13.60	4244	21	1 0
	N2692	8 53.40	52 16.02	14.10	3992	30	1 0
30	N2778	9 9.20	35 13.02	13.10	2174	22	-7 0
	N2780	9 9.60	35 7.02	14.20	2108	32	3 0

Table 2: continued

No.	Name	R.A.	Dec.	mag.	V	E	Mor.
31	N2804	9 14.00	20 24.00	14.00	8519	23	-2 0
	N2809	9 14.30	20 16.02	13.90	8077	75	-2 0
32	N2798	9 14.20	42 13.02	13.29	1923	35	1B0P
	N2799	9 14.30	42 12.00	14.40	2072	30	9B0S
33	N2832	9 16.80	33 58.98	13.31	7025	34	-4 0
	0919+3403	9 19.10	34 3.00	14.50	7163	23	-2 0
34	N2854	9 20.60	49 25.02	13.80	2952	20	3B0
	N2856	9 20.80	49 27.00	13.90	2858	19	5 0
35	N2911	9 31.10	10 22.02	13.82	3316	25	-2A0P
	N2914	9 31.40	10 19.98	14.19	3233	25	2B0S
36	N2927	9 34.40	23 49.02	14.10	7685	29	3X0
	N2929	9 34.60	23 22.98	14.40	7676	38	5 0
37	N2964	9 40.00	32 4.98	12.37	1488	20	4X3R
	N2968	9 40.20	32 10.02	13.25	1515	23	0 OP
38	N2998	9 45.60	44 19.02	12.62	4996	10	5X3T
	N3009	9 47.00	44 31.98	14.50	4825	36	5 0
39	N3003	9 45.60	33 39.00	12.52	1726	35	5X6
	N3021	9 48.00	33 46.98	13.23	1723	15	4A0T
40	N3020	9 47.40	13 3.00	13.20	1537	15	6B0R
	N3024	9 47.80	13 0.00	13.70	1597	25	5 0
41	0952+5932	9 52.60	59 31.98	13.30	3259	20	5 0
	N3043	9 52.70	59 32.70	13.66	3200	51	3 0
42	N3053	9 52.80	16 40.02	13.70	3900	30	1X0
	N3060	9 53.60	17 4.98	13.80	3860	27	3 0
43	N3073	9 57.50	55 52.02	13.80	1316	105	-3X0
	N3079	9 58.60	55 55.02	11.43	1374	25	5B3S
44	N3158	10 10.90	39 1.02	13.55	7037	25	-5 0
	N3163	10 11.20	38 52.98	14.40	6414	27	-3A0
45	N3206	10 18.50	57 10.98	12.70	1434	15	6B0S
	N3220	10 20.50	57 16.98	13.70	1500	35	0A0

Table 2: continued

No.	Name	R.A.	Dec.	mag.	V	E	Mor.
46	N3265	10 28.20	29 4.02	14.10	1626	28	-7 0
	N3277	10 30.10	28 46.02	12.60	1614	15	2A3R
47	N3259	10 29.10	65 18.00	13.02	2033	60	4X7T
	N3266	10 29.80	65 1.02	13.50	2190	86	-2X0
48	N3287	10 32.10	21 55.02	13.15	1486	33	7B7S
	N3301	10 34.20	22 7.98	12.43	1507	75	0B0T
49	1033+1358	10 33.70	13 58.02	14.20	3134	31	6 0
	N3300	10 34.00	14 25.98	13.21	3132	31	-2X0R
50	N3348	10 43.50	73 6.00	12.45	3131	21	-5 0
	N3364	10 44.70	72 40.02	13.65	3013	36	4X0T
51	1044+2648	10 44.30	26 48.00	14.40	6488	35	3A0
	1045+2651	10 45.70	26 51.00	14.50	6496	10	5A0P
52	N3425	10 48.80	8 49.98	14.50	6754	24	-2 0
	N3427	10 48.80	8 34.02	14.00	6389	45	0 0
53	1057+4600	10 57.30	46 0.00	14.40	11581	41	3A0
	1058+4555	10 58.70	45 55.02	14.10	9050	87	1 0
54	N3486	10 57.70	29 15.00	11.10	900	10	5X3R
	N3510	11 1.00	29 9.00	13.80	933	10	9B0S
55	1059+4530	10 59.10	45 30.00	13.40	6245	25	5B0
	1101+4524	11 1.80	45 24.00	13.00	6785	47	5 0
56	1059+1700	10 59.90	17 0.00	14.50	1211	10	7 0
	1100+1700	11 0.00	17 0.00	14.50	1210	10	5 0
57	1100+5029	11 0.20	50 28.98	14.50	7559	18	1B0
	1101+5005	11 1.10	50 4.98	14.40	7476	31	5A0
58	N3501	11 0.20	18 15.00	13.80	1319	15	5 0
	N3507	11 0.80	18 24.00	11.40	1161	10	3B0S
59	N3504	11 0.50	28 15.00	11.80	1755	19	2X0R
	N3512	11 1.30	28 18.00	13.12	1615	19	5X5T
60	N3521	11 3.30	0 13.98	9.82	902	10	4X3T
	I 678	11 6.80	0 10.02	14.50	1068	47	1A0

Table 2: continued

No.	Name	R.A.	Dec.	mag.	V	E	Mor.
61	1106+4705	11 6.80	47 4.98	14.30	7776	30	-3 0
	1108+4719	11 8.60	47 19.02	14.30	7861	32	-3 0
62	N3615	11 15.40	23 40.02	14.00	6898	30	-7 0
	N3618	11 15.90	23 45.00	14.40	7020	25	3A0
63	N3631	11 18.20	53 27.00	11.27	1458	8	5A1S
	N3657	11 21.10	53 12.00	13.10	1513	10	5X0T
64	N3646	11 19.10	20 27.00	12.12	4399	24	4 1
	N3649	11 19.60	20 28.02	14.50	4647	44	1 0
65	N3658	11 21.30	38 49.98	13.30	2312	15	-2A0R
	N3665	11 22.00	39 1.98	12.01	2349	16	-2A0S
66	1122+6401	11 22.40	64 1.02	14.10	4032	9	5A0T
	N3668	11 22.50	63 43.02	13.10	3758	27	4 0
67	I 694	11 25.69	58 49.98	12.60	3422	35	9B0P
	N3690	11 25.72	58 50.40	12.73	3408	32	9B0P
68	I 696	11 26.00	9 22.02	14.50	6472	41	5B0
	I 698	11 26.40	9 22.98	14.40	6351	28	-1 0
69	N3713	11 29.00	28 25.02	14.40	7231	26	-3 0
	N3714	11 29.20	28 37.98	14.30	7227	29	-5 0P
70	N3719	11 29.70	1 6.00	13.80	6031	40	3A0T
	N3720	11 29.80	1 4.98	13.00	6103	25	2 0
71	N3718	11 29.80	53 21.00	11.72	1290	10	1B0P
	N3729	11 31.10	53 24.00	12.26	1400	37	1B0R
72	N3733	11 32.30	55 7.98	13.20	1494	10	5X0S
	N3756	11 34.10	54 34.02	12.42	1589	10	4X3T
73	N3770	11 35.20	59 52.98	13.50	3526	27	1B0
	N3809	11 38.50	60 10.02	13.60	3757	44	-2 0
74	N3773	11 35.60	12 22.98	13.34	1156	9	-2A0
	N3810	11 38.40	11 45.00	11.40	1175	15	5A1T
75	N3786	11 37.10	32 10.98	13.50	2917	30	1X0T
	N3788	11 37.10	32 13.02	13.20	2887	23	2X0T

Table 2: continued

No.	Name	R.A.	Dec.	mag.	V	E	Mor.
76	N3799	11 37.60	15 36.00	14.40	3523	28	3BOP
	N3800	11 37.60	15 37.02	13.10	3508	11	3XOT
77	N3872	11 43.20	14 3.00	13.30	3406	22	-5 0
	1144+1359	11 44.50	13 58.98	14.40	3300	33	8 0
78	N3894	11 46.20	59 42.00	12.90	3573	25	-5 0
	N3895	11 46.40	59 43.02	14.00	3526	26	1B0T
79	N3900	11 46.60	27 18.00	12.63	2049	10	-1A5R
	N3912	11 47.50	26 46.02	13.00	2040	19	3X5P
80	N3902	11 46.70	26 24.00	14.00	3869	31	3X0S
	1147+2615	11 47.70	26 15.00	14.40	4004	46	2 0P
81	N3958	11 52.00	58 39.00	13.10	3640	23	1B0S
	N3963	11 52.40	58 46.02	12.52	3503	20	4X2T
82	I 749	11 56.00	43 1.02	13.40	1105	10	5B5T
	I 750	11 56.29	43 0.12	13.00	1004	22	2 0
83	1159+3007	11 59.50	30 7.02	14.30	3354	30	5 0
	1159+3008	11 59.80	30 7.98	14.40	3442	23	3 0
84	N4049	12 0.40	19 1.98	14.20	1068	25	10 0
	N4064	12 1.60	18 43.02	12.60	1262	47	1B5P
85	N4067	12 1.60	11 7.98	13.20	2600	25	3A0S
	N4078	12 2.20	10 52.02	13.90	2725	28	-2 0
86	N4073	12 1.90	2 10.98	12.98	6121	20	-3A0
	N4077	12 2.10	2 4.02	14.50	7185	20	-3 0
87	N4108	12 4.30	67 27.00	13.00	2808	40	5A0P
	N4108A	12 4.70	67 30.00	14.50	2898	37	5B0
88	N4116	12 5.10	2 58.02	12.71	1484	10	8B5T
	N4123	12 5.60	3 9.00	12.04	1490	10	5B5R
89	N4131	12 6.20	29 34.98	14.10	4002	25	3 0
	N4134	12 6.60	29 27.00	13.80	4099	26	3 0
90	N4145	12 7.50	40 10.02	11.68	1313	10	7X3T
	N4151	12 8.00	39 40.98	11.20	1269	0	2X0T

Table 2: continued

No.	Name	R.A.	Dec.	mag.	V	E	Mor.
91	N4185	12 10.80	28 46.98	13.50	4115	42	3 0
	N4196	12 11.90	28 42.00	13.70	4254	100	-2 0P
92	N4227	12 14.00	33 48.00	13.80	6738	26	0X0
	N4229	12 14.10	33 49.98	14.30	7101	21	-2 0
93	1216+4938	12 16.70	49 37.98	14.30	3960	30	5A0
	1217+5005	12 17.00	50 4.98	13.70	4429	21	0 0
94	N4335	12 20.60	58 43.98	13.70	4944	22	-5 0
	N4364	12 21.60	58 40.02	14.30	4825	27	-2 0
95	N4391	12 23.00	65 13.02	13.80	1666	74	-3A0
	N4441	12 25.10	65 4.02	13.50	1769	44	-1X0P
96	N4410A	12 23.93	9 17.82	14.30	7768	31	2 0P
	N4410B	12 23.95	9 17.82	14.30	7771	75	-2 0P
97	N4494	12 28.90	26 3.00	11.31	1623	13	-5 0
	N4565	12 33.90	26 16.02	10.61	1504	10	3A1S
98	N4517A	12 29.91	0 39.90	12.89	1696	10	8B9T
	N4517	12 30.20	0 22.98	11.43	1297	7	6A0S
99	N4527	12 31.60	2 55.98	11.68	1909	10	4X3S
	N4536	12 31.90	2 28.02	11.21	1991	8	4X3T
100	N4599	12 37.90	1 27.00	13.70	2054	23	1 0
	1238+0140	12 38.70	1 40.02	14.30	1915	30	5 0
101	N4614	12 39.00	26 18.00	14.20	5063	26	0B0
	N4615	12 39.10	26 19.98	13.80	4969	30	5 0
102	N4612	12 39.00	7 34.98	12.59	2090	24	-2X0R
	N4623	12 39.60	7 57.00	13.03	1996	56	-1B0
103	N4646	12 40.60	55 7.02	13.80	4886	127	-5 0
	1241+5510	12 41.50	55 10.02	14.50	5277	31	11 0P
104	N4686	12 44.40	54 49.02	13.70	5355	28	1 0
	N4695	12 45.30	54 39.00	14.50	5264	21	5X0
105	N4687	12 45.00	35 37.02	14.30	4572	23	-5 0
	N4711	12 46.40	35 36.00	14.40	4372	25	3 0

Table 2: continued

No.	Name	R.A.	Dec.	mag.	V	E	Mor.
106	N4725	12 48.00	25 46.02	10.21	1490	10	2X1R
	N4747	12 49.30	26 3.00	13.22	1474	10	6BOP
107	N4750	12 48.30	73 9.00	12.60	1846	60	2AOT
	1253+7328	12 53.20	73 28.02	14.40	1880	36	5 0
108	N4765	12 50.70	4 43.98	12.90	977	28	15 0
	N4808	12 53.30	4 34.02	12.64	963	15	6A5S
109	N4795	12 52.50	8 19.98	13.10	3030	21	1BOR
	N4796	12 52.50	8 19.98	14.50	2993	75	-6 0
110	1252+5902	12 52.50	59 1.98	14.40	2861	35	6 0
	N4814	12 53.20	58 37.02	13.16	2871	65	3A3S
111	N4868	12 56.80	37 34.98	13.15	5007	28	3A3
	N4914	12 58.40	37 34.98	12.85	4983	25	-3A0
112	N4952	13 2.60	29 24.00	13.60	6167	71	-5 0
	N4966	13 3.90	29 19.98	13.90	7332	40	-2 0
113	N5056	13 13.80	31 12.00	13.60	5919	15	5 0
	N5065	13 15.20	31 19.98	14.30	5878	20	5A0
114	N5107	13 19.10	38 48.00	13.70	1271	15	6BOS
	N5112	13 19.70	39 0.00	12.72	1310	10	6B3T
115	N5129	13 21.70	14 15.00	13.30	7167	26	-7 0
	N5132	13 22.00	14 21.00	14.30	7579	27	-2B0
116	N5173	13 26.30	46 51.00	14.12	2749	50	-5 0
	N5198	13 28.10	46 55.98	13.30	2833	44	-5 0
117	N5194	13 27.76	47 27.30	9.03	820	23	4A1P
	N5195	13 27.88	47 31.80	10.94	904	23	0 OP
118	N5208	13 29.90	7 34.98	14.40	6995	38	-2 0
	N5210	13 30.30	7 25.98	14.40	7067	32	1A0
119	N5216	13 30.40	62 57.00	14.00	3296	26	-5 0
	N5218	13 30.50	63 1.02	13.10	3207	25	3BOP
120	N5223	13 32.10	34 57.00	14.40	7543	27	-5 0
	N5228	13 32.30	35 1.98	14.50	8034	28	-3 0

Table 2: continued

No.	Name	R.A.	Dec.	mag.	V	E	Mor.
121	N5257	13 37.30	1 6.00	13.70	7105	30	3XOP
	N5258	13 37.40	1 4.98	13.80	6892	40	3AOP
122	1339+5554	13 39.50	55 54.00	14.10	7945	23	-2 0
	N5278	13 39.80	55 55.32	13.70	7921	25	3AOP
123	N5289	13 43.00	41 45.00	13.50	2860	15	2XOR
	N5290	13 43.20	41 58.02	13.00	2927	15	3 0
124	I 946	13 49.70	14 21.00	14.50	7114	25	1A0
	I 948	13 50.00	14 19.98	14.40	7183	25	-7 0
125	N5341	13 50.40	38 4.02	14.10	3988	10	9 0
	N5351	13 51.30	38 10.02	12.77	3972	11	3A3R
126	N5362	13 52.80	41 34.02	13.16	2524	0	3 OP
	N5383	13 55.00	42 6.00	12.14	2606	4	3B3T
127	1354+1541	13 54.90	15 40.98	14.50	5807	24	-1 0
	1355+1532	13 55.60	15 31.98	14.30	5865	30	9 0
128	N5406	13 58.20	39 9.00	13.05	5495	40	4X2T
	N5407	13 58.70	39 22.98	14.50	5776	28	-2 0
129	N5417	13 59.70	8 16.98	13.80	5065	21	1 0
	N5418	13 59.80	7 55.98	14.40	4791	36	3A0
130	N5448	14 0.93	49 24.78	12.53	2379	10	1X4R
	N5448	14 1.00	49 25.02	12.70	2352	27	3B0
131	N5480	14 4.50	50 58.02	12.90	2217	20	5A2S
	N5481	14 4.80	50 57.00	13.50	2361	23	-3A0
132	N5490	14 7.60	17 46.98	13.40	5298	23	-5B0
	I 983	14 7.70	17 58.02	14.30	5742	17	2B0
133	1412+1421	14 12.50	14 21.00	14.30	5244	31	1A0
	N5525	14 13.20	14 31.02	14.00	5834	18	-2 0
134	N5536	14 14.30	39 43.98	14.50	6197	16	1B0
	N5541	14 14.40	39 49.02	13.40	8047	26	5 OP
135	N5546	14 15.70	7 48.00	14.10	7575	29	-7 0
	N5549	14 16.10	7 36.00	14.20	7981	29	-2 0

Table 2: continued

No.	Name	R.A.	Dec.	mag.	V	E	Mor.
136	I 999	14 17.20	18 6.00	14.50	6032	33	-1 0
	I1000	14 17.30	18 4.98	14.40	5921	28	-2 0
137	N5598	14 20.50	40 33.00	14.30	5819	20	-2 0
	N5603	14 21.10	40 36.00	14.00	5977	25	-2 0
138	1426+7010	14 26.70	70 10.02	14.50	9735	89	-6 OP
	N5671	14 26.90	69 55.98	14.40	9360	27	3B0
139	N5638	14 27.10	3 27.00	12.67	1882	19	-5 0
	I1024	14 28.90	3 13.02	14.00	1737	38	-2 0
140	N5641	14 27.10	29 3.00	12.97	4676	23	2X2R
	N5657	14 28.50	29 24.00	14.40	4242	30	3B0
141	N5689	14 33.70	48 58.02	13.17	2524	22	0B0S
	N5693	14 34.40	48 48.00	14.50	2637	15	7B0T
142	N5684	14 33.80	36 45.00	14.20	4430	26	-2 0
	N5695	14 35.30	36 46.02	13.90	4610	31	20 0
143	N5740	14 41.90	1 52.98	12.89	1804	20	3X4T
	N5746	14 42.40	2 10.02	11.81	1954	10	3X0T
144	1448+3547	14 48.90	35 46.98	14.50	1554	34	11 OP
	1449+3545	14 49.20	35 45.00	14.20	1620	32	11 OP
145	N5784	14 52.40	42 45.00	13.70	5821	26	-2 0
	N5787	14 53.40	42 42.00	14.10	5854	22	0 0
146	N5789	14 54.40	30 25.02	13.90	2144	35	8 0
	N5798	14 55.50	30 10.02	13.50	2129	8	10 0
147	N5806	14 57.50	2 4.98	12.70	1585	10	3X5S
	N5813	14 58.70	1 54.00	12.09	2194	18	-5 0
148	N5857	15 5.20	19 46.98	14.29	5079	21	3B0S
	N5859	15 5.30	19 46.02	13.57	5069	31	4B0S
149	N5874	15 6.50	54 57.00	14.10	3492	10	4X0T
	N5876	15 8.10	54 42.00	13.90	3454	72	2B0R
150	N5879	15 8.50	57 10.98	12.32	1139	15	4A4T
	N5906	15 14.60	56 30.00	11.40	1030	7	5X0S

Table 2: continued

No.	Name	R.A.	Dec.	mag.	V	E	Mor.
151	N5905	15 14.00	55 42.00	12.41	3755	9	3B1R
	N5908	15 15.40	55 34.98	12.96	3673	10	3AOS
152	N5929	15 24.30	41 51.00	14.00	2909	22	2 OP
	N5930	15 24.40	41 51.00	13.60	2976	29	3XOT
153	N5934	15 26.40	43 4.98	14.50	5960	33	5 OP
	N5945	15 28.00	43 4.98	14.10	5881	27	1B0
154	N5956	15 32.60	11 55.02	13.30	2176	8	5 0
	N5957	15 33.00	12 13.02	13.30	2108	12	3XOR
155	N5992	15 42.60	41 15.00	14.20	9875	28	3B0
	N5993	15 42.70	41 16.98	13.90	9935	37	3 0
156	N6003	15 47.10	19 10.98	14.40	4364	29	-2 0
	N6004	15 48.10	19 4.98	13.40	4122	40	5B0
157	1554+4800	15 54.20	48 0.00	14.10	6358	21	-2 0
	I1152	15 55.30	48 13.98	14.40	6293	25	-7 0
158	N6127	16 18.20	58 6.00	13.00	4969	34	-7 0
	N6130	16 18.50	57 45.00	14.20	5426	32	4B0
159	1626+4120	16 26.80	41 19.98	14.30	8766	35	5 OP
	N6173	16 28.10	40 55.02	14.00	9151	25	-5 0
160	I5285	23 4.40	22 40.02	14.40	6210	23	0 0
	N7489	23 5.10	22 43.98	14.30	6260	15	5 0
161	N7537	23 12.00	4 13.98	14.13	2566	28	4A0
	N7541	23 12.20	4 16.02	12.80	2525	30	4B3T
162	N7550	23 12.80	18 40.98	13.90	5134	31	-3A0
	N7549	23 12.80	18 46.02	14.10	4666	38	6BOP
163	N7563	23 13.40	12 55.02	14.50	4277	25	1B0
	N7570	23 14.20	13 13.02	14.30	4618	28	1B0
164	N7673	23 25.20	23 19.02	12.70	3411	12	5AOP
	N7677	23 25.60	23 15.00	13.90	3551	15	4XOR
165	N7679	23 26.23	3 14.16	13.47	5021	25	-2BOP
	N7682	23 26.50	3 15.00	14.30	5009	29	2BOR

Table 2: continued

No.	Name	R.A.	Dec.	mag.	V	E	Mor.
166	N7720	23 36.00	26 45.00	13.90	9160	29	-3 OP
	N7728	23 37.40	26 52.02	14.30	9517	42	-7 0
167	2338+2557	23 38.10	25 57.00	14.50	770	8	9 8
	N7741	23 41.40	25 48.00	12.26	760	10	6B3S
168	N7731	23 39.00	3 28.02	14.30	2759	30	1B0
	N7732	23 39.10	3 27.00	14.50	2848	37	8 OP
169	N7752	23 44.50	29 10.98	14.30	5169	20	0 0
	N7753	23 44.60	29 12.00	13.20	5207	26	4X0T
170	N7767	23 48.30	26 49.02	14.20	8024	27	0 0
	N7768	23 48.40	26 52.98	14.00	8134	24	-5 0
171	N7769	23 48.50	19 52.02	13.04	4169	25	3A0T
	N7771	23 48.90	19 49.98	13.39	4336	31	1B0S
172	N7803	23 58.80	12 49.98	13.80	5226	27	0 0
	N7810	23 59.80	12 40.98	14.30	5456	29	-2 0
173	N7805	23 58.90	31 9.00	14.30	4976	21	-2XOP
	N7806	23 58.90	31 10.02	14.40	4855	22	4XOP
174	2359+2313	23 59.10	23 13.02	13.20	4367	26	6 OR
	2359+2314	23 59.20	23 13.98	13.90	4514	56	7B0P

Table 3: Unculled Binaries, $\Omega_0 = 0.03$

No.	BCPT	R.A.	Dec.	mag.	V	ΔV	θ
1	B P	0 7.50	25 36.83	12.69	4563	16	0.1643
2		0 18.68	22 6.56	13.20	5900	606	0.0791
3		0 34.23	23 42.72	13.13	4525	15	0.0050
4	B P	0 45.48	27 22.22	13.01	5035	216	0.1493
5	B P	0 55.04	30 4.05	12.28	4934	126	0.1065
6	BCP	1 17.37	3 9.00	11.87	2174	37	0.0766
7		1 19.61	8 52.30	12.83	2335	14	0.2894
8		1 25.08	-3 51.18	13.45	5380	274	0.0839
9	B	1 34.06	15 32.11	10.05	542	23	0.8509
10	C	1 44.94	27 8.58	11.21	368	16	0.1342
11		1 46.25	12 18.28	13.34	5222	254	0.2646
12	B	1 46.39	5 40.85	10.43	1347	77	0.4614
13	B T	1 56.59	18 45.80	11.34	2389	54	0.0559
14	B P	1 58.78	26 16.16	13.37	5007	93	0.0625
15	B PT	2 1.05	14 29.06	13.50	3513	7	0.0395
16	B	2 3.24	29 37.25	13.47	4898	166	0.1856
17	B P	2 15.14	14 19.02	12.52	3741	169	0.1938
18	P	2 25.39	20 4.57	13.00	3983	3	0.1493
19	B T	2 36.67	10 36.69	13.19	3380	163	0.1119
20	B P	2 37.31	1 18.94	13.70	5778	165	0.1047
21	C	2 39.93	-1 52.14	10.05	902	149	0.5120
22	B P	2 50.96	12 44.96	12.81	3438	19	0.1736
23	B	2 52.63	-1 36.93	13.11	8354	176	0.0122

Table 3: continued

No.	BCPT	R.A.	Dec.	mag.	V	ΔV	θ
24	B P	2 55.65	3 11.22	13.11	2912	28	0.1413
25	B PT	8 53.22	52 17.23	13.07	4147	252	0.0559
26	B PT	9 9.31	35 11.42	12.76	2156	66	0.1282
27		9 10.97	30 14.27	13.41	6922	197	0.2624
28	B P	9 14.16	20 19.83	13.20	8288	442	0.1506
29	B P	9 14.23	42 12.75	12.96	1962	149	0.0251
30	B P	9 20.70	49 25.96	13.10	2907	94	0.0484
31	B P	9 31.22	10 21.17	13.24	3282	83	0.0815
32	BCP	9 40.06	32 6.53	11.97	1496	27	0.0949
33	B	9 47.55	13 1.84	12.67	1560	60	0.1101
34	B	9 52.64	59 32.28	12.71	3234	59	0.0280
35	B	9 58.49	55 54.72	11.31	1368	58	0.1631
36	B	10 10.99	38 58.50	13.14	6842	623	0.1467
37	B	10 19.07	57 12.69	12.34	1453	66	0.2887
38	CPT	10 20.76	20 7.76	11.70	1363	105	0.0484
39	B	10 29.37	65 11.36	12.48	2094	157	0.2921
40		10 39.58	13 58.94	11.46	1428	122	0.3449
41	P	10 48.51	28 15.88	12.10	1614	138	0.1356
42	B	10 48.80	8 40.19	13.47	6530	365	0.2654
43		10 56.74	46 20.50	12.79	6886	256	0.2341
44	B	10 59.95	17 0.00	13.75	1211	1	0.0342
45	B	11 0.74	18 23.11	11.29	1177	158	0.2056
46	BC	11 0.68	28 15.69	11.52	1723	140	0.1824
47	B	11 3.35	0 13.93	9.81	904	166	0.8774

Table 3: continued

No.	BCPT	R.A.	Dec.	mag.	V	ΔV	θ
48	B P	11 15.60	23 42.06	13.43	6948	122	0.1426
49		11 16.04	58 13.87	12.04	2340	87	0.3202
50	BC	11 18.65	53 24.65	11.09	1467	55	0.4997
51	B	11 19.15	20 27.10	12.01	4424	248	0.1170
52	BC	11 21.84	38 59.18	11.72	2340	37	0.2423
53		11 24.05	57 15.49	12.53	2109	199	0.2357
54	BC T	11 25.71	58 50.18	11.91	3415	14	0.0079
55	B	11 26.21	9 22.52	13.70	6409	121	0.1028
56	B P	11 29.10	28 31.80	13.60	7229	4	0.2203
57	B PT	11 29.77	1 5.31	12.58	6080	72	0.0280
58	BC	11 30.29	53 22.13	11.20	1332	110	0.1998
59		11 30.51	62 8.46	13.07	3583	34	0.1342
60		11 33.39	55 10.72	13.33	5889	9	0.2167
61		11 34.07	58 37.79	13.08	1564	43	0.2357
62	B PT	11 37.10	32 12.14	12.59	2900	30	0.0342
63		11 37.58	17 59.75	12.99	3508	179	0.1203
64	B PT	11 37.60	15 36.78	12.81	3511	15	0.0198
65		11 39.38	20 28.37	12.94	5762	11	0.2502
66		11 43.17	20 41.55	13.47	7067	55	0.2661
67	B PT	11 46.25	59 42.27	12.56	3560	47	0.0280
68		11 50.42	20 58.18	13.34	6680	367	0.1998
69	BCP	11 52.25	58 43.43	12.02	3554	137	0.1282
70		11 54.96	53 38.45	10.75	1367	32	0.2324
71	CPT	11 56.17	43 0.49	12.43	1045	101	0.0559

Table 3: continued

No.	BCPT	R.A.	Dec.	mag.	V	ΔV	\bar{G}
72	B PT	11 59.64	30 7.48	13.60	3396	88	0.0625
73		12 1.35	64 41.64	13.14	1681	134	0.2140
74	B P	12 1.81	11 2.49	12.74	2643	125	0.3032
75	C	12 2.97	50 47.13	11.19	1067	3	0.1877
76		12 3.40	20 49.34	13.70	7260	590	0.1251
77	B	12 4.38	67 27.60	12.76	2826	90	0.0625
78		12 4.58	43 21.34	11.95	1118	164	0.1370
79	BCP	12 5.42	3 5.15	11.57	1488	6	0.2220
80	B	12 6.43	29 30.44	13.19	4057	97	0.1595
81	BC	12 7.80	39 52.34	10.66	1286	44	0.4934
82	B	12 11.30	28 44.72	12.84	4178	139	0.2549
83	B PT	12 14.04	33 48.77	13.27	6878	363	0.0395
84	C	12 14.35	7 34.72	12.27	2809	55	0.3045
85	P	12 15.06	6 57.36	13.18	2431	27	0.1282
86	CPT	12 18.86	11 46.98	12.10	517	131	0.0969
87	CPT	12 19.08	14 52.98	11.78	1370	30	0.0523
88	B P	12 20.97	58 42.53	13.21	4901	119	0.1454
89	C T	12 21.25	16 59.03	11.52	1321	315	0.0766
90	C T	12 23.00	18 28.22	10.18	1032	157	0.1203
91	C	12 23.25	16 36.51	12.15	1953	47	0.3292
92	B P	12 24.19	65 7.90	12.89	1725	103	0.2669
93		12 24.22	15 26.81	11.98	300	29	0.6691
94	B	12 23.94	9 17.82	13.55	7770	3	0.0198
95		12 24.15	9 9.51	13.65	1479	11	0.0766

Table 3: continued

No.	BCPT	R.A.	Dec.	mag.	V	ΔV	θ
96	C	12 24.87	13 10.32	11.65	311	7	0.4949
97	C	12 25.25	9 57.86	11.30	698	85	0.4302
98	C	12 27.08	14 3.50	11.02	1523	139	0.4126
99	C T	12 28.19	41 55.34	10.17	883	122	0.0484
100		12 31.53	7 56.46	10.92	803	31	0.5546
101	BCP	12 31.78	2 39.02	10.67	1959	82	0.4715
102	C	12 33.08	12 45.76	11.04	560	57	0.3334
103	CPT	12 34.06	11 31.41	11.41	2434	46	0.0342
104	CP	12 37.87	10 26.63	11.39	2075	12	0.3202
105	B PT	12 39.06	26 19.17	13.23	5007	94	0.0395
106	C	12 39.24	7 43.79	12.04	2052	94	0.3951
107	C	12 39.17	41 27.46	11.38	877	64	0.1532
108	C	12 41.08	3 5.44	10.56	1072	149	0.6813
109	B P	12 40.91	55 8.05	13.34	5021	391	0.1385
110	B	12 44.69	54 45.78	13.28	5326	91	0.2112
111	BC	12 48.08	25 47.02	10.14	1489	16	0.4073
112	B	12 52.50	8 19.98	12.84	3022	37	0.0000
113		12 55.37	27 47.89	13.19	7772	105	0.2832
114	BCP	12 57.71	37 34.98	12.24	4993	24	0.3165
115		12 57.54	28 14.68	12.76	7018	664	0.1119
116		12 58.89	27 59.52	13.37	8183	222	0.2669
117	C	13 9.76	37 6.45	10.17	1285	130	0.6714
118	B P	13 19.53	38 56.54	12.35	1299	39	0.2315
119	B P	13 21.79	14 16.71	12.94	7284	412	0.1235

Table 3: continued

No.	BCPT	R.A.	Dec.	mag.	V	ΔV	θ
120	P	13 22.70	36 38.95	13.20	5576	53	0.0559
121	BC T	13 27.77	47 27.96	8.86	832	84	0.0791
122	B	13 30.10	7 30.48	13.65	7031	72	0.1802
123	B P	13 30.47	62 59.80	12.71	3234	89	0.0685
124	B	13 32.20	34 59.38	13.70	7777	491	0.0906
125	B PT	13 37.35	1 5.51	13.00	7003	213	0.0280
126	B	13 39.68	55 54.78	13.13	7931	24	0.0484
127	B P	13 43.12	41 52.98	12.47	2901	67	0.2185
128	P	13 47.38	40 13.36	12.59	2936	156	0.1724
129	B	13 49.86	14 20.47	13.70	7150	69	0.0713
130	B P	13 51.10	38 8.66	12.49	3976	16	0.2027
131	B	13 55.28	15 36.07	13.64	5839	58	0.2247
132	B	13 58.30	39 11.91	12.80	5554	281	0.2518
133	BC	14 0.96	49 24.89	11.86	2367	27	0.0118
134	C	14 4.17	55 10.79	11.98	2354	20	0.3701
135	B PT	14 4.61	50 57.65	12.41	2270	144	0.0523
136	B	14 7.63	17 50.33	13.01	5433	444	0.1866
137	B P	14 15.89	7 42.28	13.40	7769	406	0.2238
138	B PT	14 17.25	18 5.47	13.70	5974	111	0.0342
139	P	14 17.77	4 10.48	11.44	1829	164	0.0713
140	P	14 19.43	35 26.38	13.14	3636	149	0.0766
141	B P	14 20.84	40 34.71	13.39	5909	158	0.1251
142	B	14 26.80	70 2.68	13.70	9539	375	0.2349
143	PT	14 28.30	14 12.90	13.30	5436	67	0.0815

Table 3: continued

No.	BCPT	R.A.	Dec.	mag.	V	ΔV	θ
144	B P	14 33.86	48 55.74	12.89	2550	113	0.2037
145	BCP	14 42.26	2 5.42	11.47	1914	150	0.3103
146	B PT	14 49.07	35 45.85	13.59	1592	66	0.0685
147	B P	14 52.81	42 43.77	13.13	5834	33	0.1897
148		15 3.86	1 48.12	11.56	1896	263	0.1203
149	B PT	15 5.27	19 46.35	13.12	5072	10	0.0342
150	BCP	15 14.53	55 39.36	11.90	3724	82	0.2307
151	B T	15 24.36	41 51.00	13.03	2949	67	0.0186
152	BCP	15 32.80	12 4.02	12.55	2142	68	0.3159
153	B PT	15 42.66	41 16.13	13.29	9909	60	0.0395
154	B	15 47.82	19 6.69	13.04	4191	242	0.2572
155	B P	23 4.77	22 42.09	13.60	6236	50	0.1747
156	B PT	23 12.15	4 15.56	12.52	2534	41	0.0593
157	B P	23 12.80	18 43.27	13.24	4921	468	0.0862
158	B P	23 25.30	23 18.02	12.39	3446	140	0.1153
159	B PT	23 26.31	3 14.43	13.05	5017	12	0.0685
160	B	23 36.57	26 47.87	13.33	9306	357	0.3334
161	B P	23 39.05	3 27.56	13.64	2799	89	0.0280
162	B P	23 44.57	29 11.73	12.86	5197	38	0.0280
163	B P	23 48.35	26 51.18	13.34	8084	110	0.0685
164	BCP	23 48.67	19 51.16	12.45	4239	167	0.0989
165	B P	23 58.90	31 9.49	13.60	4918	121	0.0170
166	B P	23 59.13	23 13.35	12.74	4418	147	0.0280

Table 4: Unculled Binary Galaxies, $\Omega_0 = 0.03$

No.	Name	R.A.	Dec.	mag.	V	E	Mor.
1	N 23	0 7.31	25 38.70	13.12	4558	15	1BOS
	N 26	0 7.90	25 33.00	13.90	4574	15	2AOT
2	N 80	0 18.60	22 4.98	13.74	5662	22	-3A0
	N 83	0 18.80	22 9.00	14.21	6268	28	-5 0
3	I1559	0 34.23	23 42.60	13.70	4519	31	-2XOP
	N 169	0 34.23	23 42.90	14.10	4534	25	2 0
4	N 252	0 45.30	27 21.00	13.40	4969	31	-2 0
	N 260	0 45.90	27 25.02	14.30	5185	25	5 0P
5	N 311	0 54.80	30 0.00	14.10	5037	16	-2 0
	N 315	0 55.10	30 4.98	12.50	4911	18	0-5A
6	N 470	1 17.20	3 9.00	12.75	2195	10	3AOT
	N 474	1 17.50	3 9.00	12.51	2158	21	-2AOP
7	N 489	1 19.20	8 55.98	13.40	2329	27	5 0
	N 502	1 20.20	8 46.98	13.80	2343	16	-2 0
8	N 560	1 24.90	-3 49.98	14.41	5219	74	-3 0
	N 564	1 25.20	-3 52.02	14.02	5493	74	-5 0
9	N 628	1 34.00	15 31.98	10.07	542	2	5A1S
	0137+1539	1 37.50	15 39.00	14.38	519	10	10 9
10	I1727	1 44.70	27 4.98	12.20	378	33	9B6S
	N 672	1 45.10	27 10.98	11.76	362	6	6B5S
11	0145+1221	1 45.80	12 21.00	14.00	5337	90	1BOP
	0146+1215	1 46.80	12 15.00	14.20	5083	25	0 0
12	N 676	1 46.30	5 40.02	10.50	1342	20	0 0
	N 693	1 47.90	5 54.00	13.50	1419	24	0 0
13	N 770	1 56.50	18 43.02	14.20	2439	22	-5 0
	N 772	1 56.60	18 46.02	11.42	2385	23	3A1S
14	0158+2615	1 58.70	26 15.00	13.90	5043	35	1 0
	0158+2618	1 58.90	26 18.00	14.40	4950	15	1XOS
15	I 195	2 1.00	14 28.02	14.30	3517	28	-2 0
	I 196	2 1.10	14 30.00	14.20	3510	21	-3B0

Table 4: continued

No.	Name	R.A.	Dec.	mag.	V	E	Mor.
16	0203+2933	2 3.20	29 33.00	14.00	4962	28	-3 0
	0203+2944	2 3.30	29 43.98	14.50	4796	25	3 0
17	N 871	2 14.50	14 19.02	14.30	3605	10	5BOS
	N 877	2 15.30	14 19.02	12.76	3774	10	4X1T
18	N 930	2 25.10	20 6.00	13.70	3982	37	1 0
	N 938	2 25.70	20 3.00	13.80	3985	34	-7 0
19	N1024	2 36.50	10 37.98	13.80	3310	25	2AOR
	N1029	2 36.90	10 34.98	14.10	3473	18	0 0
20	I1827	2 37.10	1 19.98	14.50	5692	26	1A0
	N1038	2 37.50	1 18.00	14.40	5857	25	1 0
21	N1055	2 39.20	0 13.98	11.77	784	10	3B4
	N1068	2 40.12	-1 46.50	10.30	933	16	3AOT
22	N1134	2 50.90	12 48.00	13.20	3444	20	2 OP
	I 267	2 51.10	12 37.98	14.10	3425	21	3B0
23	N1143	2 52.60	-1 37.20	14.20	8242	31	-2 OP
	N1144	2 52.64	-1 36.78	13.60	8418	32	10 OP
24	N1153	2 55.50	3 10.02	13.50	2921	22	-5 0
	0256+0314	2 56.00	3 13.98	14.40	2893	28	-5 OP
25	0853+5218	8 53.10	52 18.00	13.60	4244	21	1 0
	N2692	8 53.40	52 16.02	14.10	3992	30	1 0
26	N2778	9 9.20	35 13.02	13.10	2174	22	-7 0
	N2780	9 9.60	35 7.02	14.20	2108	32	3 0
27	N2783	9 10.60	30 10.98	13.90	6850	28	-7 0
	0911+3020	9 11.60	30 19.98	14.50	7047	28	-1 0
28	N2804	9 14.00	20 24.00	14.00	8519	23	-2 0
	N2809	9 14.30	20 16.02	13.90	8077	75	-2 0
29	N2798	9 14.20	42 13.02	13.29	1923	35	1BOP
	N2799	9 14.30	42 12.00	14.40	2072	30	9BOS
30	N2854	9 20.60	49 25.02	13.80	2952	20	3B0
	N2856	9 20.80	49 27.00	13.90	2858	19	5 0

Table 4: continued

No.	Name	R.A.	Dec.	mag.	V	E	Mor.
31	N2911	9 31.10	10 22.02	13.82	3316	25	-2AOP
	N2914	9 31.40	10 19.98	14.19	3233	25	2BOS
32	N2964	9 40.00	32 4.98	12.37	1488	20	4X3R
	N2968	9 40.20	32 10.02	13.25	1515	23	0 OP
33	N3020	9 47.40	13 3.00	13.20	1537	15	6BOR
	N3024	9 47.80	13 0.00	13.70	1597	25	5 0
34	0952+5932	9 52.60	59 31.98	13.30	3259	20	5 0
	N3043	9 52.70	59 32.70	13.66	3200	51	3 0
35	N3073	9 57.50	55 52.02	13.80	1316	105	-3X0
	N3079	9 58.60	55 55.02	11.43	1374	25	5B3S
36	N3158	10 10.90	39 1.02	13.55	7037	25	-5 0
	N3163	10 11.20	38 52.98	14.40	6414	27	-3A0
37	N3206	10 18.50	57 10.98	12.70	1434	15	6BOS
	N3220	10 20.50	57 16.98	13.70	1500	35	0A0
38	N3226	10 20.70	20 9.00	12.77	1429	24	-5 OP
	N3227	10 20.80	20 7.02	12.20	1324	41	1XOP
39	N3259	10 29.10	65 18.00	13.02	2033	60	4X7T
	N3266	10 29.80	65 1.02	13.50	2190	86	-2X0
40	N3338	10 39.50	14 1.02	11.59	1442	7	5A3S
	1040+1343	10 40.20	13 43.02	13.80	1320	35	7BOP
41	N3414	10 48.50	28 15.00	12.23	1629	20	-2 OP
	N3418	10 48.60	28 22.98	14.50	1491	24	0 0
42	N3425	10 48.80	8 49.98	14.50	6754	24	-2 0
	N3427	10 48.80	8 34.02	14.00	6389	45	0 0
43	N3478	10 56.60	46 22.98	13.04	6939	20	4B2T
	1057+4611	10 57.30	46 10.98	14.50	6683	24	-7 0
44	1059+1700	10 59.90	17 0.00	14.50	1211	10	7 0
	1100+1700	11 0.00	17 0.00	14.50	1210	10	5 0
45	N3501	11 0.20	18 15.00	13.80	1319	15	5 0
	N3507	11 0.80	18 24.00	11.40	1161	10	3BOS

Table 4: continued

No.	Name	R.A.	Dec.	mag.	V	E	Mor.
46	N3504	11 0.50	28 15.00	11.80	1755	19	2XOR
	N3512	11 1.30	28 18.00	13.12	1615	19	5X5T
47	N3521	11 3.30	0 13.98	9.82	902	10	4X3T
	I 678	11 6.80	0 10.02	14.50	1068	47	1A0
48	N3615	11 15.40	23 40.02	14.00	6898	30	-7 0
	N3618	11 15.90	23 45.00	14.40	7020	25	3A0
49	N3613	11 15.70	58 16.02	12.25	2356	75	-5 0
	N3625	11 17.60	58 4.02	13.90	2269	31	3XOS
50	N3631	11 18.20	53 27.00	11.27	1458	8	5A1S
	N3657	11 21.10	53 12.00	13.10	1513	10	5XOT
51	N3646	11 19.10	20 27.00	12.12	4399	24	4 1
	N3649	11 19.60	20 28.02	14.50	4647	44	1 0
52	N3658	11 21.30	38 49.98	13.30	2312	15	-2AOR
	N3665	11 22.00	39 1.98	12.01	2349	16	-2AOS
53	N3674	11 23.60	57 19.98	13.10	2190	50	-2 0
	N3683	11 24.70	57 9.00	13.50	1991	18	5BOS
54	I 694	11 25.69	58 49.98	12.60	3422	35	9BOP
	N3690	11 25.72	58 50.40	12.73	3408	32	9BOP
55	I 696	11 26.00	9 22.02	14.50	6472	41	5B0
	I 698	11 26.40	9 22.98	14.40	6351	28	-1 0
56	N3713	11 29.00	28 25.02	14.40	7231	26	-3 0
	N3714	11 29.20	28 37.98	14.30	7227	29	-5 OP
57	N3719	11 29.70	1 6.00	13.80	6031	40	3AOT
	N3720	11 29.80	1 4.98	13.00	6103	25	2 0
58	N3718	11 29.80	53 21.00	11.72	1290	10	1BOP
	N3729	11 31.10	53 24.00	12.26	1400	37	1BOR
59	1129+6206	11 29.90	62 6.00	14.10	3562	15	5A0
	N3725	11 30.90	62 10.02	13.60	3596	44	5B0
60	N3737	11 32.90	55 13.98	13.90	5893	120	-2B0
	N3759	11 34.10	55 6.00	14.30	5884	25	-2 0

Table 4: continued

No.	Name	R.A.	Dec.	mag.	V	E	Mor.
61	1133+5829	11 33.60	58 28.98	14.30	1535	38	5A0
	N3757	11 34.30	58 42.00	13.50	1578	21	-2 0
62	N3786	11 37.10	32 10.98	13.50	2917	30	1X0T
	N3788	11 37.10	32 13.02	13.20	2887	23	2X0T
63	N3790	11 37.20	17 58.98	14.50	3642	27	0 0
	N3801	11 37.70	18 0.00	13.30	3463	70	-2 0P
64	N3799	11 37.60	15 36.00	14.40	3523	28	3B0P
	N3800	11 37.60	15 37.02	13.10	3508	11	3X0T
65	N3816	11 39.20	20 22.02	13.60	5767	49	-2 0
	N3821	11 39.60	20 36.00	13.80	5756	44	1B0
66	1142+2044	11 42.50	20 43.98	14.50	7101	27	-2 0
	N3884	11 43.60	20 40.02	14.00	7046	30	1 0
67	N3894	11 46.20	59 42.00	12.90	3573	25	-5 0
	N3895	11 46.40	59 43.02	14.00	3526	26	1B0T
68	N3937	11 50.10	20 55.02	14.00	6847	100	-3 0
	N3947	11 50.80	21 1.98	14.20	6480	33	3B0
69	N3958	11 52.00	58 39.00	13.10	3640	23	1B0S
	N3963	11 52.40	58 46.02	12.52	3503	20	4X2T
70	1154+5327	11 54.20	53 27.00	14.10	1398	15	10 0
	N3992	11 55.00	53 39.00	10.80	1366	10	4B1T
71	I 749	11 56.00	43 1.02	13.40	1105	10	5B5T
	I 750	11 56.29	43 0.12	13.00	1004	22	2 0
72	1159+3007	11 59.50	30 7.02	14.30	3354	30	5 0
	1159+3008	11 59.80	30 7.98	14.40	3442	23	3 0
73	1200+6439	12 0.10	64 39.00	14.30	1769	28	-2 0
	N4081	12 2.00	64 43.02	13.60	1635	37	1 0
74	N4067	12 1.60	11 7.98	13.20	2600	25	3A0S
	N4078	12 2.20	10 52.02	13.90	2725	28	-2 0
75	N4085	12 2.83	50 37.92	13.11	1065	10	5X5S
	N4088	12 3.00	50 49.02	11.39	1068	10	4X2T

Table 4: continued

No.	Name	R.A.	Dec.	mag.	V	E	Mor.
76	N4092	12 3.30	20 46.02	14.40	6979	29	4 0
	N4098	12 3.50	20 52.98	14.50	7569	34	9 0
77	N4108	12 4.30	67 27.00	13.00	2808	40	5A0P
	N4108A	12 4.70	67 30.00	14.50	2898	37	5B0
78	N4111	12 4.50	43 21.00	12.08	1099	14	-1A0R
	N4117	12 5.20	43 24.00	14.30	1263	28	-2 0
79	N4116	12 5.10	2 58.02	12.71	1484	10	8B5T
	N4123	12 5.60	3 9.00	12.04	1490	10	5B5R
80	N4131	12 6.20	29 34.98	14.10	4002	25	3 0
	N4134	12 6.60	29 27.00	13.80	4099	26	3 0
81	N4145	12 7.50	40 10.02	11.68	1313	10	7X3T
	N4151	12 8.00	39 40.98	11.20	1269	0	2X0T
82	N4185	12 10.80	28 46.98	13.50	4115	42	3 0
	N4196	12 11.90	28 42.00	13.70	4254	100	-2 OP
83	N4227	12 14.00	33 48.00	13.80	6738	26	0X0
	N4229	12 14.10	33 49.98	14.30	7101	21	-2 0
84	N4224	12 14.00	7 43.98	13.21	2841	36	1A0S
	N4235	12 14.60	7 28.02	12.86	2786	18	1A0S
85	N4241	12 14.90	6 58.02	13.60	2422	25	0A0S
	I3115	12 15.40	6 55.98	14.40	2449	23	5B0
86	N4294	12 18.70	11 46.98	12.67	571	8	6B6S
	N4299	12 19.10	11 46.98	13.06	440	15	8X7S
87	N4298	12 19.00	14 52.98	12.34	1358	22	5A0T
	N4302	12 19.20	14 52.98	12.76	1388	22	5 0
88	N4335	12 20.60	58 43.98	13.70	4944	22	-5 0
	N4364	12 21.60	58 40.02	14.30	4825	27	-2 0
89	N4340	12 21.10	17 0.00	12.25	1167	10	-1B0R
	N4350	12 21.40	16 58.02	12.30	1482	20	-2A0
90	N4382	12 22.90	18 28.02	10.43	1000	13	-1A0P
	N4394	12 23.40	18 28.98	11.90	1157	8	3B3R

Table 4: continued

No.	Name	R.A.	Dec.	mag.	V	E	Mor.
91	N4383	12 22.90	16 45.00	12.90	1930	31	1 OP
	N4405	12 23.60	16 28.02	12.90	1977	31	0AOT
92	N4391	12 23.00	65 13.02	13.80	1666	74	-3A0
	N4441	12 25.10	65 4.02	13.50	1769	44	-1XOP
93	N4396	12 23.50	15 57.00	13.70	78	26	7A0
	N4419	12 24.40	15 19.02	12.23	49	12	1BOS
94	N4410A	12 23.93	9 17.82	14.30	7768	31	2 OP
	N4410B	12 23.95	9 17.82	14.30	7771	75	-2 OP
95	N4411A	12 24.00	9 9.00	14.40	1484	20	7X0
	N4411B	12 24.30	9 10.02	14.40	1473	20	7A0
96	N4413	12 24.00	12 52.98	13.04	316	9	3BOT
	N4438	12 25.20	13 16.98	12.00	309	23	0AOP
97	N4424	12 24.70	9 42.00	12.57	639	15	1B5S
	N4442	12 25.50	10 4.98	11.70	724	19	-2BOS
98	N4459	12 26.50	14 15.00	11.95	1443	16	-1AOR
	N4477	12 27.50	13 55.02	11.62	1582	11	-2BOS
99	N4485	12 28.10	41 58.02	12.60	774	50	10B6P
	N4490	12 28.20	41 55.02	10.29	896	26	7B5P
100	N4526	12 31.50	7 58.02	10.97	805	15	-2XOS
	I3521	12 32.10	7 25.98	14.20	774	35	10 0
101	N4527	12 31.60	2 55.98	11.68	1909	10	4X3S
	N4536	12 31.90	2 28.02	11.21	1991	8	4X3T
102	N4550	12 33.00	12 30.00	12.73	605	15	-1B0
	N4552	12 33.10	12 49.98	11.30	548	13	-5 0
103	N4567	12 34.00	11 31.98	12.37	2407	43	4AOT
	N4568	12 34.10	11 31.02	11.98	2453	40	4AOT
104	N4596	12 37.40	10 27.00	11.88	2071	28	-1BOR
	N4608	12 38.70	10 25.98	12.48	2083	24	-2BOR
105	N4614	12 39.00	26 18.00	14.20	5063	26	0B0
	N4615	12 39.10	26 19.98	13.80	4969	30	5 0

Table 4: continued

No.	Name	R.A.	Dec.	mag.	V	E	Mor.
106	N4612	12 39.00	7 34.98	12.59	2090	24	-2XOR
	N4623	12 39.60	7 57.00	13.03	1996	56	-1B0
107	N4618	12 39.10	41 25.98	11.60	865	8	9B0T
	N4625	12 39.50	41 34.02	13.22	929	10	9X0T
108	N4636	12 40.30	2 58.02	11.01	1122	15	-5 0
	N4665	12 42.60	3 19.98	11.74	973	50	0B0S
109	N4646	12 40.60	55 7.02	13.80	4886	127	-5 0
	1241+5510	12 41.50	55 10.02	14.50	5277	31	11 0P
110	N4686	12 44.40	54 49.02	13.70	5355	28	1 0
	N4695	12 45.30	54 39.00	14.50	5264	21	5X0
111	N4725	12 48.00	25 46.02	10.21	1490	10	2X1R
	N4747	12 49.30	26 3.00	13.22	1474	10	6B0P
112	N4795	12 52.50	8 19.98	13.10	3030	21	1B0R
	N4796	12 52.50	8 19.98	14.50	2993	75	-6 0
113	N4839	12 55.00	27 46.02	13.60	7739	67	-3A0
	N4853	12 56.20	27 52.02	14.46	7844	50	-3A0
114	N4868	12 56.80	37 34.98	13.15	5007	28	3A3
	N4914	12 58.40	37 34.98	12.85	4983	25	-3A0
115	N4874	12 57.20	28 13.98	14.01	7472	24	-4 0
	N4889	12 57.70	28 15.00	13.17	6808	23	-4 0
116	N4911	12 58.50	28 3.00	13.90	8269	30	4X0R
	N4926	12 59.50	27 54.00	14.40	8047	54	-3A0
117	N5005	13 8.60	37 19.02	10.85	1346	16	4X3T
	N5033	13 11.10	36 52.02	11.00	1216	16	5A2S
118	N5107	13 19.10	38 48.00	13.70	1271	15	6B0S
	N5112	13 19.70	39 0.00	12.72	1310	10	6B3T
119	N5129	13 21.70	14 15.00	13.30	7167	26	-7 0
	N5132	13 22.00	14 21.00	14.30	7579	27	-2B0
120	N5141	13 22.60	36 37.98	13.90	5551	33	-2 0
	N5142	13 22.80	36 40.02	14.00	5604	31	-2 0

Table 4: continued

No.	Name	R.A.	Dec.	mag.	V	E	Mor.
121	N5194	13 27.76	47 27.30	9.03	820	23	4A1P
	N5195	13 27.88	47 31.80	10.94	904	23	0 OP
122	N5208	13 29.90	7 34.98	14.40	6995	38	-2 0
	N5210	13 30.30	7 25.98	14.40	7067	32	1A0
123	N5216	13 30.40	62 57.00	14.00	3296	26	-5 0
	N5218	13 30.50	63 1.02	13.10	3207	25	3BOP
124	N5223	13 32.10	34 57.00	14.40	7543	27	-5 0
	N5228	13 32.30	35 1.98	14.50	8034	28	-3 0
125	N5257	13 37.30	1 6.00	13.70	7105	30	3XOP
	N5258	13 37.40	1 4.98	13.80	6892	40	3AOP
126	1339+5554	13 39.50	55 54.00	14.10	7945	23	-2 0
	N5278	13 39.80	55 55.32	13.70	7921	25	3AOP
127	N5289	13 43.00	41 45.00	13.50	2860	15	2XOR
	N5290	13 43.20	41 58.02	13.00	2927	15	3 0
128	N5311	13 46.80	40 13.98	13.70	3036	23	0 0
	N5313	13 47.70	40 13.02	13.07	2880	25	3 3
129	I 946	13 49.70	14 21.00	14.50	7114	25	1A0
	I 948	13 50.00	14 19.98	14.40	7183	25	-7 0
130	N5341	13 50.40	38 4.02	14.10	3988	10	9 0
	N5351	13 51.30	38 10.02	12.77	3972	11	3A3R
131	1354+1541	13 54.90	15 40.98	14.50	5807	24	-1 0
	1355+1532	13 55.60	15 31.98	14.30	5865	30	9 0
132	N5406	13 58.20	39 9.00	13.05	5495	40	4X2T
	N5407	13 58.70	39 22.98	14.50	5776	28	-2 0
133	N5448	14 0.93	49 24.78	12.53	2379	10	1X4R
	N5448	14 1.00	49 25.02	12.70	2352	27	3B0
134	N5473	14 3.00	55 7.98	12.66	2363	38	-3XOS
	N5485	14 5.50	55 13.98	12.80	2343	50	-2AOP
135	N5480	14 4.50	50 58.02	12.90	2217	20	5A2S
	N5481	14 4.80	50 57.00	13.50	2361	23	-3A0

Table 4: continued

No.	Name	R.A.	Dec.	mag.	V	E	Mor.
136	N5490	14 7.60	17 46.98	13.40	5298	23	-5B0
	I 983	14 7.70	17 58.02	14.30	5742	17	2B0
137	N5546	14 15.70	7 48.00	14.10	7575	29	-7 0
	N5549	14 16.10	7 36.00	14.20	7981	29	-2 0
138	I 999	14 17.20	18 6.00	14.50	6032	33	-1 0
	I1000	14 17.30	18 4.98	14.40	5921	28	-2 0
139	N5560	14 17.60	4 13.02	13.48	1968	20	3B0P
	N5566	14 17.80	4 10.02	11.62	1804	24	2B4R
140	N5589	14 19.30	35 28.98	14.30	3734	30	1B0
	N5590	14 19.50	35 25.02	13.60	3585	26	-2 0
141	N5598	14 20.50	40 33.00	14.30	5819	20	-2 0
	N5603	14 21.10	40 36.00	14.00	5977	25	-2 0
142	1426+7010	14 26.70	70 10.02	14.50	9735	89	-6 OP
	N5671	14 26.90	69 55.98	14.40	9360	27	3B0
143	N5648	14 28.20	14 15.00	14.10	5401	30	5 0
	N5649	14 28.40	14 10.98	14.00	5468	31	5 0
144	N5689	14 33.70	48 58.02	13.17	2524	22	0B0S
	N5693	14 34.40	48 48.00	14.50	2637	15	7B0T
145	N5740	14 41.90	1 52.98	12.89	1804	20	3X4T
	N5746	14 42.40	2 10.02	11.81	1954	10	3X0T
146	1448+3547	14 48.90	35 46.98	14.50	1554	34	11 OP
	1449+3545	14 49.20	35 45.00	14.20	1620	32	11 OP
147	N5784	14 52.40	42 45.00	13.70	5821	26	-2 0
	N5787	14 53.40	42 42.00	14.10	5854	22	0 0
148	N5845	15 3.47	1 49.62	13.51	1677	10	-5 0
	N5846	15 3.94	1 47.82	11.76	1940	11	-5 0
149	N5857	15 5.20	19 46.98	14.29	5079	21	3B0S
	N5859	15 5.30	19 46.02	13.57	5069	31	4B0S
150	N5905	15 14.00	55 42.00	12.41	3755	9	3B1R
	N5908	15 15.40	55 34.98	12.96	3673	10	3A0S

Table 4: continued

No.	Name	R.A.	Dec.	mag.	V	E	Mor.
151	N5929	15 24.30	41 51.00	14.00	2909	22	2 OP
	N5930	15 24.40	41 51.00	13.60	2976	29	3XOT
152	N5956	15 32.60	11 55.02	13.30	2176	8	5 0
	N5957	15 33.00	12 13.02	13.30	2108	12	3XOR
153	N5992	15 42.60	41 15.00	14.20	9875	28	3BO
	N5993	15 42.70	41 16.98	13.90	9935	37	3 0
154	N6003	15 47.10	19 10.98	14.40	4364	29	-2 0
	N6004	15 48.10	19 4.98	13.40	4122	40	5BO
155	I5285	23 4.40	22 40.02	14.40	6210	23	0 0
	N7489	23 5.10	22 43.98	14.30	6260	15	5 0
156	N7537	23 12.00	4 13.98	14.13	2566	28	4AO
	N7541	23 12.20	4 16.02	12.80	2525	30	4B3T
157	N7550	23 12.80	18 40.98	13.90	5134	31	-3AO
	N7549	23 12.80	18 46.02	14.10	4666	38	6BOP
158	N7673	23 25.20	23 19.02	12.70	3411	12	5AOP
	N7677	23 25.60	23 15.00	13.90	3551	15	4XOR
159	N7679	23 26.23	3 14.16	13.47	5021	25	-2BOP
	N7682	23 26.50	3 15.00	14.30	5009	29	2BOR
160	N7720	23 36.00	26 45.00	13.90	9160	29	-3 OP
	N7728	23 37.40	26 52.02	14.30	9517	42	-7 0
161	N7731	23 39.00	3 28.02	14.30	2759	30	1BO
	N7732	23 39.10	3 27.00	14.50	2848	37	8 OP
162	N7752	23 44.50	29 10.98	14.30	5169	20	0 0
	N7753	23 44.60	29 12.00	13.20	5207	26	4XOT
163	N7767	23 48.30	26 49.02	14.20	8024	27	0 0
	N7768	23 48.40	26 52.98	14.00	8134	24	-5 0
164	N7769	23 48.50	19 52.02	13.04	4169	25	3AOT
	N7771	23 48.90	19 49.98	13.39	4336	31	1BOS
165	N7805	23 58.90	31 9.00	14.30	4976	21	-2XOP
	N7806	23 58.90	31 10.02	14.40	4855	22	4XOP

Table 4: continued

No.	Name	R.A.	Dec.	mag.	V	E	Mor.
166	2359+2313	23 59.10	23 13.02	13.20	4367	26	6 OR
	2359+2314	23 59.20	23 13.98	13.90	4514	56	7BOP

Table 5: Effect of Culling Procedure on Sample Size

Cull	Ω_0^{in}							
	0.01	0.02	0.03	0.04	0.05	0.10	0.20	1.00
14.5	133	155	165	174	173	171	173	172
14.4	116	134	138	143	141	142	141	140
14.3	105	120	122	125	121	118	116	112
14.2	92	105	103	107	103	99	96	87
14.1	80	93	91	93	89	85	80	69
14.0	65	78	77	79	75	71	68	58
13.9	57	72	72	74	70	63	61	48
13.8	50	65	66	67	63	55	53	40
13.7	44	56	57	58	53	48	46	33
13.6	39	49	50	51	46	40	40	28
13.5	39	48	49	50	46	40	39	27
13.4	34	42	42	43	39	34	34	21
13.3	31	40	40	39	37	30	30	19
13.2	26	35	34	33	31	25	25	15
13.1	22	30	31	30	28	22	19	10
13.0	20	26	26	25	23	18	16	9

Table 6: Omega Determination

Ω_0^{in}	Cull	#	$\langle M/L \rangle_c$	$\langle M/L \rangle_t$	Ω_0^{out}
1.00	13.4	21	302.	1020	0.66
0.20	13.8	53	46.3	157.	0.10
0.10	13.3	30	18.1	61.3	0.039
0.05	13.4	39	13.3	45.1	0.029
0.04	13.3	39	9.64	32.7	0.021
0.03	13.4	42	12.2	38.6	0.025
0.02	13.0	26	10.8	36.7	0.023
0.01	13.6	39	5.61	19.0	0.012

Table 7: Velocity Dispersion Comparisons
(unculled binaries)

Ω_0	Rp in kpc			
	10	30	90	270
1.00	98	79	172	611
0.20	85	93	342	380
0.10	85	116	280	274
0.05	80	92	148	295
0.04	81	114	147	257
0.03	81	113	162	265
0.02	76	116	125	248
0.01	68	93	114	250
Turner	193	205	267	---

FIGURES

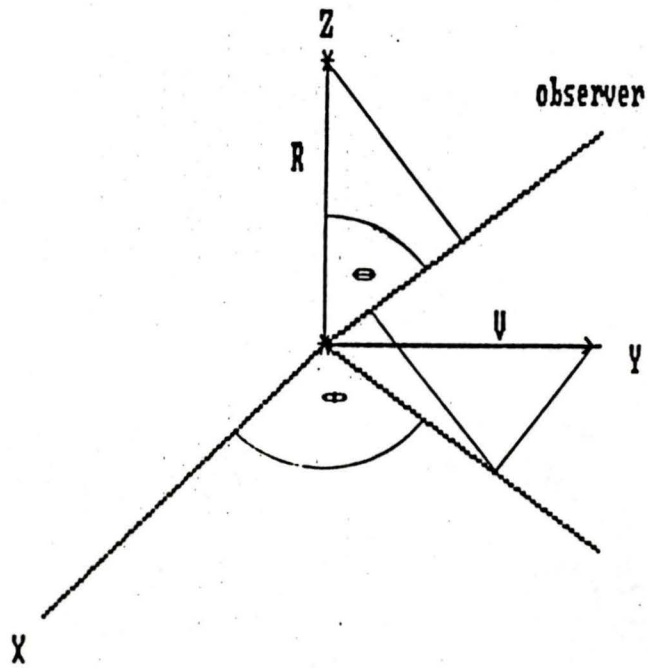


Figure 1: Projection Geometry

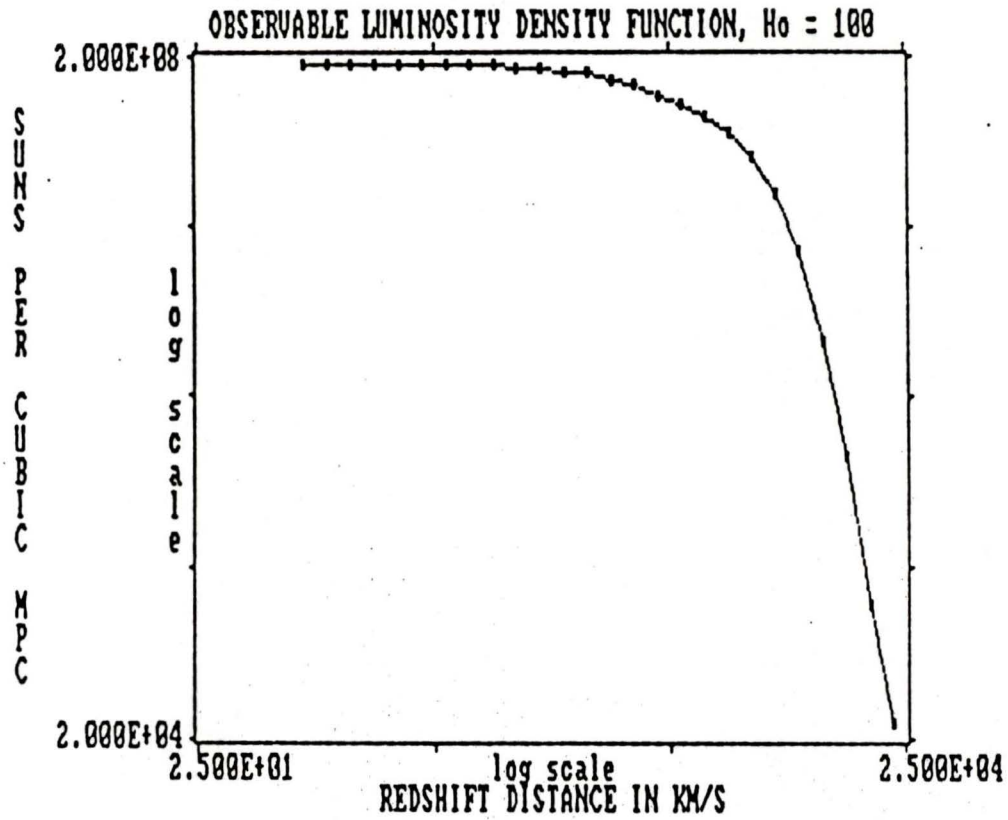


Figure 2: Observable Luminosity Density Function, $H_0 = 100$

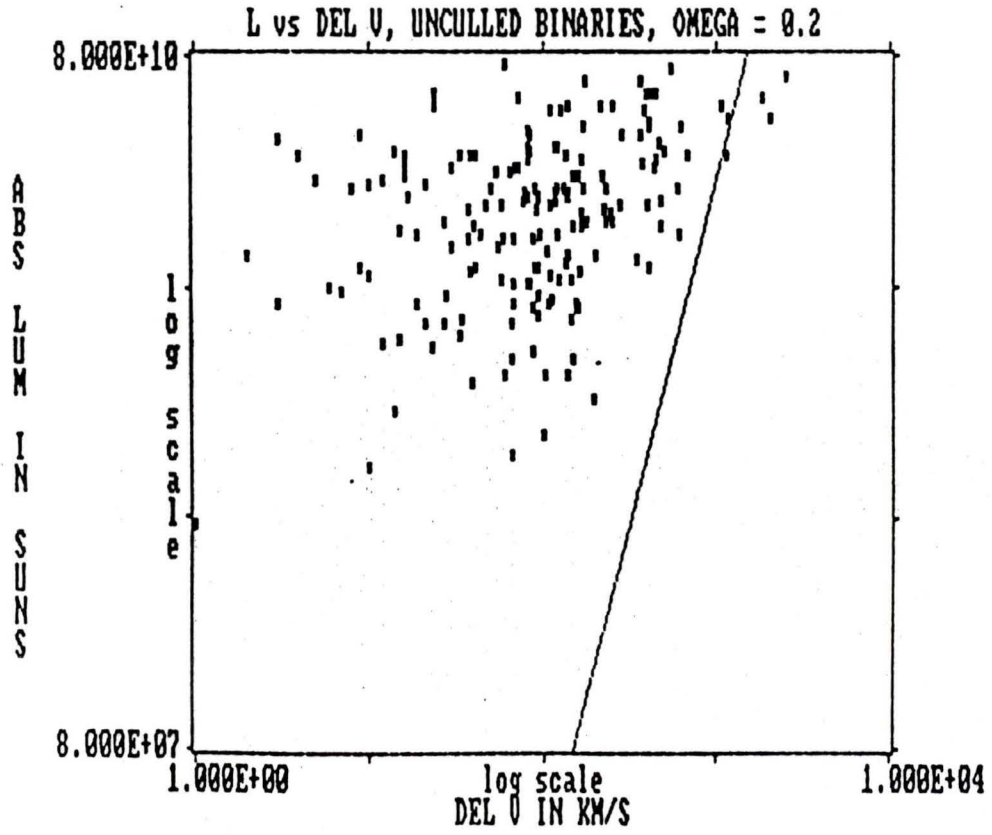


Figure 3: L vs Del V, Unculled Binaries, Omega = 0.2

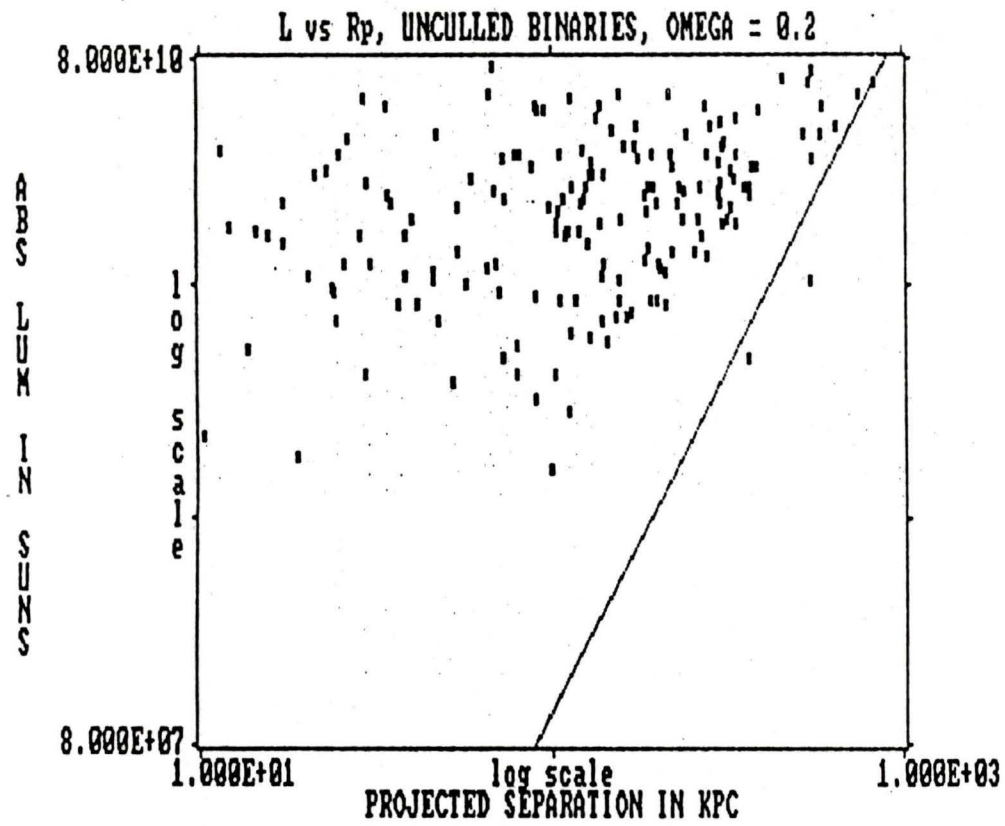


Figure 4: L vs Rp, Unculled Binaries, Omega = 0.2

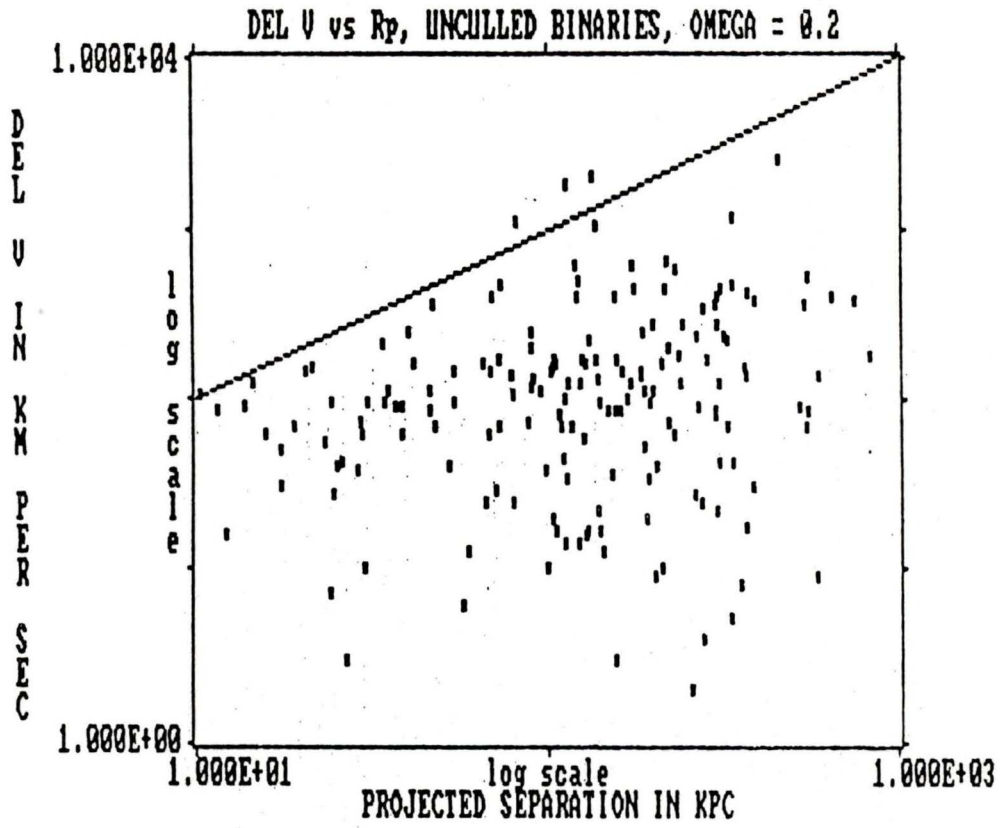


Figure 5: Del V vs Rp, Uncultured Binaries, Omega = 0.2

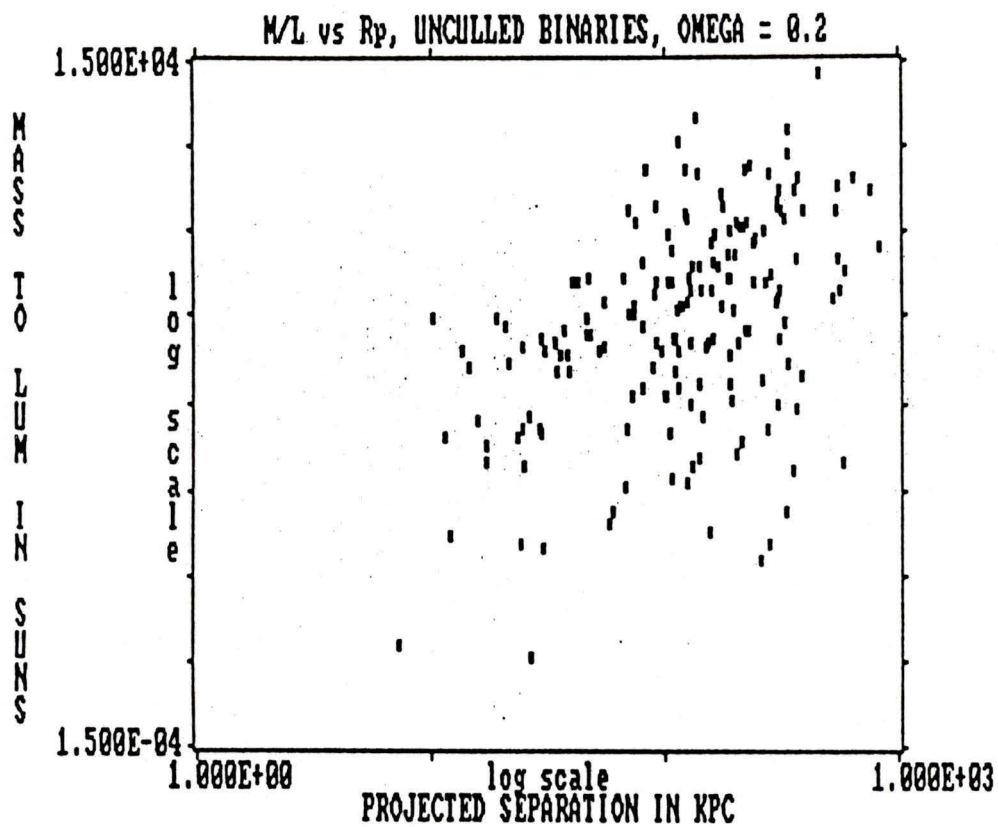


Figure 6: M/L vs R_p , Unculled Binaries, $\Omega = 0.2$

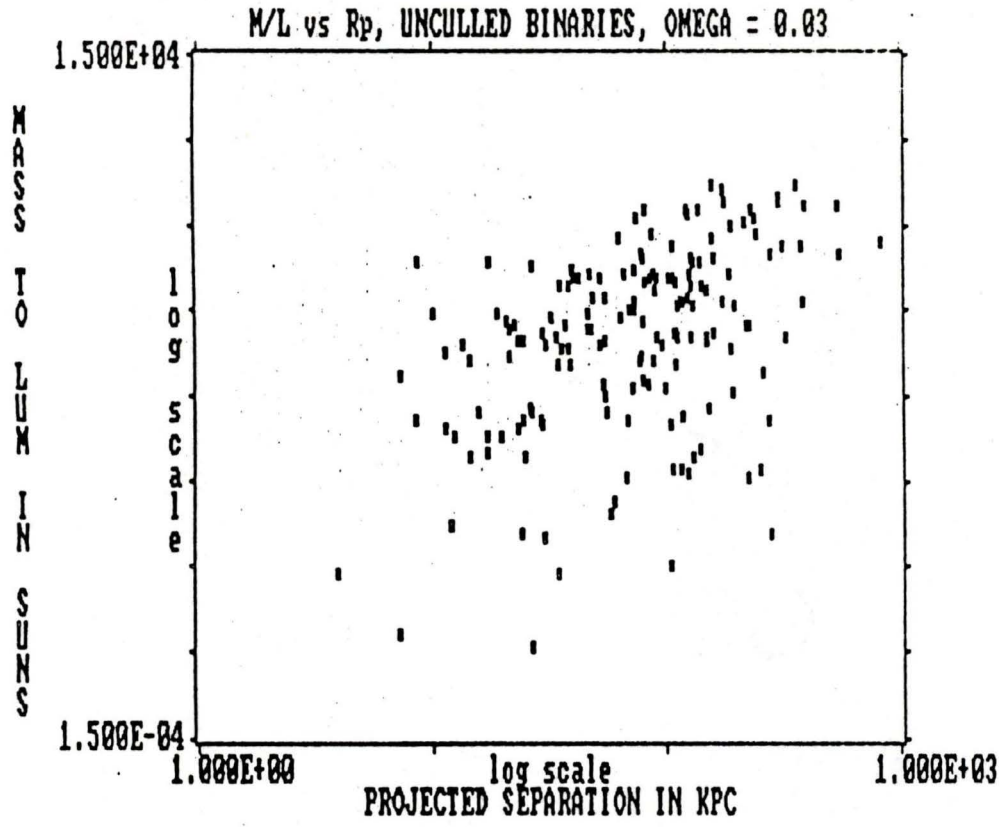


Figure 7: M/L vs R_p , Unculled Binaries, $\Omega = 0.03$

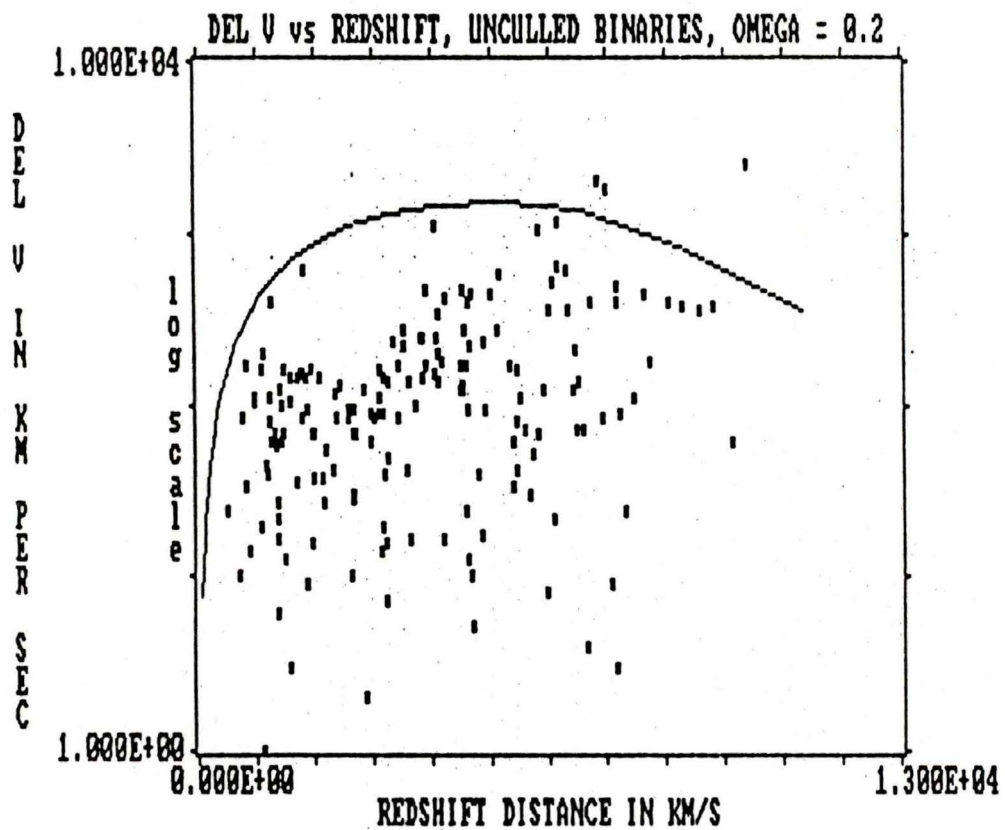


Figure 8: Del V vs Redshift, Unculled Binaries, Omega = 0.2

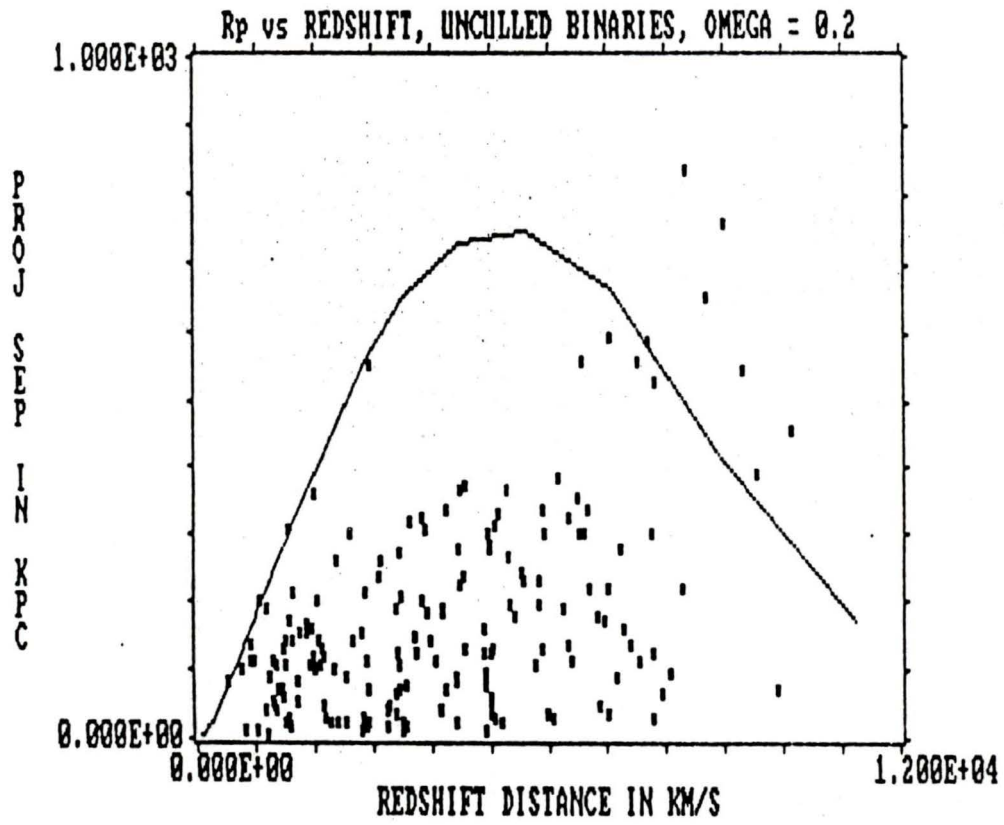


Figure 9: Rp vs Redshift, Uncultured Binaries, Omega = 0.2

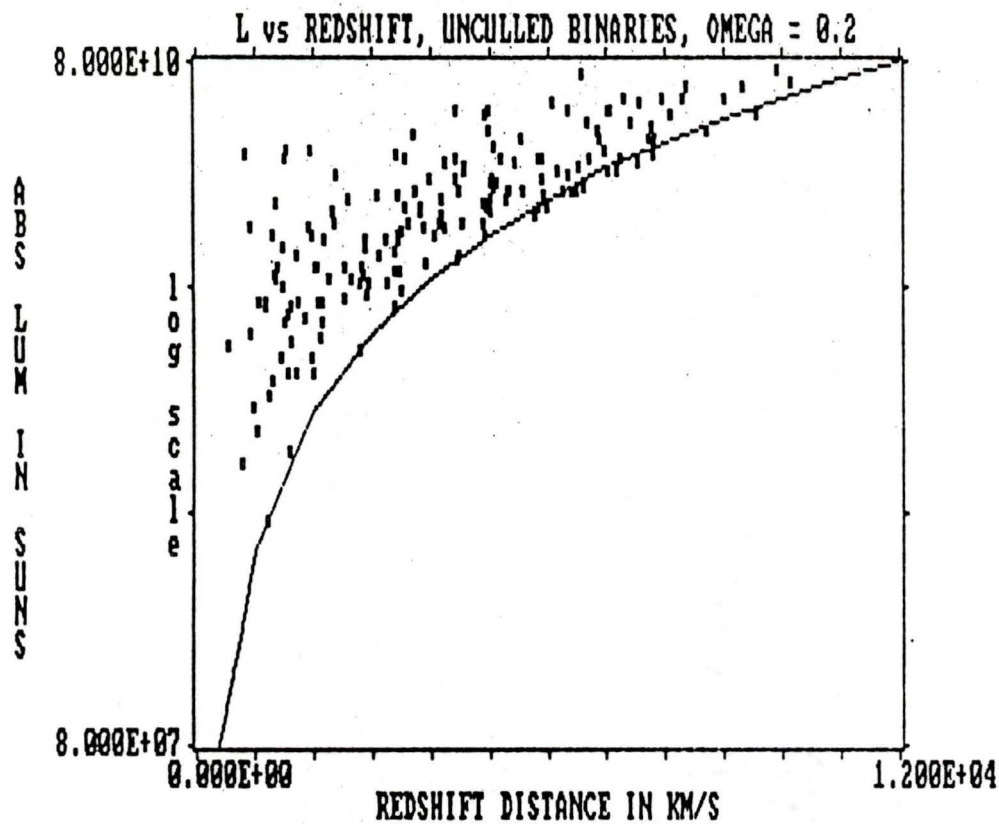


Figure 10: L vs Redshift, Unculled Binaries, Omega = 0.2

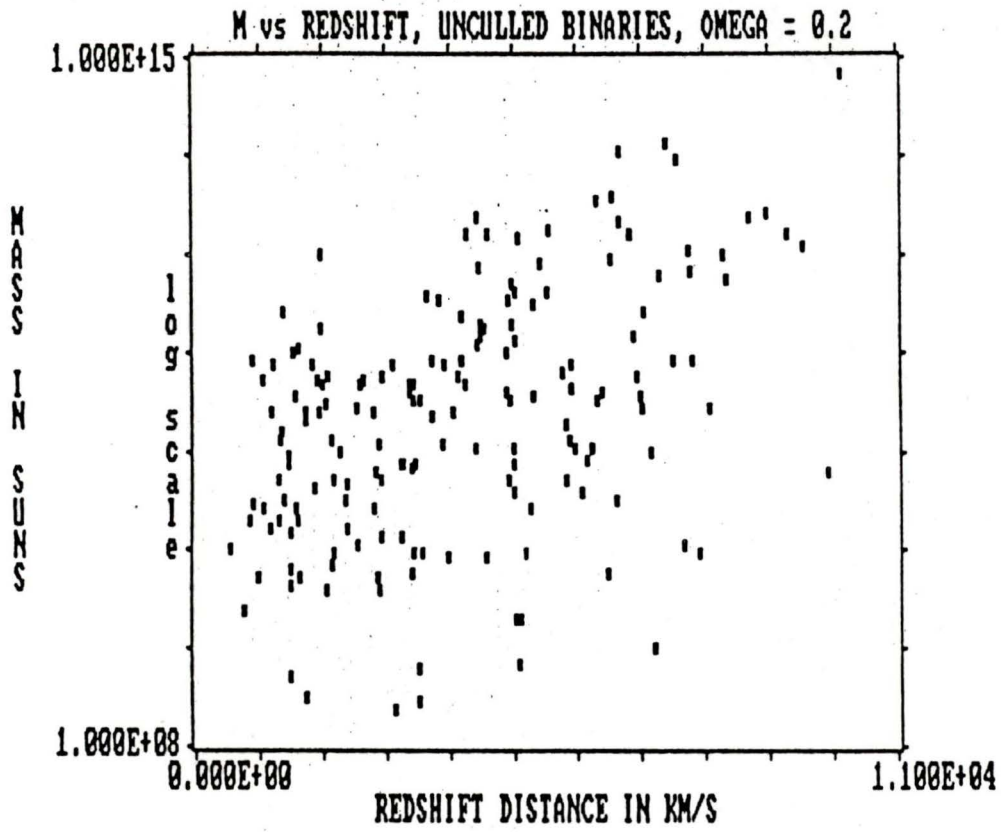


Figure 11: M vs Redshift, Unculled Binaries, Omega = 0.2

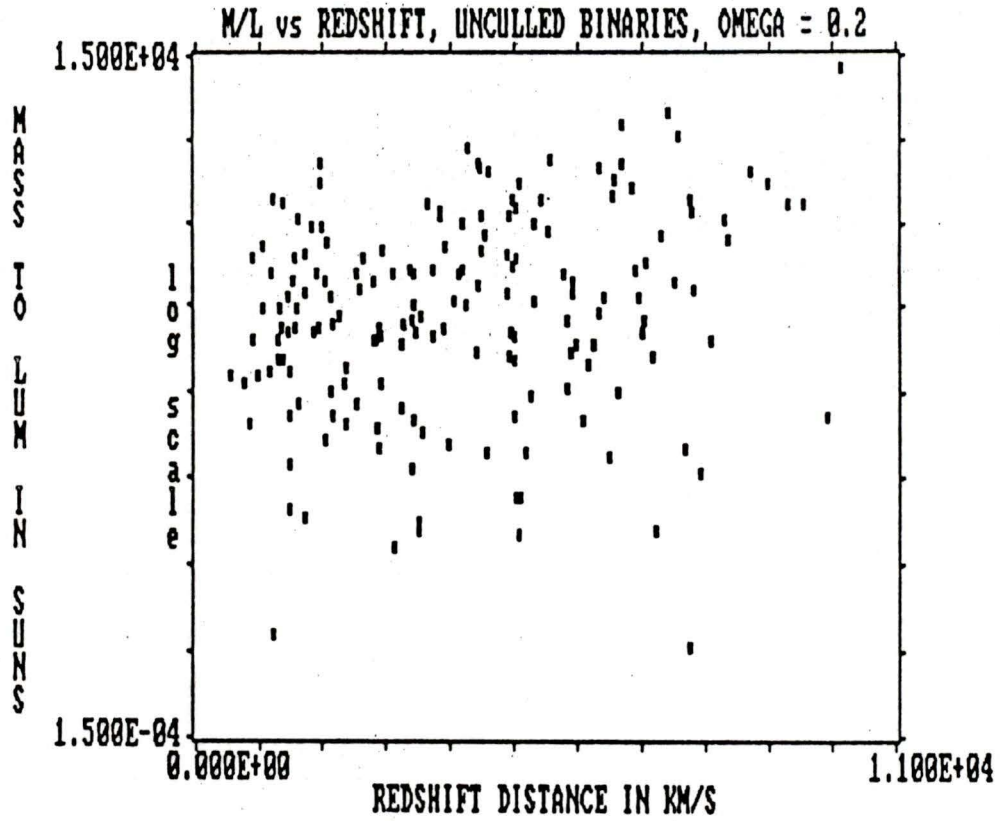


Figure 12: M/L vs Redshift, Unculled Binaries, Omega = 0.2

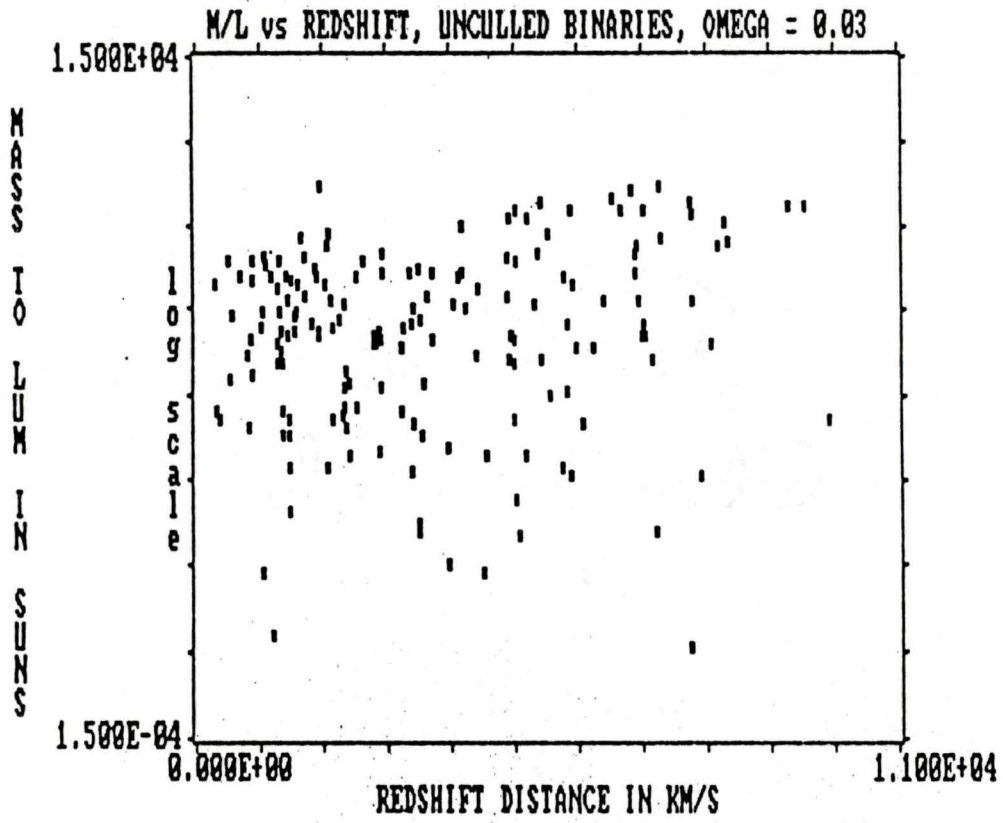


Figure 13: M/L vs Redshift, Uncultured Binaries, Omega = 0.03

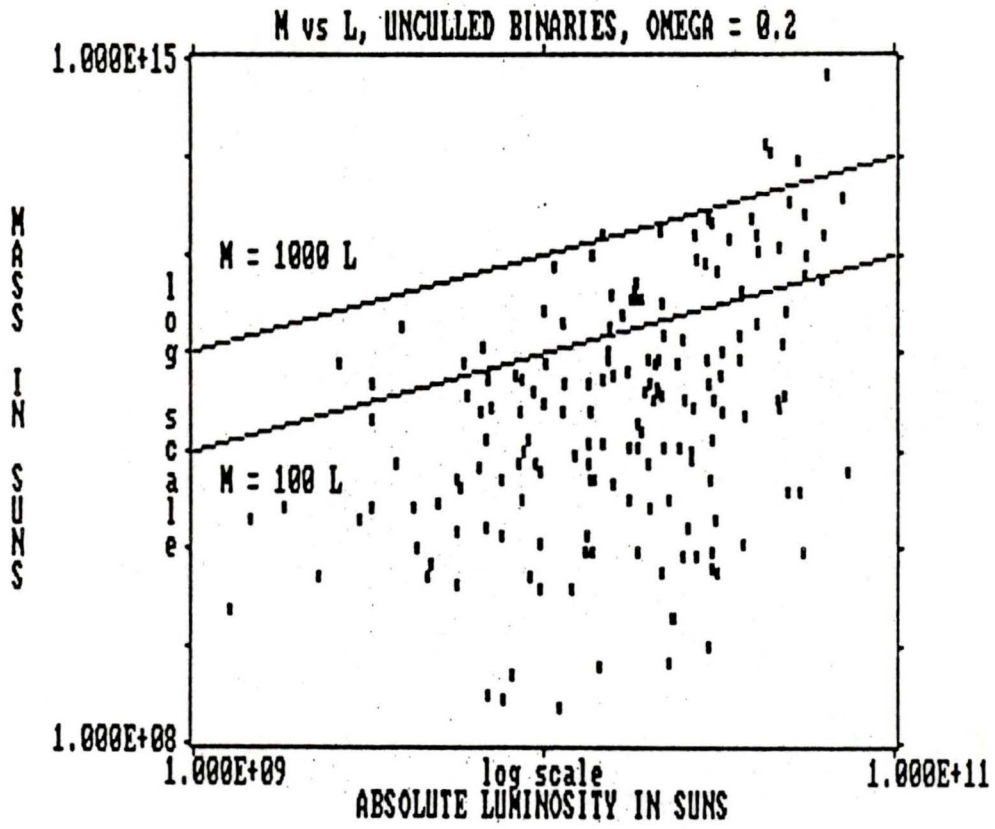


Figure 14: M vs L, Unculled Binaries, Omega = 0.2

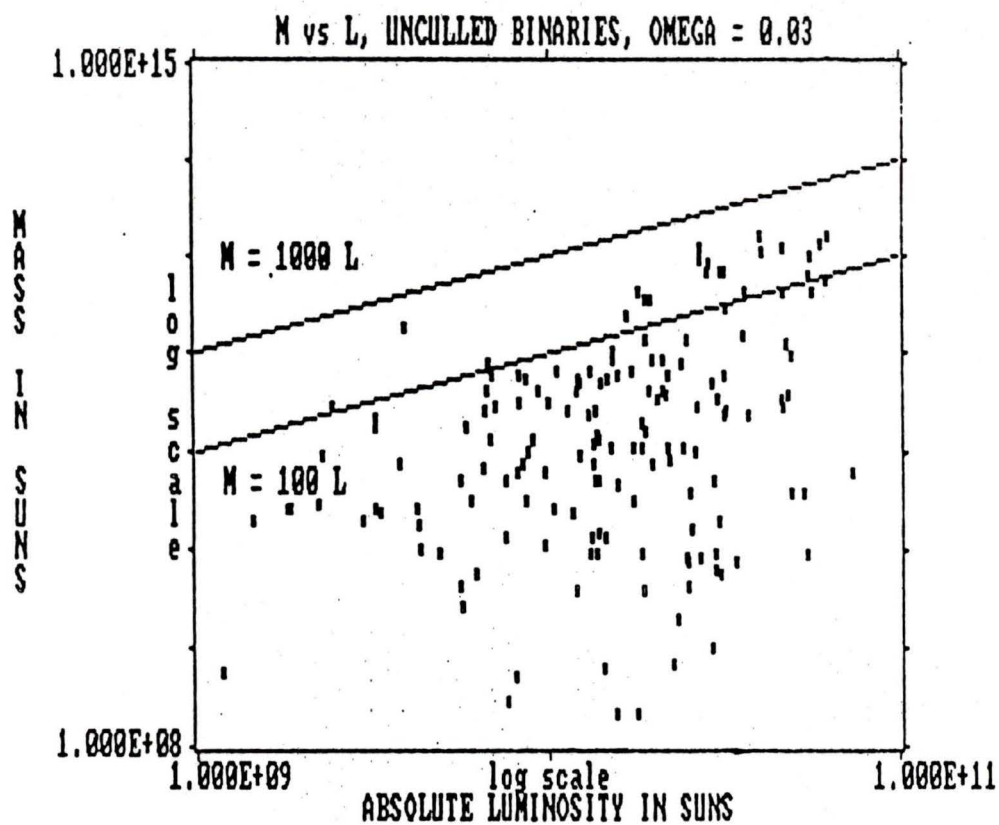


Figure 15: M vs L, Unculled Binaries, Omega = 0.03

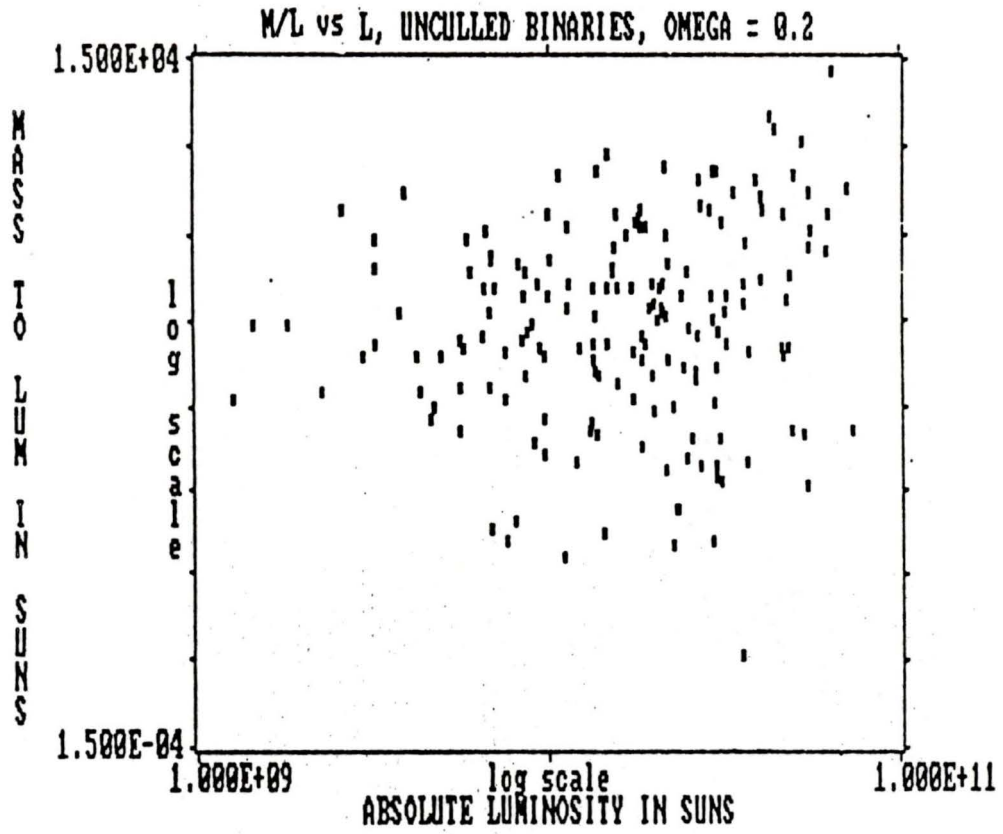


Figure 16: M/L vs L, Unculled Binaries, Omega = 0.2

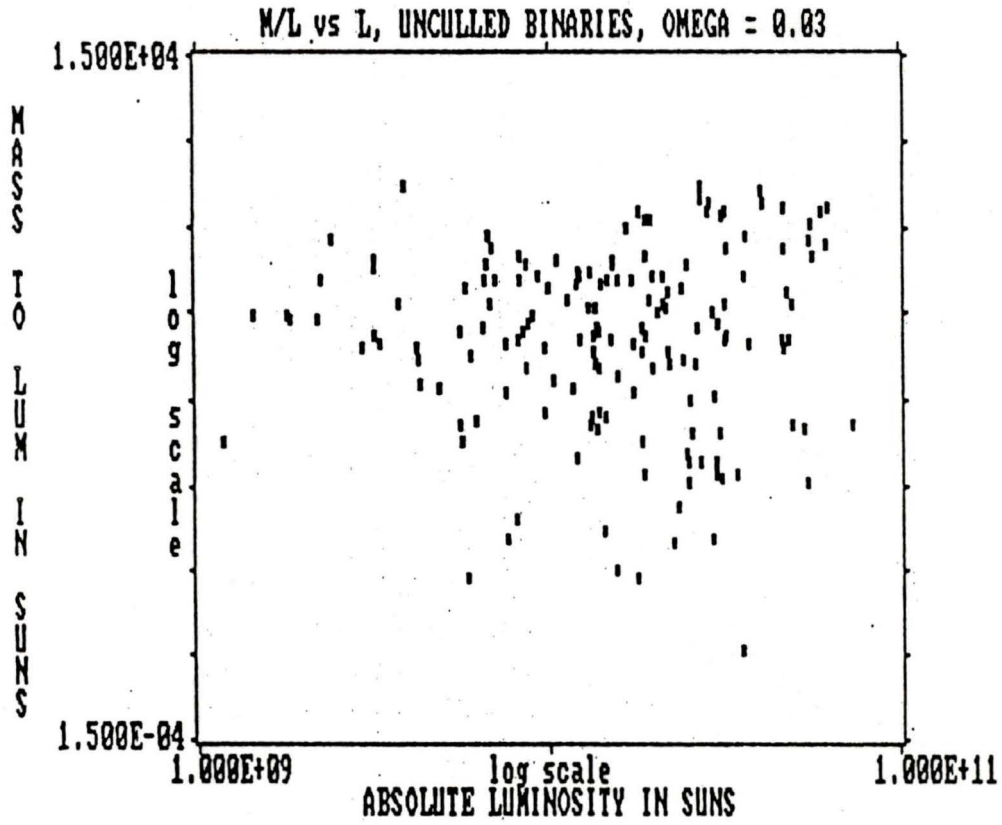


Figure 17: M/L vs L, Unculled Binaries, Omega = 0.03

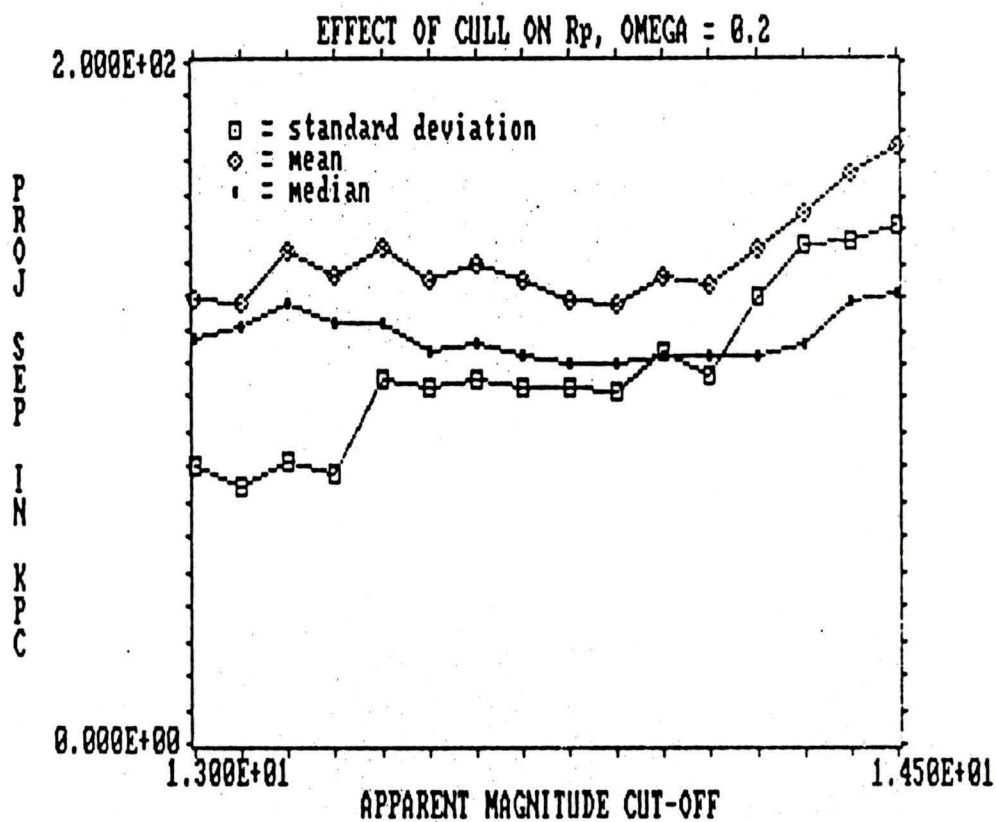


Figure 18: Effect of Cull on R_p , Omega = 0.2

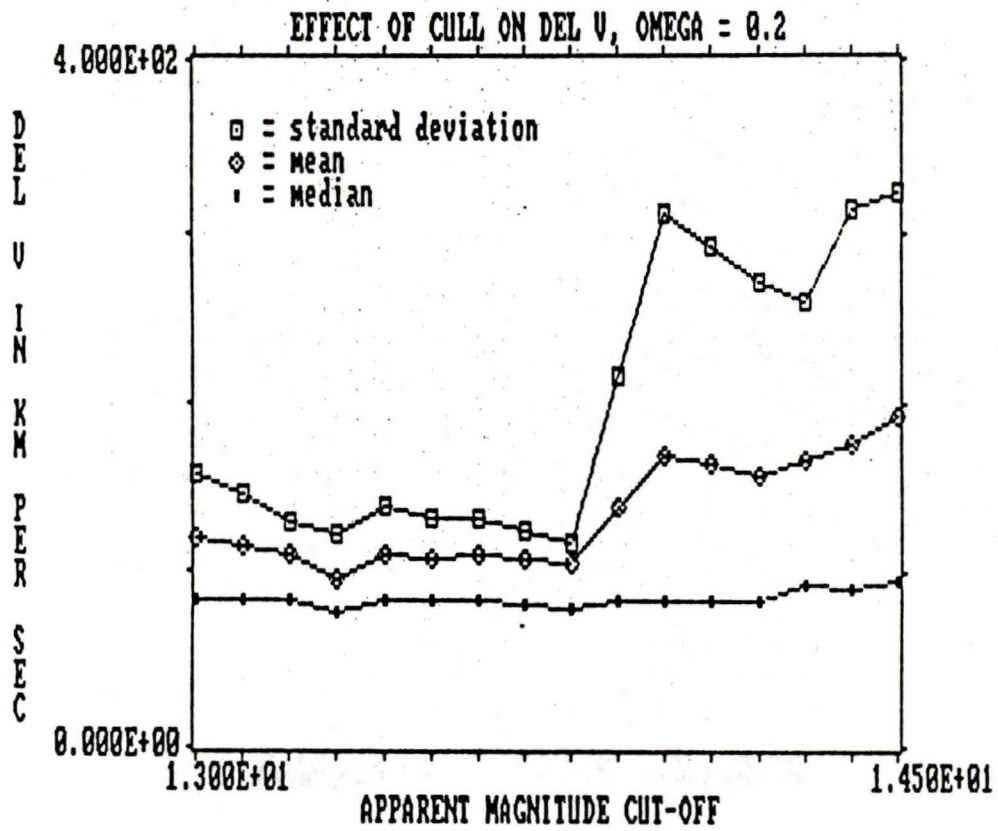


Figure 19: Effect of Cull on Del V, Omega = 0.2

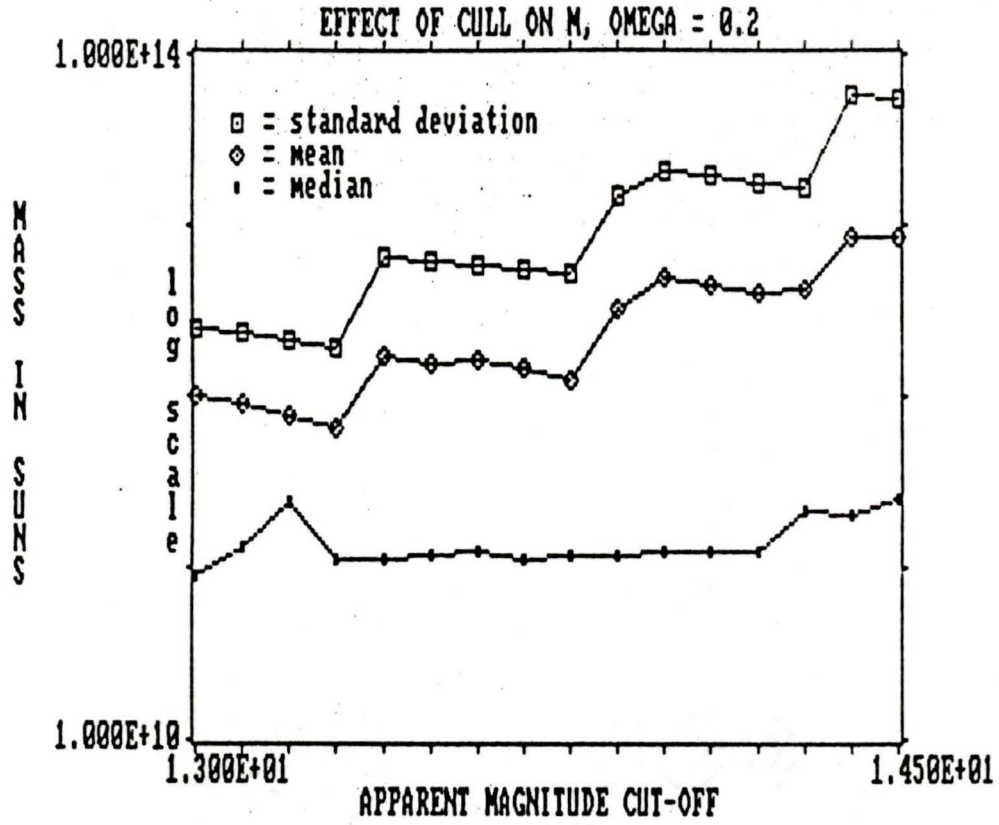


Figure 20: Effect of Cull on M, Omega = 0.2

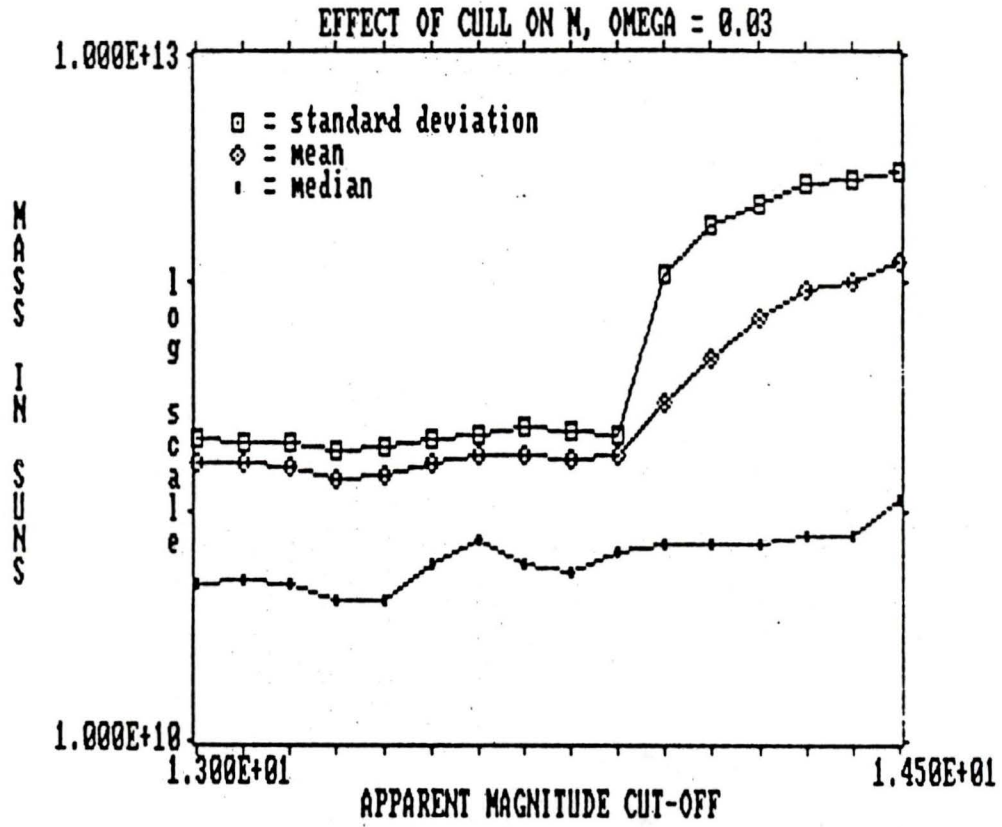


Figure 21: Effect of Cull on M, Omega = 0.03

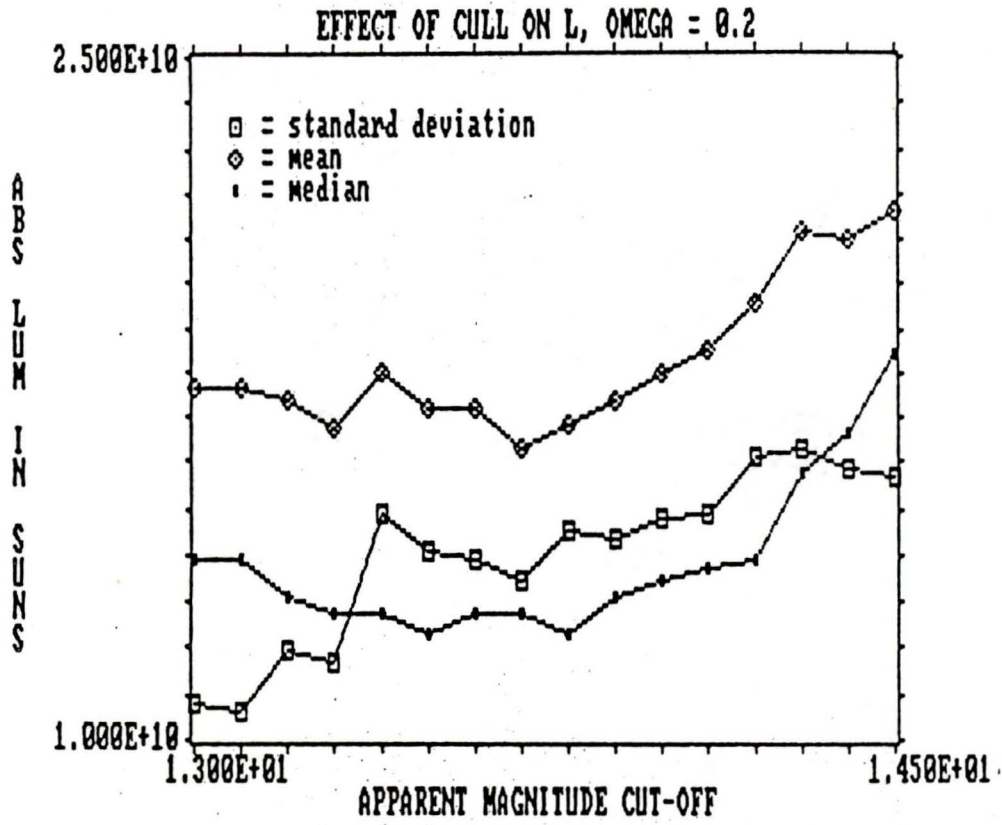


Figure 22: Effect of Cull on L, Omega = 0.2

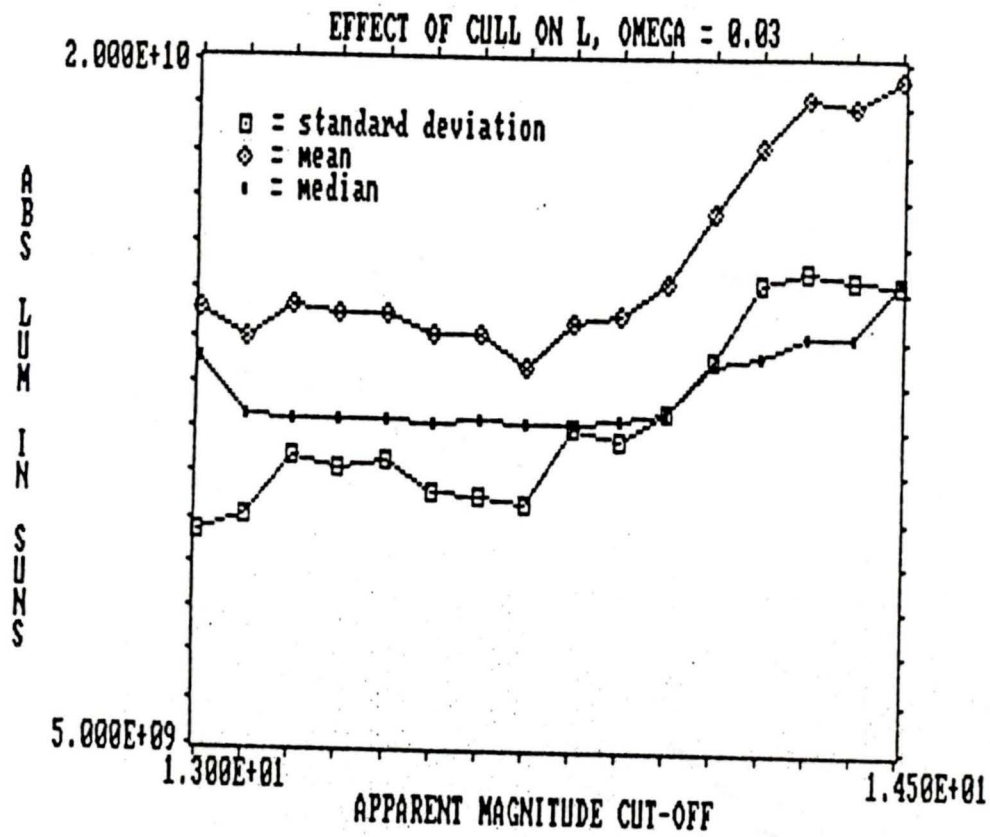


Figure 23: Effect of Cull on L, Omega = 0.03

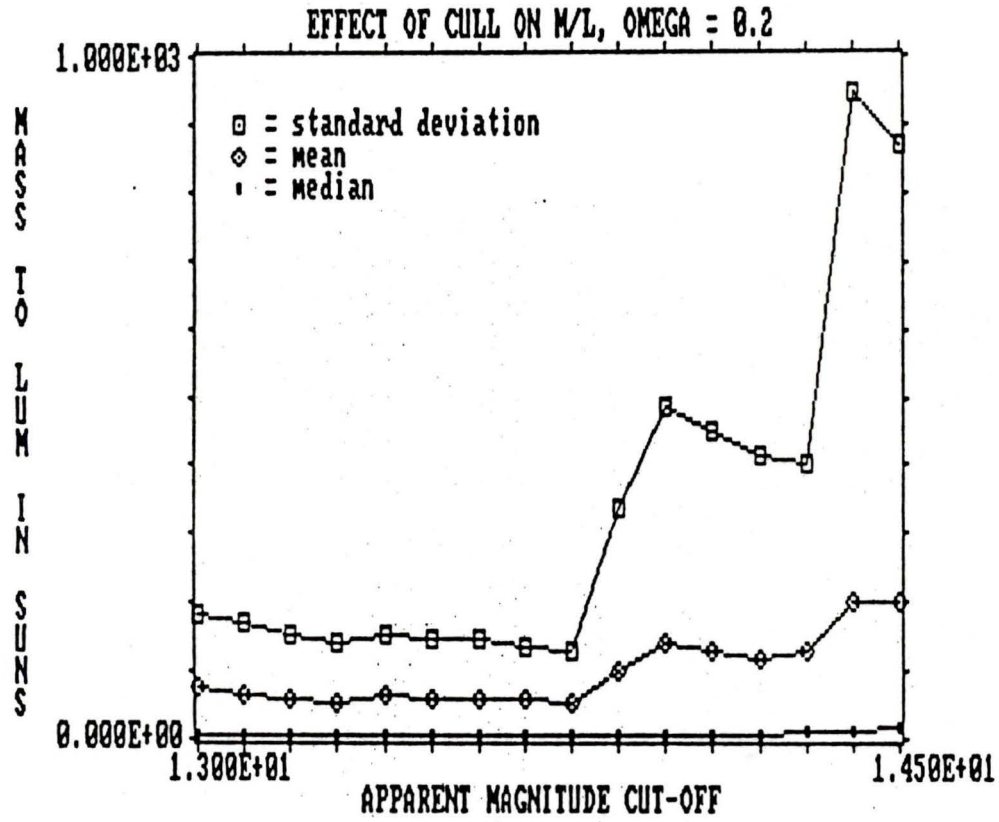


Figure 24: Effect of Cull on M/L, Omega = 0.2

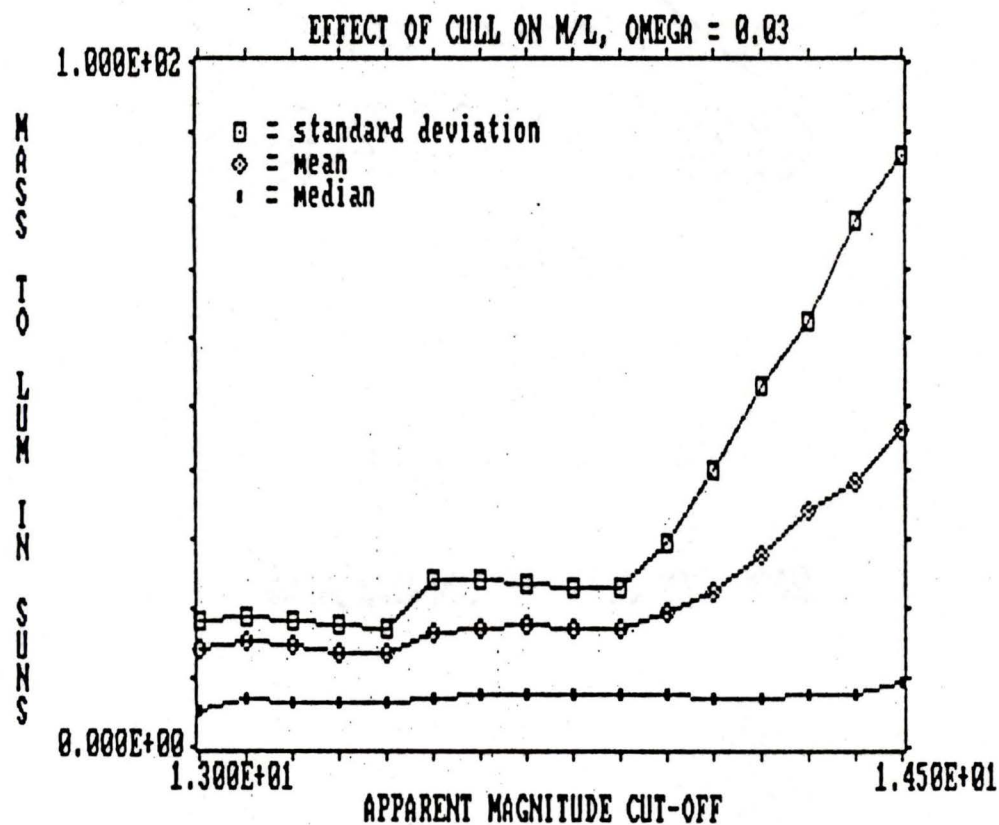


Figure 25: Effect of Cull on M/L, Omega = 0.03

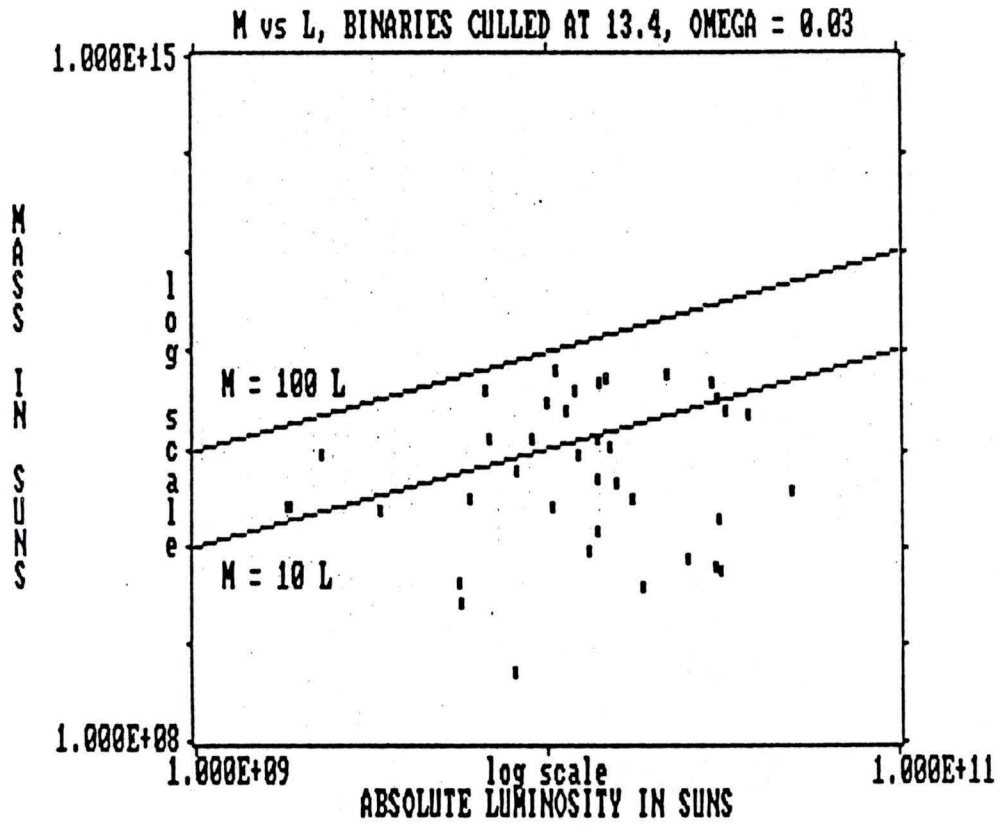


Figure 27: M vs L, Binaries Culled at 13.4, Omega = 0.03

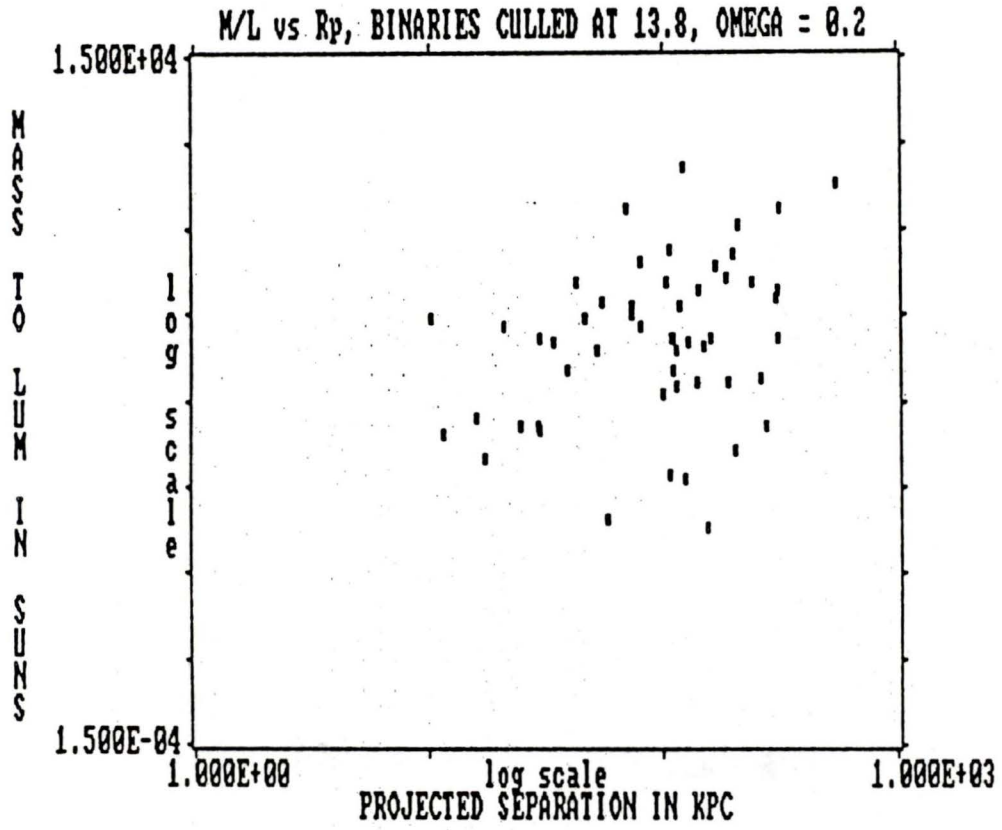


Figure 28: M/L vs R_p , Binaries Culled at 13.8, Omega = 0.2

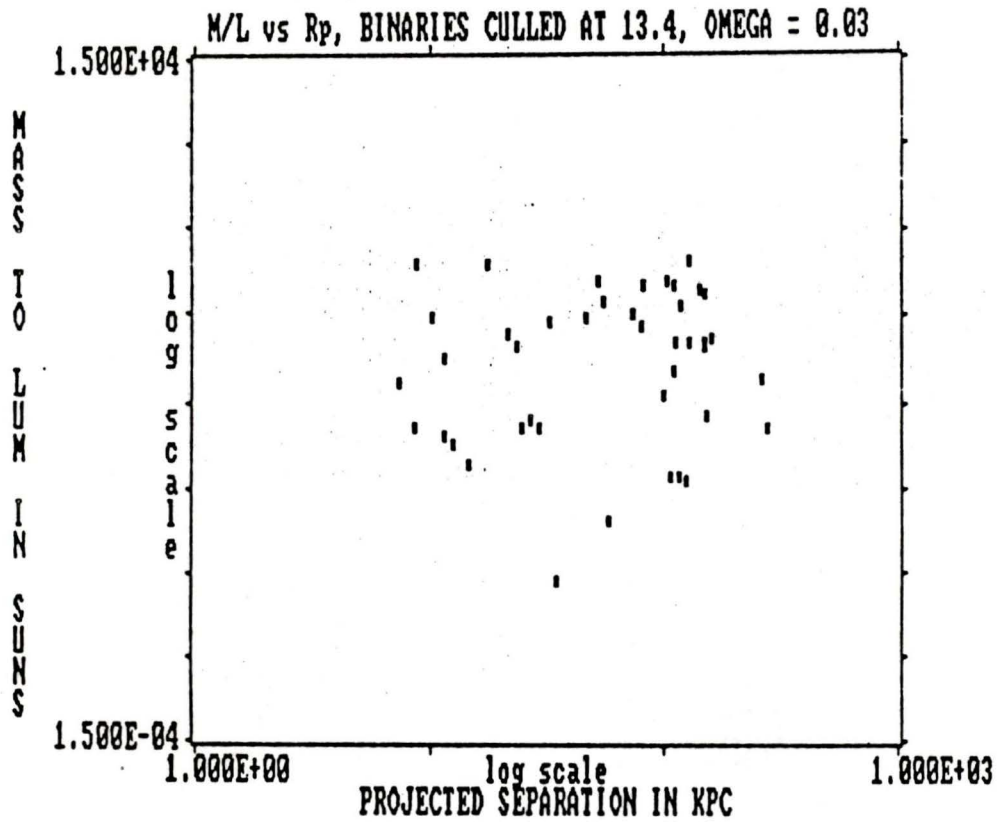


Figure 29: M/L vs Rp, Binaries Culled at 13.4, Omega = 0.03

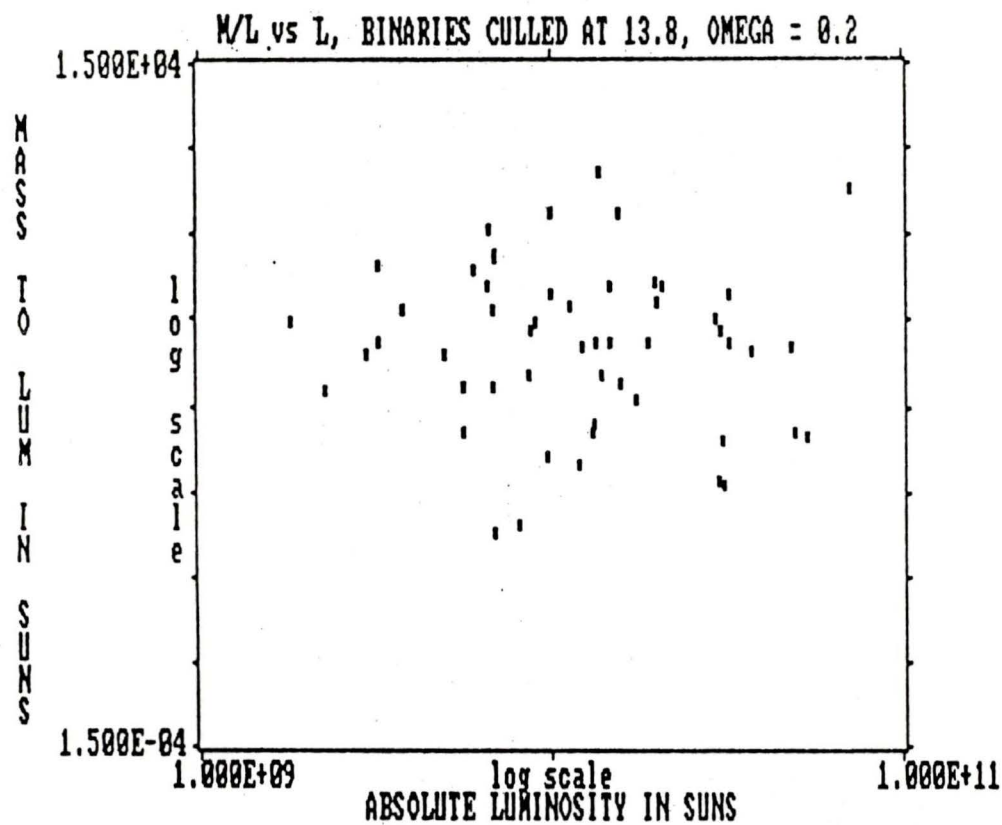


Figure 30: M/L vs L, Binaries Culled at 13.8, Omega = 0.2

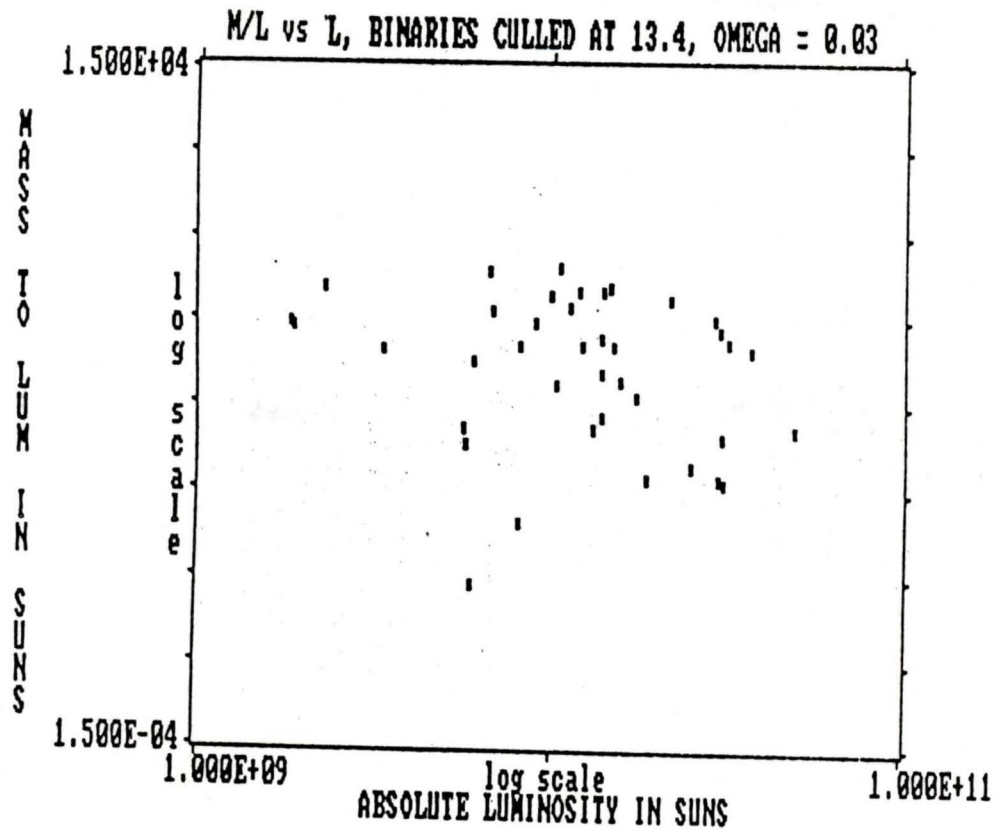


Figure 31: M/L vs L, Binaries Culled at 13.4, Omega = 0.03

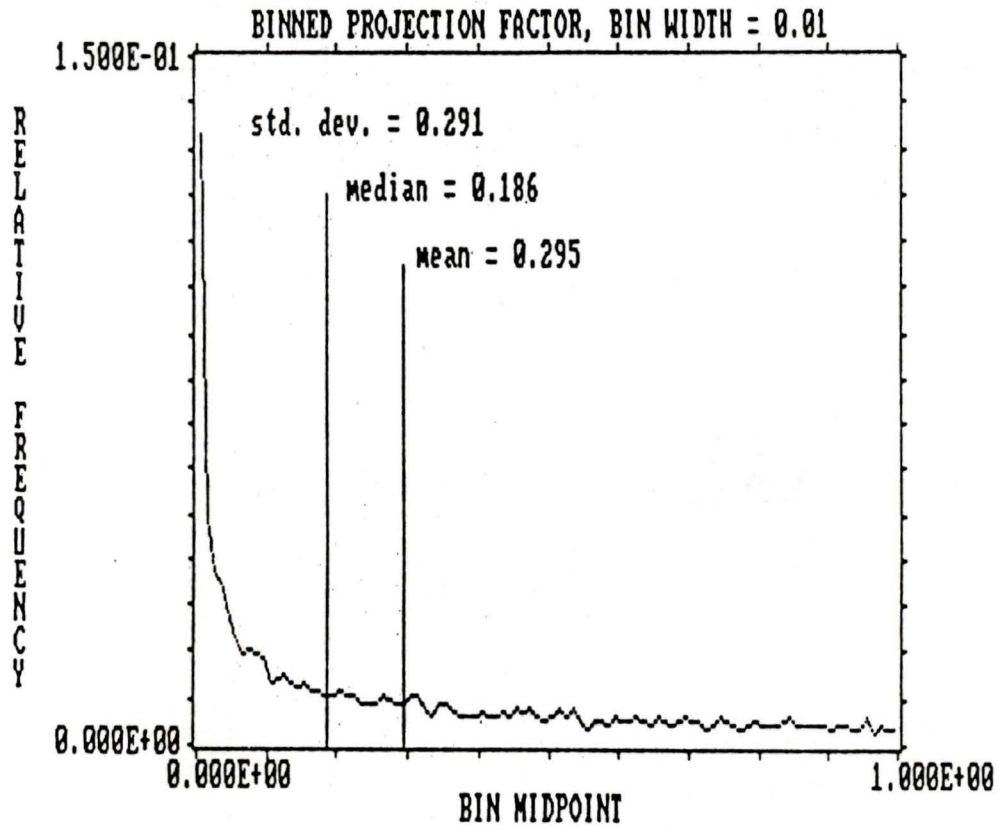


Figure 32: Binned Projection Factor, Bin Width = 0.01

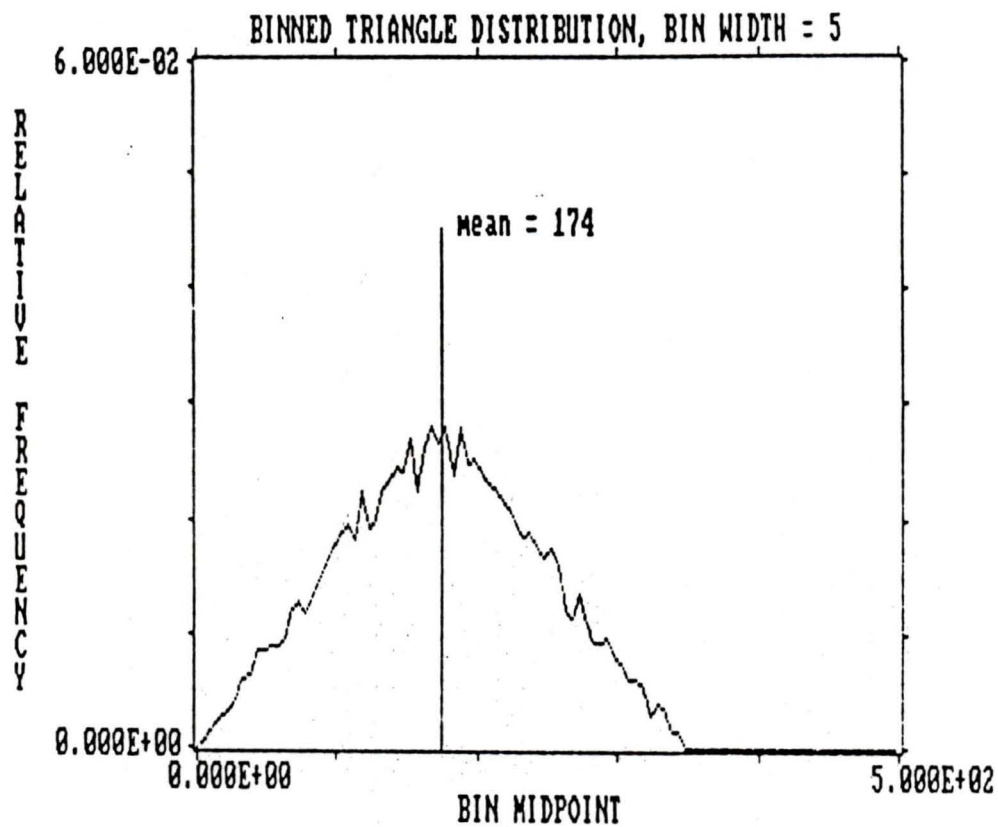


Figure 33: Binned Triangle Distribution, Bin Width = 5

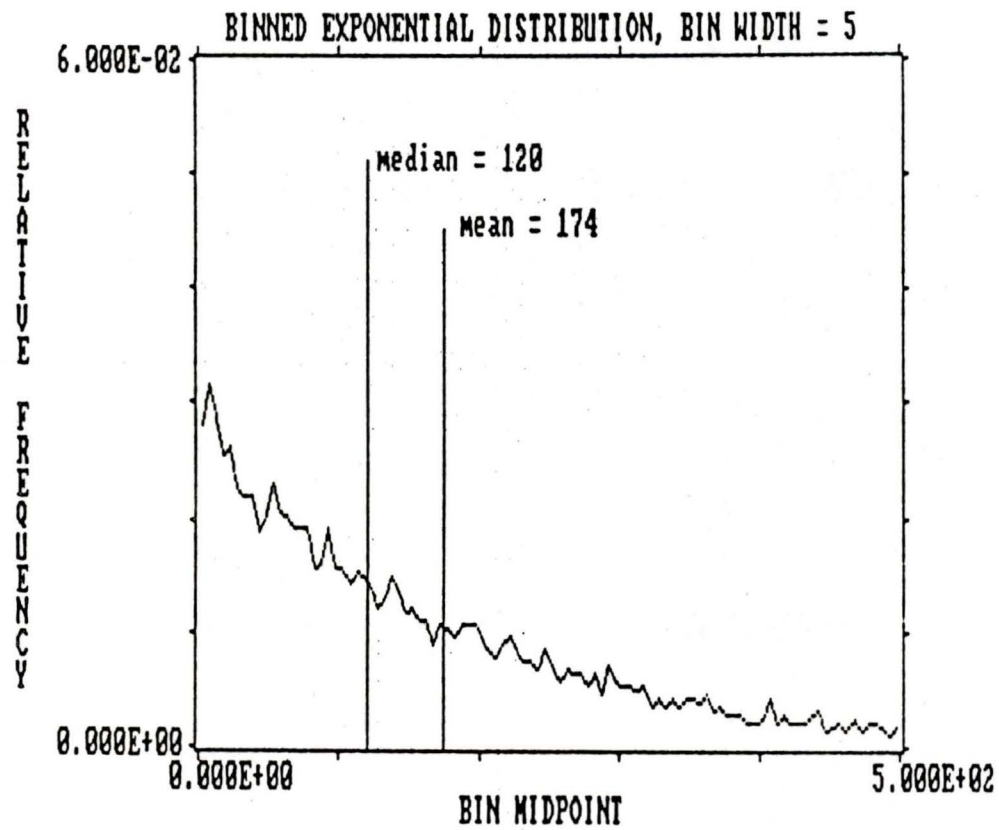


Figure 34: Binned Exponential Distribution, Bin Width = 5

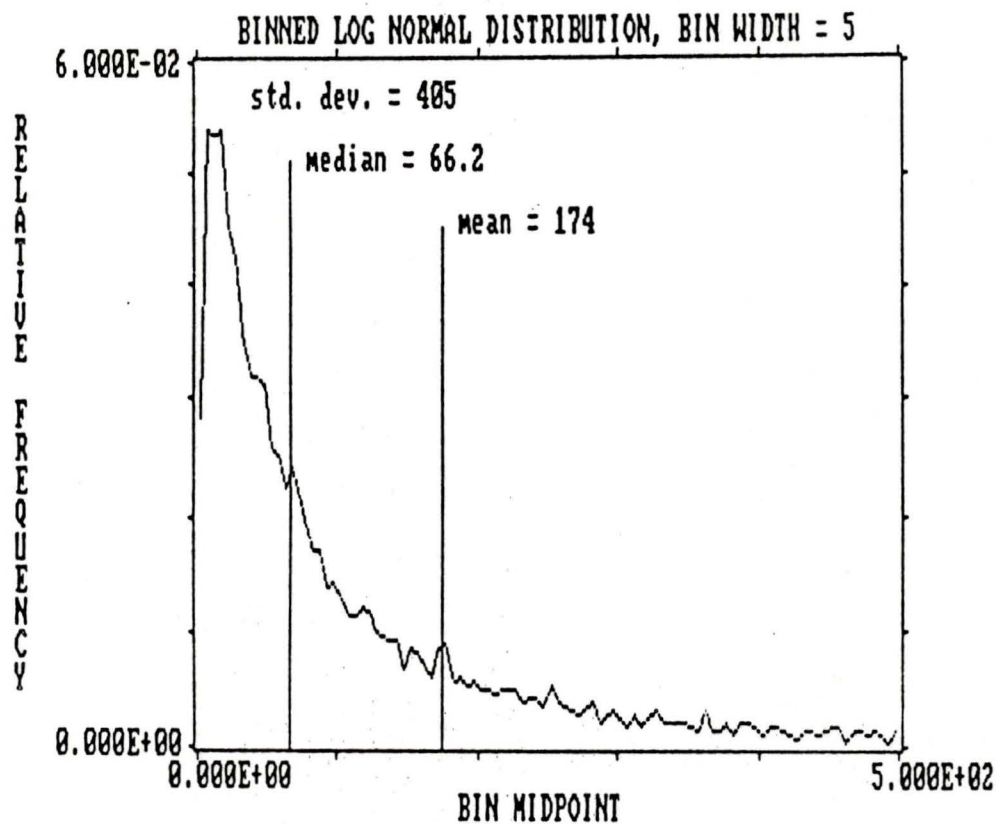


Figure 35: Binned Log Normal Distribution, Bin Width = 5

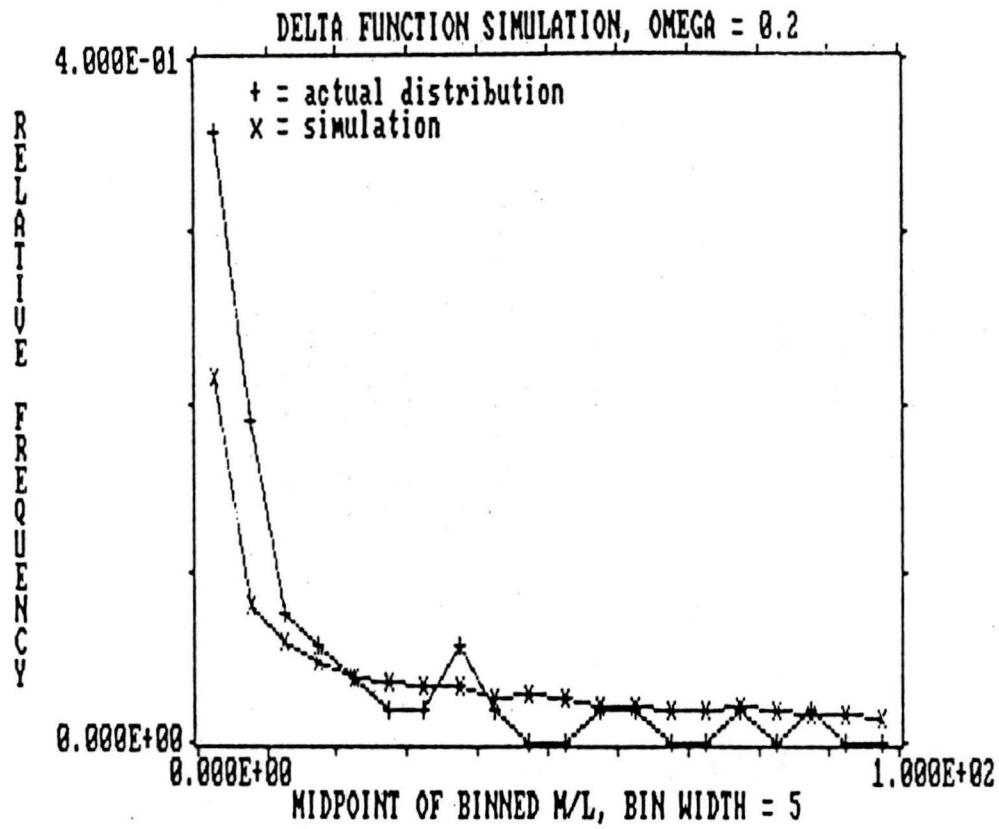


Figure 36: Delta Function Simulation, Omega = 0.2

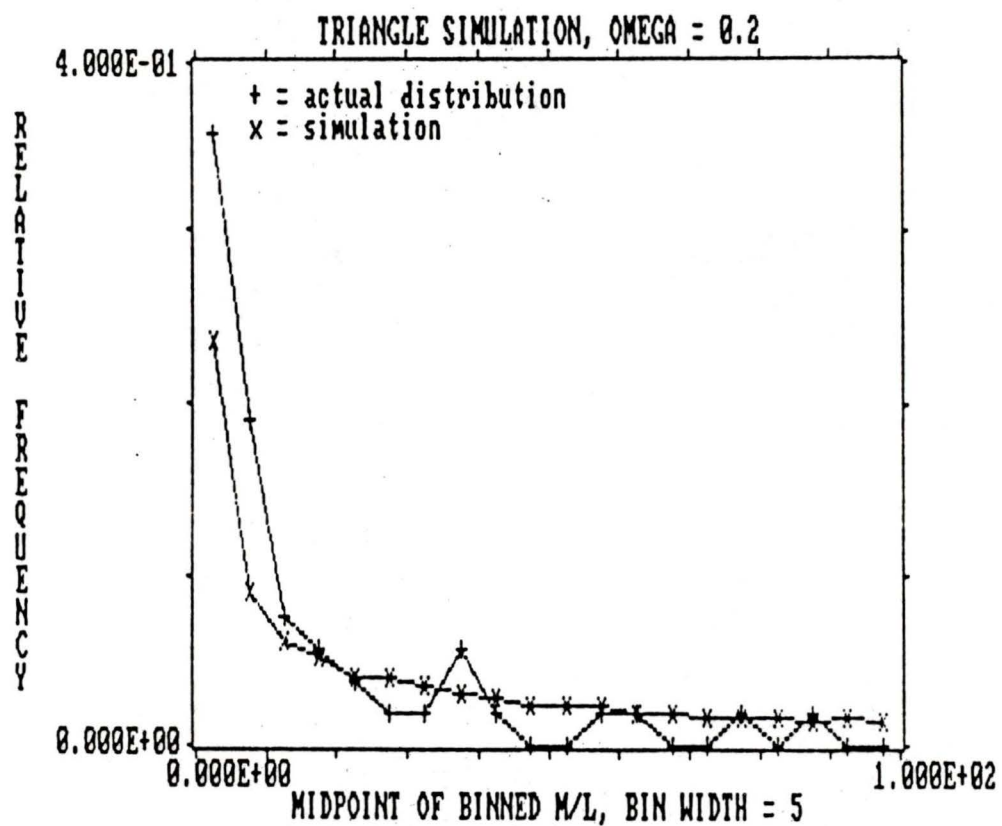


Figure 37: Triangle Simulation, Omega = 0.2

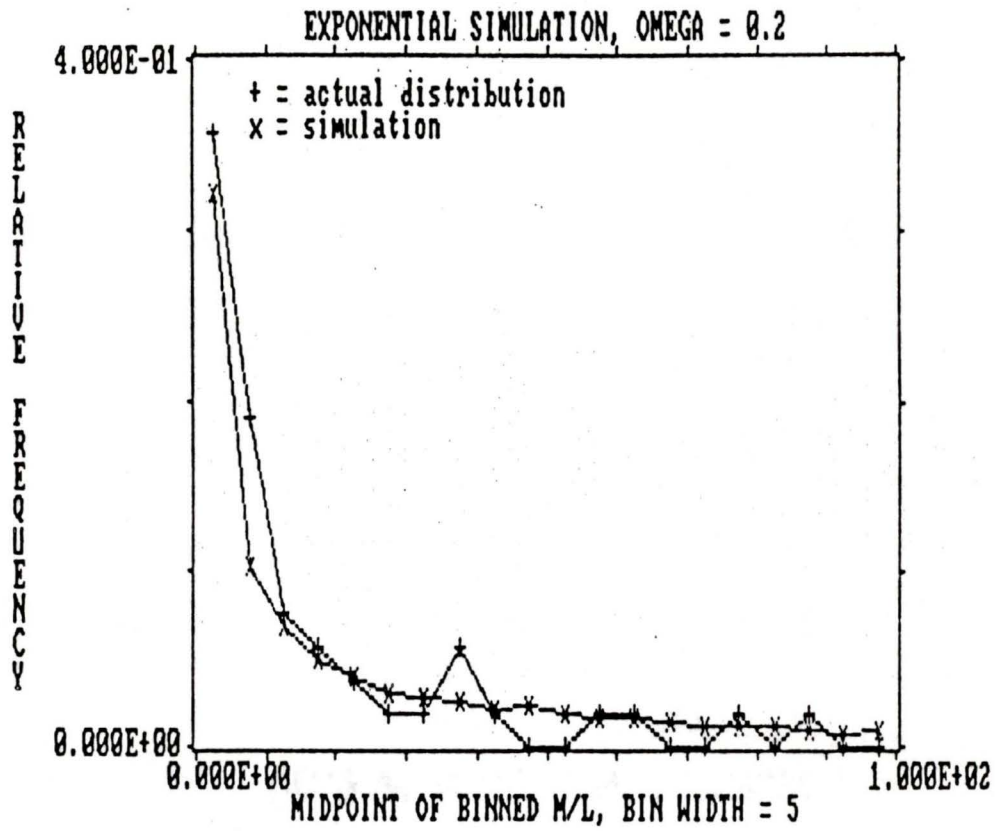


Figure 38: Exponential Simulation, Omega = 0.2

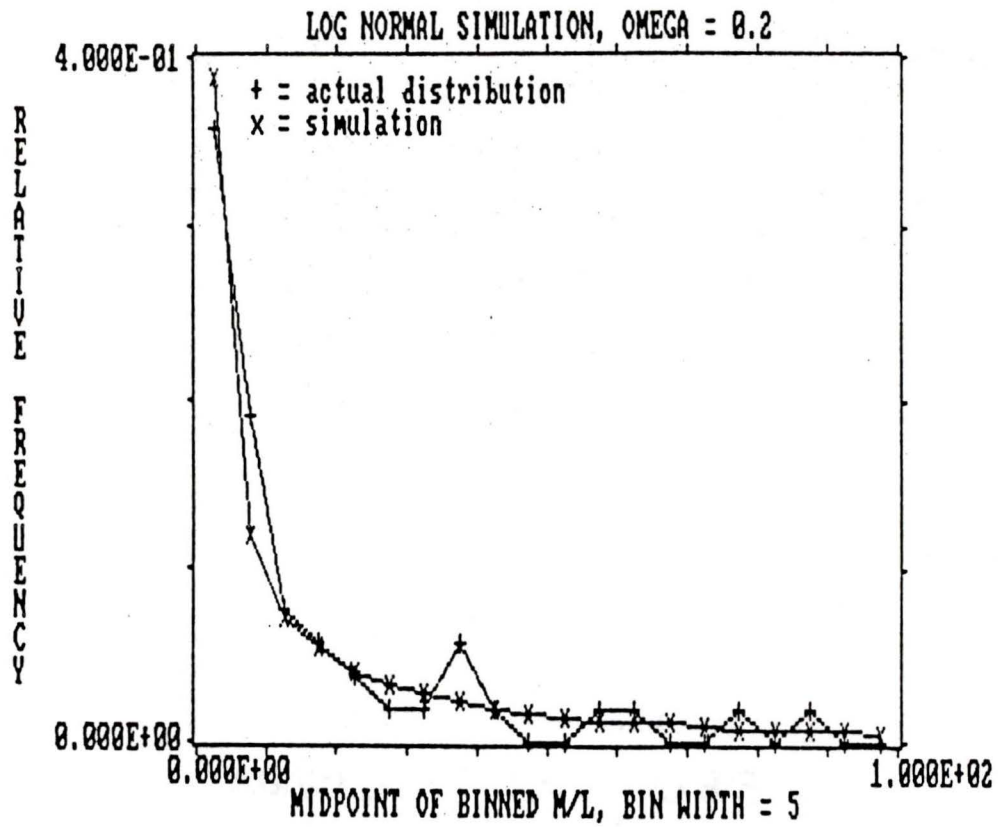


Figure 39: Log Normal Simulation, Omega = 0.2

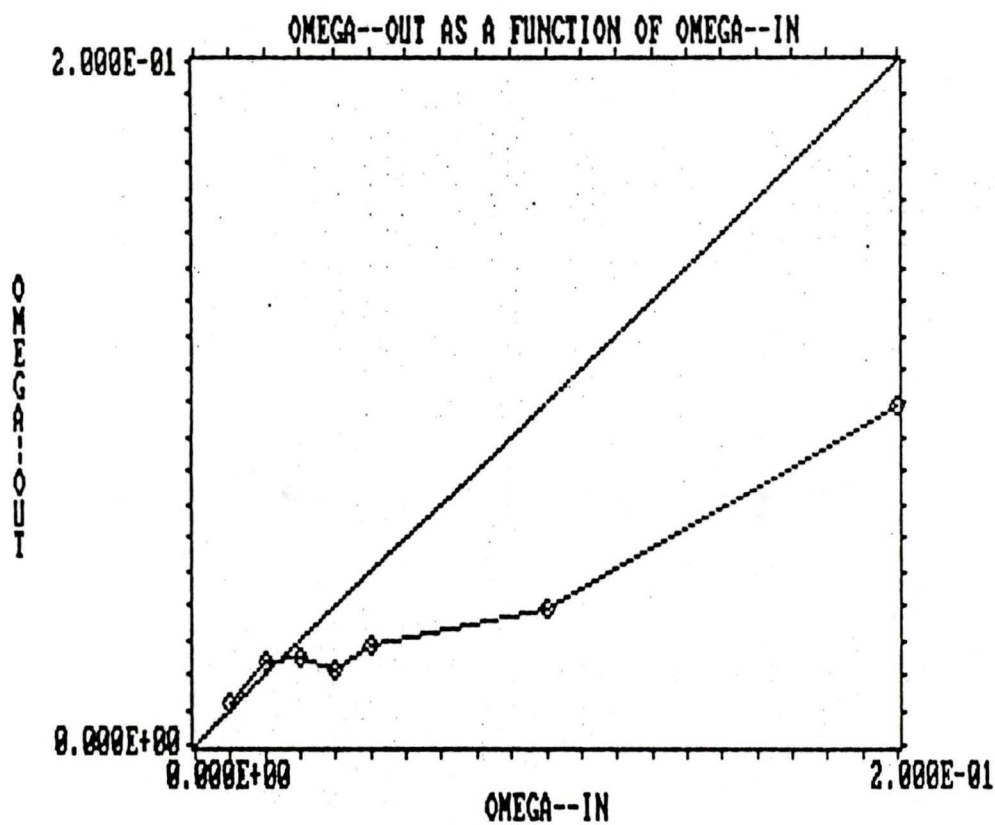


Figure 40: Omega--out as a Function of Omega--in

BIBLIOGRAPHY

Davis, M., and Peebles, P.J.E. 1983, Ap. J., 267, 465.

Einasto, J., Kaasik, A. and Saar, E. 1974, Nature, 250, 309.

Faber, S.M. 1982, in Astrophysical Cosmology, Pontificia Academia Scientiarum, Citta del Vaticano, p. 219.

Faber, S.M., and Gallagher, J.S. 1979, Ann. Rev. Astron. Astrophys., 17, 135.

Geller, M.J., and Huchra, J.P. 1983, Ap. J. Suppl., 52, 61.

Gott, R., and Rees, M.J. 1975, Astron. & Astrophys., 45, 365.

Huchra, J., Davis, M., Latham, D., and Tonry, J. 1983, Ap. J. Suppl., 52, 89.

Huchra, J., and Geller, M. 1982, Ap. J., 257, 423.

Karachentsev, I.D. 1972, Catalog of Isolated Pairs of Galaxies in the Northern Hemisphere, Soobshch. Spec. Astrophys. Obs., 7, 3.

Page, T. 1952, Ap. J., 116, 63.

Peebles, P.J.E. 1980, The Large Scale Structure of the Universe, Princeton University Press, Princeton.

Peebles, P.J.E. 1984, Ap. J., 284, 439.

Peterson, S.D. 1979, Ap. J. Suppl., 40, 527.

Press, W.H., and Davis, M. 1982, Ap. J., 259, 449.

Reif, F. 1965, Fundamentals of Statistical and Thermal Physics, McGraw-Hill, New York.

Schmidt, M. 1968, Ap. J., 151, 393.

Schmidt, M., and Green, R. F. 1983, Ap. J., 269, 352.

Squires, G.L. 1976, Practical Physics, McGraw-Hill, London.

Turner, E.L. 1976, Ap. J., 208, 20.

Weinberg, S. 1972, Gravitation and Cosmology: Principles and Applications of the General Theory of Relativity, John Wiley & Sons, Inc., New York.

White, S.D.M., and Rees, M.J. 1978, Mon. Not. R. Astr. Soc., 183, 341.

White, S. D. M., Huchra, J., Latham, D., and Davis, D. 1983, Mon. Not. R. Astr. Soc., 203, 701.

Yang, J., Turner, M.S., Steigman, G., Schramm, D.N., and Olive, K.A. 1984, Ap. J., 281, 493.

VITA

Surname: Morgan

Given Names: Charles Grady

Date and Place of Birth:

December 1, 1944 San Antonio, Texas

Educational Institutions Attended, with Dates:

Memphis State University, Memphis, Tenn.	1962 to 1966
Johns Hopkins University, Baltimore, Md.	1966 to 1969
University of Alberta, Edmonton, Alta.	1969 to 1975
University of Victoria, Victoria, B. C.	1975 to 1986

Degrees with Dates and Names of Institutions:

B.S., <u>cum laude</u>	1966	Memphis State University
M.S.	1969	Johns Hopkins University
Ph.D., with honors	1970	Johns Hopkins University
M.Sc.	1972	University of Alberta

Publications:

1. "Kim on deductive explanation," Philosophy of Science, vol. 37 (1970), pp. 434-439.
2. "Hypothesis generation by machine," Artificial Intelligence, vol. 2 (1971), pp. 179-187.
3. "On two proposed models of explanation," Philosophy of Science, vol. 39 (1972), pp. 74-81.

4. "Omer on scientific explanation," Philosophy of Science, vol. 40 (1973), pp. 110-117.
5. "Archaeology and explanation," World Archaeology, vol. 4 (1973), pp. 110-117.
6. "Sentential calculus for logical falsehoods," Notre Dame Journal of Formal Logic, vol. 14 (1973), pp. 347-353.
7. "Truth, falsehood, and contingency in first-order predicate calculus," Notre Dame Journal of Formal Logic, vol. 14 (1973), pp. 536-542.
8. "Systems of modal logic for impossible worlds," Inquiry, vol. 16 (1973), pp. 280-289.
9. "Drawing dichotomies via formal languages," The Southern Journal of Philosophy, vol. 11 (1973), pp. 216-227.
10. "Proper definitions in Principia Mathematica," International Logic Review, vol. 4 (1973), pp. 80-85.
11. "On the algorithmic generation of hypotheses," Scientia, vol. 108 (1973), pp. 585-598.
12. "Explanation and scientific archaeology," World Archaeology, vol. 6 (1974), pp. 133-137.
13. "A theory of equality for a class of many-valued logics," Zeitschrift fur mathematische Logik, vol 20 (1974), pp. 427-432.
14. "Notes on Garden of Eden configurations of higher degree," Kybernetes, vol. 3 (1974), pp. 129-134.

15. "Liberated Brouwerian modal logic," Dialogue, vol. 13 (1974), pp. 505-514.
16. "Liberated versions of T, S4, and S5," Archive fur mathematische Logik, vol. 17 (1975), pp. 85-90.
17. "Weak liberated versions of T and S4," Journal of Symbolic Logic, vol. 40 (1975), pp. 25-30.
18. "Automated hypothesis generation using extended inductive resolution," Proceedings of the Fourth International Joint Conference on Artificial Intelligence, (1975), pp. 351-356.
19. "Similarity as a theory of graded equality for a class of many-valued logics," Proceedings of the 1975 International Symposium on Multiple Valued Logics, (1975), pp. 436-449.
20. "Some undecidability results for construction problems in tessellation automata," Cybernetica, vol XIX (1976), pp. 133-139.
21. "Methods for automated theorem proving in nonclassical logics," I.E.E.E. Transactions on Computers, vol. C-25 (1976), pp. 852-862.
22. "Tuomela on deductive explanation," Journal of Philosophical Logic, vol. 5 (1976), pp. 511-525.
23. "A resolution principle for a class of many-valued logics," Logique et Analyse, no. 74-75-76 (1976), pp. 311-339.

24. "Some notes concerning fuzzy logics," Linguistics and Philosophy, vol. 1 (1976), pp. 79-97 (with F. J. Pelletier).
25. "Peirce semantics for modal logics," Proceedings of the 1976 International Peirce Congress, (1981).
26. "Comment on 'Descriptive statements, covering laws, and theories in archaeology'," Current Anthropology, vol. 19 (1978), pp. 325-326.
27. "Modality, analogy, and ideal experiments according to C. S. Peirce," Synthese, vol. 41 (1979), pp. 65-83.
28. "Local and global operators and many-valued modal logics," Notre Dame Journal of Formal Logic, vol. 20 (1979), pp. 401-411.
29. "Note on a strong liberated modal logic and its relevance to possible world skepticism," Notre Dame Journal of Formal Logic, vol. 20 (1979), pp. 718-721.
30. "There is a probabilistic semantics for every extension of classical sentence logic," The Journal of Philosophical Logic, vol. 11 (1982), pp. 431-442.
31. "Simple probabilistic semantics for propositional K, T, B, S4, and S5," The Journal of Philosophical Logic, vol. 11 (1982), pp. 443-458.
32. "Probabilistic semantics for intuitionistic logic," Notre Dame Journal of Formal Logic, vol. 24 (1983), pp. 161-180 (with H. Leblanc).

33. "Probability theory, intuitionism, semantics, and the Dutch book argument," Notre Dame Journal of Formal Logic, vol. 24 (1983), pp. 289-304 (with H. Leblanc).
34. "The truebeliever, the unbeliever, and a new modal semantics," Essays in Epistemology and Semantics, ed. by H. Leblanc, R. Stern, and R. D. Gumb. Haven Publications, New York (1983), pp. 33-53.
35. "Probabilistic semantics for propositional modal logics," Essays in Epistemology and Semantics, ed. by H. Leblanc, R. Stern, and R. D. Gumb. Haven Publications, New York (1983), pp. 97-116.
36. "Satisfiability in probabilistic semantics," Essays in Epistemology and Semantics, ed. by H. Leblanc, R. Stern, and R. D. Gumb. Haven Publications, New York (1983), pp. 153-159 (with H. Leblanc).
37. "Probabilistic semantics for orthologic and quantum logic," Logique et Analyse, no. 103-104 (1983), pp. 323-339.
38. "Probability functions and their assumption sets-the binary case," Synthese, vol. 60 (1984), pp. 91-106 (with H. Leblanc).
39. "Weak conditional comparative probability as a formal semantic theory," Zeitschrift fur mathematische Logik, vol. 30 (1984), pp. 199-212.
40. "Autologic," Logique et Analyse, no. 110-111 (1985), pp. 257-282.

PARTIAL COPYRIGHT LICENSE

I hereby grant the right to lend my thesis or dissertation (the title of which is shown below) to users of the University of Victoria Library, and to make single copies only for such users or in response to a request from the Library of any other university, or similar institution, on its behalf or for one of its users. I further agree that permission for extensive copying of this thesis for scholarly purposes may be granted by me or a member of the University designated by me. It is understood that copying or publication of this thesis for financial gain shall not be allowed without my written permission.

Title of Thesis/Dissertation:

GALAXY GROUPS AND BINARIES AND THE VALUE OF Ω_0

Author


Charles G. Morgan

July 12, 1986